

1 **Drainage reorganization and divide migration induced by the excavation of the Ebro**  
2 **basin (NE Spain)**

3

4 Arnaud Vacherat <sup>1</sup>, Stéphane Bonnet <sup>1</sup>, Frédéric Mouthereau <sup>1</sup>

5

6 <sup>1</sup>Géosciences Environnement Toulouse (GET), Université de Toulouse, CNRS, IRD, UPS,  
7 (Toulouse), France

8

9 *Correspondance to:* Stéphane Bonnet (stephane.bonnet@get.omp.eu)

10

11 **Abstract**

12

13 Intracontinental endorheic basins are key elements of source-to-sink systems as they preserve  
14 sediments eroded from the surrounding catchments. Drainage reorganization in such a basin in  
15 response to changing boundary conditions has strong implications on the sediment routing  
16 system and on landscape evolution. The Ebro and Duero basins represent two foreland basins,  
17 which developed in response to the growth of surrounding compressional orogens, the Pyrenees  
18 and the Cantabrian mountains to the north, the Iberian Ranges to the south, and the Catalan  
19 Coastal Range to the east. They were once connected as endorheic basins in the early Oligocene.  
20 By the end of the Miocene, new post-orogenic conditions led to the current setting in which the  
21 Ebro and Duero basins are flowing in opposite directions, towards the Mediterranean Sea and  
22 the Atlantic Ocean. Although these two hydrographic basins recorded a similar history, they are  
23 characterized by very different morphologic features. The Ebro basin is highly excavated,  
24 whereas relicts of the endorheic stage are very well preserved in the Duero basin. The  
25 contrasting morphological preservation of the endorheic stage represents an ideal natural  
26 laboratory to study the drivers (internal / external) of post-orogenic drainage divide mobility,  
27 drainage network and landscape evolution. To that aim, we use field and map observations and  
28 we apply the  $\chi$ -analysis of river profiles along the divide between the Ebro and Duero drainage  
29 basins. We show here that the contrasting excavation of the Ebro and Duero basins drives a  
30 reorganization of their drainage network through a series of captures, which resulted in the  
31 southwestward migration of their main drainage divide. Fluvial captures have strong impact on  
32 drainage areas, fluxes, and so on their respective incision capacity. We conclude that drainage  
33 reorganization driven by the capture of the Duero rivers by the Ebro drainage system explains

34 the first-order preservation of endorheic stage remnants in the Duero basin, due to drainage area  
35 loss, independently from tectonics and climate.

36

## 37 **1. Introduction**

38

39 Landscapes subjected to contrasted erosion rates between adjacent drainage basins show a  
40 migration of their drainage divide toward the area of lower erosion rates (Bonnet, 2009; Willett  
41 et al., 2014). This is the case for mountain ranges characterized by gradients in precipitation  
42 rates due to orography, once landscapes are in a transient state and are not adjusted to  
43 precipitation differences (Bonnet, 2009). It also occurs when drainage reorganized in response  
44 to capture (Yanites et al., 2013; Willett et al., 2014). River capture actually drives a drop in the  
45 spatial position of drainage divide (Prince et al. 2011) but also produces a wave of erosion in  
46 the captured reach (Yanites et al., 2013) that may impact divide position. Historically, migration  
47 of divides has been inferred by changes in the provenance of sediments stored in sedimentary  
48 basins (*e.g.* Kuhlemann et al., 2001). It is however a process that is generally very difficult to  
49 document in erosional landscapes. Recent developments have provided models and analytical  
50 approaches to identify divide migration in the landscape (Bonnet, 2009; Castelltort et al., 2012;  
51 Willett et al., 2014; Whipple et al., 2017). Among them the recently-developed  $\chi$ -analysis of  
52 longitudinal profiles of rivers (Perron and Royden, 2012) is based on the recognition of  
53 disequilibrium along river profiles, disequilibrium being defined by the departure from an ideal  
54 equilibrium shape. The application of this method to both natural and numerically-simulated  
55 landscapes, has allowed to demonstrate contrasts in the equilibrium state of rivers across divide  
56 and then to infer their migration (Willett et al., 2014). The applicability of this method is  
57 however limited to settings where the response time of rivers is larger compared to the rate of  
58 divide migration, so they can actually show disequilibrium in their longitudinal profiles  
59 (Whipple et al., 2017).

60

61 The Ebro and Duero drainage basins in the Northern Iberian Peninsula show geological and  
62 geomorphological evidence of very contrasted erosional histories during the Neogene. They  
63 initially recorded a long endorheic stage from the Early Oligocene to the Late Miocene (Riba  
64 et al., 1983; Garcia-Castellanos et al., 2003). Since then, both basins opened toward the Atlantic  
65 Ocean (Duero) or the Mediterranean Sea (Ebro). The Ebro basin's opening is reflected in the  
66 landscape by evidence of river incision (Garcia-Castellanos et al., 2003), whereas the Duero  
67 Basin does not show significant incision in its upstream part as a large relict of its endorheic

68 morphology is preserved (Antón et al., 2012). The Duero river long profile actually shows a  
69 pronounced knickpoint (knickzone) defining an upstream domain of high mean elevation (~800  
70 m) and low relief where the sediments deposited during the endorheic stage are relatively well  
71 preserved. Then, these two adjacent basins are characterized by differences in incision and in  
72 the preservation of their endorheic stages. They thus represent an ideal natural laboratory to  
73 evaluate divide migration in response to differential post-orogenic incision. Following a  
74 presentation of the geological context, we first compile evidence of fluvial captures along the  
75 Ebro-Duero divide, based on previous studies and our own investigations, and we map the  
76 location of knickpoints and relict portions of the drainage network. We use all these  
77 observations to reconstruct a paleo-divide position and to estimate the impact of divide  
78 migration in terms of drainage area and stream power. We complement this dataset by providing  
79 a map of  $\chi$  across divide (Willett et al., 2014) to highlight potential disequilibrium state between  
80 rivers of the Ebro and Duero catchments.

81

## 82 **2. Geological setting**

83

### 84 2.1 The Ebro and Duero basins

85

86 The Ebro and Duero basins represent two hydrographic basins located in the northern part of  
87 the Iberian Peninsula (Fig. 1). The bedrock of the Ebro and Duero drainage basins mainly  
88 consists of Cenozoic deposits, and Mesozoic and Paleozoic rocks in their headwaters (Fig. 2).  
89 They formed once a unique foreland basin during the Cenozoic controlled by the flexural  
90 loading by the surrounding mountain belts: the Pyrenees and the Cantabrian mountains to the  
91 north (Pulgar et al., 1999), the Iberian and Central Ranges to the south (Guimerà et al., 2004;  
92 De Vicente et al., 2007), and the Catalan Coastal Range (CCR) to the east (López-Blanco et al.,  
93 2000 ; Salas et al., 2001), during collision between Iberia and Europe since the Late Cretaceous.

94

95 From the Late Cretaceous, the Ebro and Duero basins were essentially filled by clastic deposits,  
96 and opened toward the Atlantic Ocean in the Bay of Biscay (Alonso-Zarza et al., 2002). During  
97 the Late Eocene – Early Oligocene, the uplift in the Western Pyrenees (Puigdefàbregas et al.,  
98 1992) led to the closure of the Ebro and Duero basins as attested by the Ebro basin  
99 continentalization dated at ~36 Ma (Costa et al., 2010). The center of these two basins became  
100 long-lived lakes filled with lacustrine, sandy, and evaporitic deposits from the Oligocene to the  
101 Miocene (Riba et al., 1983; Alonso-Zarza et al., 2002; Pérez-Rivarés et al., 2002, 2004; Garcia-

102 Castellanos et al, 2003; Garcia-Castellanos, 2006; Larrasoña et al., 2006; Vázquez-Urbez et  
103 al., 2013). The opening of the Ebro basin through the Catalan Coastal Range toward the  
104 Mediterranean Sea occurred during the Late Miocene, leading to kilometer-scale excavation  
105 throughout the basin (Fillon and Van der Beek, 2012; Fillon et al., 2013; Garcia-Castellanos  
106 and Larrasoña, 2015). The exact timing and processes driving the opening, as well as the  
107 role of the Messinian Salinity Crisis, have long been debated (Coney et al., 1996 (post-  
108 Messinian); Garcia-Castellanos et al., 2003 (13-8.5 Ma); Babault et al., 2006 (post-Messinian);  
109 Urgeles et al., 2010; Cameselle et al. (2014) (Serravallian-Tortonian); Garcia-Castellanos and  
110 Larrasoña, 2015 (12-7.5 Ma)). In contrast with the Ebro basin, incision in the upper Duero  
111 basin appears much less significant. The Duero basin is characterized by a low relief topography  
112 (Fig. 1) in its upstream part, at 700-800 m above sea level to the west, and at 1000-1100 m a.s.l.  
113 to the north, northeast, and to the east in the Almazan subbasin, close to the divide with the  
114 Ebro basin. The connection of the Duero River with the Atlantic Ocean occurred from the Late  
115 Miocene-Early Pliocene to the Late Pliocene-Early Pleistocene (Martín-Serrano, 1991). The  
116 current Ebro and Duero drainage networks are separated by a divide running from the  
117 Cantabrian belt to the NW, toward the SE in the Iberian Range (Figs. 1, 2, 3). In the following,  
118 we review the geological evolution of the different domains that constitute this drainage divide  
119 between the Ebro and Duero drainage basins.

120

## 121 2.2 The Iberian Range

122

123 The Iberian Range (Figs. 2, 4) is a double vergent fold-and-thrust belt resulting from Late  
124 Cretaceous inversion of Late Jurassic-Early Cretaceous rift basins during Iberia – Europe  
125 convergence (Salas et al., 2001; Guimerà et al., 2004; Martín-Chivelet et al., 2002). It is divided  
126 into two NW-SE directed branches, the Aragonese and the Castilian branches, separated by the  
127 Tertiary Almazan subbasin (Bond, 1996). The Almazan subbasin is connected to the Duero  
128 basin since the Early Miocene (Alonso-Zarza et al., 2002).

129 The Iberian Range is essentially made of marine carbonates and continental clastic sediments  
130 ranging from Late Permian to Albian, overlying a Hercynian basement. The Cameros subbasin  
131 to the NW represents a late Jurassic-Early Cretaceous trough almost exclusively filled by  
132 continental siliciclastic deposits (Martín-Chivelet et al., 2002 and references therein; Del Rio  
133 et al., 2009). Shortening in the Iberian Range occurred from the Late Cretaceous to the Early  
134 Miocene, along inherited Hercynian NW-SE structures (Gutiérrez-Elorza and Gracia, 1997;  
135 Guimerà et al., 2004; Gutiérrez-Elorza et al., 2002). The opening of the Calatayud basin in the



136 Aragonese branch occurred during the Early Miocene in response to right-lateral transpression  
137 on the southern margin of the Iberian Range (Daroca area) (Colomer and Santanach, 1988). It  
138 is followed during the Pliocene and the Pleistocene, by pulses of extension reactivating faults  
139 in the Calatayud basin, and the formation of grabens such as the Daroca, Munébrega,  
140 Gallocanta, and Jiloca grabens (Fig. 4; Colomer and Santanach, 1988; Gutiérrez-Elorza et al.,  
141 2002; Capote et al., 2002). This is also outlined by the occurrence of Late Pliocene to Early  
142 Pleistocene breccias and glaciais levels in the Daroca and Jiloca grabens (Gracia, 1992, 1993a;  
143 Gracia and Cuchi, 1993; Gutiérrez-Santolalla et al., 1996). These Neogene troughs are filled by  
144 continental deposits and pediments, up to the Quaternary (Fig. 4). The Neogene tectonic pulses  
145 in the Iberian are interrupted by periods of quiescence during which erosion surfaces developed  
146 (Gutiérrez-Elorza and Gracia, 1997).

147 Deformation and uplift of the Iberian Range and Cameros basin resulted in the development of  
148 a new drainage divide between the Duero and Ebro basins and in the isolation of the Almazan  
149 subbasin (Alonso-Zarza et al., 2002). In contrast, the connection between the Duero the Ebro  
150 basins has not been affected by significant deformation and uplift in the proto-Rioja trough  
151 (Mikes, 2010).

152

### 153 2.3 The Rioja trough and Bureba high

154

155 The Rioja trough (Figs. 2, 5) recorded important subsidence, especially during the Cenozoic (>  
156 5 km), related to compression and thrusting on its borders (Jurado and Riba, 1996). As thrusting  
157 initiated in the Pyrenean-Cantabrian belt and in the Iberian Range and Cameros basin, the Rioja  
158 trough became domain of important synorogenic sediment transfer between the Ebro and Duero  
159 basins. During the Paleocene, the Rioja trough was a marine depositional environment. With  
160 the increase of sediment fluxes that originated from the exhumation of surrounding mountain  
161 belts, sedimentation became essentially continental in the Eocene. Thrusting continued during  
162 the Oligocene resulting in the formation of an anticline connecting the Cantabrian domain and  
163 the Cameros inverted basin. This morphologic high (the Bureba anticline, Fig. 5) located in the  
164 center of the area is supposed to have triggered the disconnection between the Duero and Ebro  
165 basins (Mikes, 2010), as suggested by the repartition of alluvial fans on both sides of this  
166 structure (Muñoz-Jiménez and Casas-Sainz, 1997; Villena et al., 1996). During the Miocene,  
167 deformation ceased as evidenced by the deposition of undeformed middle Miocene to Holocene  
168 strata. The Bureba anticline is cored by Albian strata and topped by Santonian limestones and

169 Oligocene conglomerates controlling the location of the current main drainage divide between  
170 the Ebro and Duero river networks (Fig. 5).

171

## 172 2.4 Climate evolution

173

174 Climate exerts a major control on valley incision, sediment discharge, and on the evolution of  
175 drainage networks (Willet, 1999; Garcia-Castellanos, 2006; Bonnet, 2009; Whipple, 2009;  
176 Whitfield and Harvey, 2012; Stange et al., 2014). The mean annual precipitation map for the  
177 North Iberian Peninsula (Hijmans et al., 2005) shows a similar pattern for both the Ebro and  
178 Duero basins as they record very low precipitation, associated with global subarid conditions,  
179 with the exception of the Cameros basin that record a slightly higher precipitation rate (Fig. 6).  
180 There is a strong contrast to the north, toward the Mediterranean Sea and the most elevated  
181 areas in the Cantabrian and Pyrenean belts, where precipitation drastically increases.

182 The paleoclimatic evolution from the Late Cretaceous to the Neogene is linked both with the  
183 effects of surrounding mountains uplift, and with the latitudinal variation drift of Iberia from  
184 30°N in the Cretaceous to ~40°N during Late Neogene times. The hot-humid tropical climate  
185 of the Late Cretaceous became drier and arid from the Paleocene to the Middle Miocene (López-  
186 Martínez et al., 1986), favouring the development of endorheic lakes (Garcia-Castellanos,  
187 2006). During the Middle-Late Miocene and Early Pliocene, the northern Iberia recorded more  
188 humid and seasonal conditions (Calvo et al., 1993; Alonso-Zarza and Calvo, 2000) with  
189 alternations of cold-wet and hot-dry periods (Bessais and Cravatte, 1988; Rivas-Carballo et al.,  
190 1994; Jiménez-Moreno et al., 2010). More humid and colder conditions took place in the Late  
191 Pliocene, characterized by dry glacial periods and humid interglacials (Suc and Popescu, 2005;  
192 Jiménez-Moreno et al., 2013). Climatic contrasts increased, triggering intense glaciers  
193 fluctuations in the surrounding mountain ranges during the Lower-Middle Pleistocene transition  
194 (1.4-0.8 Ma) (Moreno et al., 2012; Duval et al., 2015; Sancho et al., 2016), and throughout the  
195 Late Pleistocene period, which record glacial / interglacial oscillations, as evidenced by pollen  
196 identification (Suc and Popescu, 2005; Jiménez-Moreno et al., 2010, 2013; Barrón et al., 2016;  
197 García-Ruiz et al., 2016) and speleothem studies (Moreno et al., 2013; Bartolomé et al., 2015).  
198 Glaciers are considered as very efficient erosion tool in continental environment. They are  
199 likely to influence drainage divide migration (Brocklehurst and Whipple, 2002). There is large  
200 evidence of glaciers development especially for the Late Pleistocene in the Pyrenees (Delmas  
201 et al., 2009; Nivière et al., 2016; García-Ruiz et al., 2016), in the Cantabrian belt (Serrano et  
202 al., 2013, 2016; García-Ruiz et al., 2016), and in the Central Range (Palacios et al., 2011, 2012;

203 García-Ruiz et al., 2016). However, although numerous moraines have been mapped throughout  
204 the Iberian Range (Ortigosa, 1994; García-Ruiz et al., 1998; Pellicer and Echeverría, 2004),  
205 there is no evidence of U-shaped valleys and because of the lack of very high elevated massifs  
206 (>2500 m), the occurrence of active ice tongues are considered as limited, if not precluded  
207 (García-Ruiz et al., 2016).

208

### 209 **3. Evidence of divide mobility between the Duero and Ebro catchments**

210

211 The easternmost part of the Duero river is opposed to the Ebro tributaries that are the Jalon,  
212 Huecha, Queiles, Alama, Cidacos, Iregua, and Najerilla rivers, whereas the Arlanzon and  
213 Pisuerga rivers (Duero tributaries) are opposed to the Najerilla, Tiron, Oca, and Rudron rivers,  
214 and to the westernmost part of the Ebro river (Fig. 3). The northeastern part of the Duero basin  
215 (the easternmost Duero river, the Arlanzon and Pisuerga rivers) mainly consists of broad flat  
216 valleys characterized by low incision depth and low-gradient streams with concave longitudinal  
217 profiles (Antón et al., 2012, 2014). By contrast, the western part of the Ebro basin is  
218 characterized by more incised valleys, especially in the Cantabrian and in the Cameros – Iberian  
219 Range domains, with more complex longitudinal profiles (knickpoints, remnants of high  
220 elevated surfaces). Previous studies (Gutiérrez-Santolalla et al., 1996; Pineda, 1997; Mikes,  
221 2010) already shown that the Jalon and Homino rivers, which belong to the Ebro basin, have  
222 recently captured parts of the Duero basin in the Iberian Range and in the Rioja trough,  
223 respectively. Such evolution has been recorded by the occurrence of geomorphological markers  
224 as wind gaps and elbows of captures, as well as by the presence of knickpoints and/or remnants  
225 of high elevated surfaces in river long profiles. To highlight this dynamic evolution, we  
226 performed a morphometric analysis of rivers all around the divide separating the Ebro basin  
227 from the Duero basin, with particular attention given to the Aragonese branch of the Iberian  
228 Range (Fig. 4) and to the Rioja Trough (Fig. 5), where captures have already been described.  
229 The studied basins were digitally mapped using high-resolution (~30 meters) digital elevation  
230 models (DEMs) from SRTM 1 Arc-Second Global elevation data available at the U.S.  
231 Geological Survey ([www.usgs.gov](http://www.usgs.gov)). The different DEMs were assembled using the ENVI  
232 software. We also used 1:50,000 geological maps from the Instituto Geológico y Minero de  
233 España ([www.igme.es](http://www.igme.es)). We used the TopoToolbox, a MATLAB-based software developed by  
234 Schwanghart and Scherler (2014), to extract the river network and longitudinal profiles and the  
235  $\chi$ -analysis Tool developed by Mudd et al. (2014).

236

### 237 3.1 Fluvial captures and related knickpoints in the Iberian Range

238

239 Neogene tectonics in the Iberian range controlled the uplift of topographic ranges and the  
240 formation of several basins whose connection with the Ebro or the Duero has occasionally  
241 changed through time. Nowadays, the western part of the Almazan subbasin (Figs. 2, 4) belongs  
242 to the Duero catchment, its eastern part being drained by the Ebro drainage network and  
243 especially by the Jalon river and its tributaries (Fig. 4). Gutiérrez-Santolalla et al. (1996)  
244 proposed that the Jalon river captured this domain after cutting into the Mesozoic and Neogene  
245 strata and the two Paleozoic ridges of the Aragonese branch of the Iberian Range. They used  
246 chronostratigraphic evidence to build a relative chronology of capture events in the Jalon area.  
247 First, the incision of the northern Paleozoic ridge and capture of the Calatayud basin by the  
248 Jalon river is attributed to a post-Messinian age. The Jiloca river, the easternmost main Jalon  
249 tributary, is then thought to capture the Daroca graben area to the east during the Late Pliocene  
250 – Early Pleistocene. This is followed from the Early to Late Pleistocene by the capture of the  
251 Jiloca graben to the southeast and finally by the capture of the Munébraga graben to the  
252 southwest, by the Jalon river (Gutiérrez-Santolalla et al., 1996), toward the easternmost part of  
253 the Almazan subbasin.

254 The Jalon river and tributaries show knickpoints in their longitudinal profiles (Fig. 4), at  
255 locations that are consistent with the events of captures proposed by Gutiérrez-Santolalla et al.  
256 (1996), suggesting that these captures are actually witnessed by knickpoints. The capture of the  
257 Jiloca graben corresponds to a major knickpoint in the Jiloca river profile that appears very  
258 smoothed, and that is followed by an upstream ~50 km long flat domain preserved at ~1000 m  
259 high above sea level. This imparts a convex shape to the Jiloca profile (Fig. 4). Due to the short  
260 period of time between the formation of the Jiloca graben (the earliest glacial deposits are  
261 attributed to the Middle Pliocene) and its capture (Early Pleistocene; Gutiérrez-Santolalla et al.,  
262 1996), we suggest this upstream domain was a short-lived endorheic domain that has never  
263 been externally drained before being captured by the Ebro network. In the northwestern part of  
264 the Jiloca graben, the Cañamaria river, a tributary of the Jiloca river, heads to the northwest,  
265 reaching the Gallocanta basin, also considered as a former graben (Gracia, 1993b; Gracia et al.,  
266 1999; Gutiérrez-Elorza et al., 2002). The upstream part of its river long profile is characterized  
267 by a sharper knickpoint at the entrance of the basin, and is followed by a ~15 km long flat  
268 domain (Fig. 4). Similarly to the Jiloca graben, the Gallocanta basin appears to be a short-lived  
269 endorheic domain that has been more recently captured by the Jiloca river network.

270 According to Gutiérrez-Santolalla et al. (1996), the Jalon river reached the southern Paleozoic  
271 ridge of the Aragonese branch, to the southwest of the Calatayud basin, captured the Munébrega  
272 graben and the Almazan subbasin (also characterized by a pronounced knickpoint) during the  
273 Pleistocene-Holocene, slightly after the capture of the Jiloca graben by the Jiloca river. This is  
274 coherent with morphological analysis of longitudinal profiles, as the major knickpoint related  
275 to the capture of the Jiloca graben appears very smoothed, whereas knickpoints observed in the  
276 west are sharper, suggesting they are younger. However we cannot ruled out some local  
277 influence of the lithology on the shape of these knickpoints.

278 Finally, the Piedra river (Jalon tributary) long profile shows major sharp knickpoints and two  
279 successive ~30 km long almost flat domains in the Almazan subbasin, at ~900-1000 m above  
280 sea level (Fig. 4). In addition, the upper reach of the river long profiles of the Jalon river, and  
281 of its tributary the Blanco river, are characterized by major sharp knickpoints, and by a ~15 km  
282 long flat domain at ~1000-1100 m above sea level, in the Mesozoic Castilian branch of the  
283 Iberian Range (Fig. 4).

284

### 285 3.2 Fluvial captures and related knickpoints in the Rioja trough area

286

287 In the Rioja trough area, the position of the Ebro-Duero divide is partly controlled by the Bureba  
288 anticline. It consists of folded Middle Cretaceous to Early Miocene series, covered by  
289 undeformed Middle Miocene to Holocene deposits (Fig. 5). The anticline is orientated E-W to  
290 the west and NE-SW to the east. The western part of the Rioja trough to the west of the NE-SW  
291 directed branch of the Bureba anticline (Fig. 5), used to be drained toward the Duero basin since  
292 the Oligocene (Pineda, 1997; Mikes, 2010). The westward migration of the divide to its current  
293 location is thought to have occurred in several steps of captures as shown by the occurrence of  
294 remnants of escarpments during the Late Miocene - Pliocene (Mikes, 2010). Once the eastern  
295 branch of the Bureba anticline has been incised, the Ebro tributaries captured the western part  
296 of the Rioja trough, up to the E-W branch of the Bureba anticline to the southwest, from the  
297 Late Miocene to the Pliocene. The western part of the anticline forms a topographic ridge that  
298 is incised by Jordan river (Fig. 5) in a place where the divide between the Ebro and Duero river  
299 networks is located to the north of the ridge. To the East of this location however, the  
300 topographic ridge formed by the Bureba anticline controls the current location of the main  
301 drainage divide (Fig. 5). Here, the ridge exhibits several wind gaps, located on the northward  
302 prolongation of the Hoz, Rioseras, and Nava Solo rivers (Figs. 5, 7). Further east, the Diablo  
303 river does not incise the ridge and its headwater is located in the core of the eastern branch of

304 the Bureba anticline, the Fuente Valley (Fig. 5). These last streams are tributaries of the Ubierna  
305 river, which is a tributary of the Arlanzon river and so, of the Duero river. To the north, the Ebro  
306 river system is represented, from west to east, by the Homino river (a tributary of the Oca river)  
307 and its four tributaries, the Molina, the Fuente Monte, the Zorica, and the San Pedro rivers (Figs.  
308 5, 7). All these streams are outlined by Late Pleistocene to Holocene alluvial series that are  
309 deposited at the bottom of their respective valleys. Valleys from the Duero side appears larger  
310 than those from the Ebro side, which are significantly more incised.

311 The Jordan river's headwater is located north of the ridge formed by the Bureba anticline. We  
312 can continuously follow its valley deposits northward along a broadly gentle slope, up to the  
313 locality of Coraegula (Fig. 5). However, the current course of the Jordan river is cut ~8 km  
314 south, in the vicinity of Hontomin, by the Homino (Ebro) river (Figs. 5B, C, 7). This fluvial  
315 capture is characterized by a well-defined and highly incised elbow of capture, already  
316 described by Pineda (1997) and Mikes (2010). The longitudinal profile of the Homino river  
317 shows a sharp knickpoint located on Hontomin (Fig. 7C). Finally, there is a small wind gap on  
318 the divide between the two opposite rivers (Figs. 5, 7).

319 To the southeast, the headwater of the Hoz river is located to the south of a wind gap cut into  
320 the Bureba ridge (Fig. 7C). To the north, in the exact prolongation of the Hoz river, the Molina  
321 river shows a bend similar to the elbow of capture previously described for the Homino river  
322 (Fig. 7) and there is a minor knickpoint located on this elbow, according to the extracted river  
323 long profile. Thus, it is likely that the Molina river used to represent the former upper reach of  
324 the Hoz river, in a period when the Ebro-Duero divide was located northward, before being  
325 captured by the Ebro network.

326 To the east, the Rioseras and the Nava Solo rivers have also their headwater located to the South  
327 of wind gaps in the Bureba ridge (Fig. 7). Similarly, in their exact prolongations, the Fuente  
328 Monte and the Zorica rivers show important elbows of capture with minor knickpoints. They  
329 may also represent former upper reaches of Duero streams that have been captured by the Ebro  
330 network (Figs. 5, 7, 8).

331 Further east, the headwater of the Diablo river is located on the depression represented by the  
332 core of the eastern branch of the Bureba anticline, the Fuente valley. In its prolongation to the  
333 northeast, the San Pedro river incises the northeastern termination of the anticline from the  
334 north before entering the valley, leading to a southward retreat of the divide (Fig. 5). Capture is  
335 again evidenced by important incision contrast between Ebro and Duero systems, and by sharp  
336 knickpoints on the upper reach of the San Pedro river long profile when crossing the Santonian  
337 dolomites (Fig. 8). According to this whole set of observations, and in agreement with previous

338 findings of Pineda (1997) and Mikes (2010), we propose that the western part of the Rioja  
339 trough, in the Bureba area has been recently captured by the Ebro drainage network leading to  
340 a sequence of southwestward retreat of the main drainage divide, toward the Duero basin (Fig.  
341 7E).

342

343 A similar capture pattern can be observed further west in the continuity of the Bureba anticline  
344 (Fig. 5). The San Anton river shows a well-defined elbow of capture accompanied by a  
345 smoothed knickpoint (See Fig. S1 in the Supplement) at its junction with the Rudron river (Ebro  
346 tributary). The river course is highly incised toward the east, along the northern flank of the  
347 WNW – ESE anticline, almost connecting to the upper reach of the Ubierna river. Valley  
348 deposits are also observed in the continuity of the Ubierna valley, which former route is  
349 suggested by a wind gap (Fig. 5). However, this domain is no longer connected to its network  
350 as it is now wandered from the North by the Nava river, a tributary of the Moradillo river, which  
351 is a tributary of the Rudron river. This domain clearly records captures leading to divide  
352 migration toward the Duero, also in favor of the Ebro basin.

353

### 354 3.3 Past position of the Ebro-Duero divide and implication for stream-power of the Duero River

355

356 We used all observations that support divide migration in the Iberian Range and Rioja trough  
357 to estimate a paleo-position of the drainage divide between the Duero and Ebro drainage basins  
358 (Fig. 9). For this purpose, we considered the location of major knickpoint along the rivers where  
359 fluvial captures are defined. Both the Ebro river and several tributaries show high elevated ~10-  
360 20 km long flat domains at ~800 – 1200 m a.s.l. and major knickpoints in the upper reach of  
361 their long profiles as the Rudron, Queiles, and Alama rivers, as well as the Homino river and  
362 its tributaries: the Puerta Nogales and Valdelanelala rivers (Figs. 5, 8; Fig. S1). All these flat  
363 domains may not be related to surface uplift as they are not clearly associated with active  
364 tectonic features. The Duero basin being characterized by a high mean elevation (~1000 m) and  
365 by a very limited incision in the vicinity of the Ebro/Duero drainage divide, a sudden divide  
366 migration toward the Duero basin is then expected to isolate such high elevated and relatively  
367 preserved surfaces. We suggest these flat domains have been recently captured by Ebro  
368 tributaries, and represent remnants of Duero drainage areas, integrated into the Ebro catchment  
369 from divide retreat toward the Duero basin. Overall, we consider a paleodrainage divide  
370 delimited by these high-elevated knickpoints and flat domains, except for the Jiloca graben area  
371 to the southeast, characterized by the occurrence of short-lived endorheic domains (Fig. 9).

372 Incision in the Ebro basin leads to the capture of new drainage areas, whereas the Duero basin  
373 recorded important loss of its own surface. The present day drainage area of the Cenozoic Duero  
374 basin, upstream of the major knickzone observed to the west in the Iberian Massif is ~63000  
375 km<sup>2</sup>. We used the paleo-divide position shown in Figure 9 to define a « recent » captured area  
376 that used to belong to the Duero basin. This area represents ~7700 km<sup>2</sup>, which corresponds to  
377 ~12% of the present-day Cenozoic Duero basin drainage area. Such a reduction of the drainage  
378 area could have strong implications on the evolution of the Duero basin, as important lowering  
379 of water and sediment fluxes, and so of incision throughout the basin. To better resolve the  
380 impact of such drainage area reduction on incision capacity, we perform a stream power analysis  
381 of the Duero river. We consider the specific stream power,  $\omega$ , defined as  $\omega = \rho g Q S / W$ , where  
382  $\rho$  is water density,  $g$  is gravitational acceleration,  $Q$  is discharge,  $S$  is local river gradient, and  
383  $W$  is river width (see the Supplement for details of the calculation). We calculate  $\omega$  for the  
384 present-day Duero river, and for a restored ancient Duero river that drained this 12% of lost  
385 area. We plot the difference (ancient – present day) between the two curves in Figure 10, with  
386 the Duero river long profile. Calculated difference in specific stream power values are relatively  
387 low ( $< 2 \text{ W m}^{-2}$ ) for the upstream part of the basin, but increase to  $\sim 5 \text{ W m}^{-2}$  when approaching  
388 the major knickzone at a distance of  $\sim 350 \text{ km}$  from the river mouth. The knickzone is  
389 characterized by peak values exceeding  $10 \text{ W m}^{-2}$ , which rapidly decrease to  $\sim 0 \text{ W m}^{-2}$  at the  
390 base of the knickzone ( $\sim 200 \text{ km}$ ) and up to the river mouth (Fig. 10). Some alternating peak  
391 and null values are observed in the lower reach of the river and may be related to the occurrence  
392 of numerous dams along the river. Overall, the specific stream power calculated for the ancient  
393 Duero river show higher values than for the present day from the base of the knickzone to the  
394 uppermost reach of the river (Fig. 10). This implies a general decrease of the Duero river's  
395 incision capacity between this ancient state to the present day, magnified on the knickzone.

396

### 397 3.4 $\chi$ map

398

399 The comparison of the shape of longitudinal profiles of rivers across divide is a way that has  
400 been proposed recently to infer disequilibrium between rivers and the potential migration of  
401 their divide (Willett et al., 2014). The  $\chi$ -analysis of river profiles (Perron and Royden, 2012)  
402 is a powerful tool to evidence differences in the equilibrium state of rivers across divide, and  
403 then to infer their migration (Willett et al., 2014). . This method is based on a coordinate  
404 transformation allowing linearizing river profiles (Perron and Royden, 2012). Considering



405 constant uplift rate (U) and erodibility (K) in time and space the  $\chi$ -transformed profile of a river  
406 is defined by the following equation (Perron and Royden, 2012; Mudd et al., 2014):

407

$$408 \quad z(x) = z_b(x_b) + \left(\frac{U}{KA_0^m}\right)^{1/n} \chi$$

409

410 with

$$411 \quad \chi = \int_{x_b}^x \left(\frac{A_0}{A(x)}\right)^{\frac{m}{n}} dx$$

412 where  $z(x)$  is the elevation of the channel,  $x$  is the longitudinal distance,  $z_b$  is the elevation at  
413 the river's base level (distance  $x_b$ ),  $A$  is the drainage area,  $A_0$  is a reference drainage area, and  
414 exponents  $m$  and  $n$  are empirical constants.

415

416 When using the  $\chi$  variable instead of the distance for plotting the elevation  $z$  along channel, ( $\chi$ -  
417 plot), the longitudinal profile of a steady-state channel is shown as a straight line (Perron and  
418 Royden, 2012). Any channel pulled away from this line is in disequilibrium and is then expected  
419 to attempt to reach equilibrium. Mapping  $\chi$  on several watersheds and comparing  $\chi$  across  
420 drainage divides is then a potential way to high disequilibrium between rivers across divide and  
421 to elucidate divide migration and drainage reorganization through captures (Willett et al., 2014).  
422 We used the  $\chi$ -analysis Tool developed by Mudd et al. (2014) to select the best  $m/n$  ratio by  
423 iteration (Perron and Royden, 2012) and to calculate  $\chi$  for rivers throughout the divide between  
424 the Ebro and Duero basins from a similar base level at 850 m a.s.l. The best mean  $m/n$  ratio for  
425 all our streams is 0.425, which falls in the typical range of values observed for rivers ( $\sim 0.4 -$   
426  $0.6$ : e.g. Kirby and Whipple, 2012). The resulting map (Fig. 11) shows  $\chi$  values calculated on  
427 different opposite streams in the vicinity of the Ebro/Duero drainage divide. Similar values on  
428 both sides of the divide suggest the two opposite streams are at equilibrium, whereas strong  
429 contrasted  $\chi$  values imply disequilibrium leading to divide migration, continuously or through  
430 fluvial capture, toward the high  $\chi$  values (Willett et al., 2014). The map of  $\chi$  values actually  
431 shows significant contrasting values across the Ebro/Duero divide. We comment here these  
432 contrasts along the divide from the SE to the NW of the area considered (Fig. 11).

433 There is a strong contrast in  $\chi$  values between the headwater of the Jalon river (Fig. 11),  
434 characterized by low values ( $\sim 300$  m), and the closest part from the divide of the Bordecorex  
435 river (Fig. 4), a tributary of the Duero river ( $\sim 500$  m). Such a disequilibrium implies divide  
436 migration toward the Duero basin, predicting the capture of the uppermost reach of the

437 Bordecorex river by the Jalon river. To the north, tributaries of the Jalon river show slightly  
438 lower  $\chi$  values than the tributaries of the Duero river. This suggests a relative stable situation  
439 although small captures may occur toward the Duero basin. A higher contrast is observed  
440 around the easternmost part of the Duero basin, which is surrounded by the Ebro basin. The  
441 Araviana river (tributary of the Duero river) seems to be taken in a bottleneck between the  
442 Manubles river to the south and the Queiles river to the north (Fig. 4), which both show lower  
443  $\chi$  values (Fig. 11). Toward the east, there is a strongest  $\chi$  values contrast between headwaters  
444 of the Araviana river (>700 m) and of the Isuela (Jalon tributary) and Huecha rivers (<100 m).  
445 This domain appears clearly in disequilibrium and is expected to be captured by the Ebro  
446 drainage network. Such high  $\chi$  values differences appear also to the northwest (Fig. 11), in the  
447 southern part of the Cameros basin where the Duero river and its tributaries' headwaters show  
448  $\chi$  values >500-700 m, whereas the facing rivers (Alama, Cidacos, Iregua, and Najerilla) are all  
449 characterized by low  $\chi$  values <100 m. This predicts important disequilibrium and divide  
450 migration and fluvial captures toward the south. Northwestward,  $\chi$  values between Duero and  
451 Ebro network are more similar indicating that the divide is relatively more stable here, up to the  
452 westernmost part of the Ebro basin (Fig. 11). However, there are some slight localized  $\chi$  value  
453 contrasts (~200 / ~450 m) as observed between the Tiron and the Arlanzon rivers, between the  
454 Rudron and the Ubierna and Urbel rivers, and between the Ebro and the Pisuerga rivers (Fig.  
455 11). It suggests minor local captures toward the Duero basin.

456

457 To sum up,  $\chi$  values calculated in the vicinity of the drainage divide between the Ebro and  
458 Duero river networks show a general disequilibrium (Fig. 11) as the Ebro network is  
459 characterized by low  $\chi$  values (up to ~200-300 m) compared to those for the Duero network  
460 (up to ~450-700 m). In complement with all the evidence of divide displacements induced by  
461 captures described previously this allows predicting a general divide migration toward the  
462 Duero basin through headwater retreat, in favor of the Ebro tributaries, especially around the  
463 Almazan subbasin, which is expected to be entirely captured by the Ebro basin.

464

## 465 **4. Discussion**

466

### 467 4.1 Long term trend of divide migration

468

469 The oldest capture evidence in our study area corresponds to the incision of the northern part  
470 of the Iberian Range by the Jalon river and by the capture of the Calatayud basin, attributed to  
471 the post-Messinian (Gutiérrez-Santolalla et al. 1996). We propose, based on morphological  
472 evidence (Fig. 4) and in agreement with stratigraphic data (Gutiérrez-Santolalla et al. 1996),  
473 that the Jalon river system captured the Jiloca graben to the east since the Early Pleistocene,  
474 before progressively capturing the Almazan subbasin toward the west in the Holocene  
475 (Gutiérrez-Santolalla et al. 1996). From  $\chi$ -analysis (Fig. 11), we deduce that the eastern part of  
476 the Duero basin, the Almazan subbasin, is being actively captured by Ebro tributaries that  
477 drained the Iberian Range and the Cameros basin. Despite low contrasts in  $\chi$  values, local  
478 captures are also suggested in the vicinity of the Ebro / Duero drainage divide toward the  
479 northwest. Capture is further implied by the occurrence of numerous high elevated (~1000 m)  
480 knickpoints and low-relief surfaces (Figs. 5, 8, 9, 11).

481 Thus, there is a good correlation between  $\chi$  evidence and morphological and stratigraphic data  
482 implying long-lasting captures and divide migration during Pliocene, Pleistocene, and  
483 Holocene times in favor of the Ebro basin.

484

485 The pursuit of such a long-term capture trend may be driven by tectonic and/or climatic forcing  
486 (Willett, 1999; Montgomery et al., 2001; Sobel et al., 2003; Sobel and Strecker, 2003; Bonnet,  
487 2009; Whipple, 2009; Castelltort et al., 2012; Kirby and Whipple, 2012; Goren et al., 2015; Van  
488 der Beek et al., 2016). However, such long-term trend in drainage reorganization may also occur  
489 in tectonically quiescent domains, independently of external forcing (Prince et al., 2011). Here,  
490 the Iberian Range and the Cameros basin recorded extension pulses from the Late Miocene to  
491 the Early Pleistocene, responsible for the formation of several grabens as previously described  
492 (Gutiérrez-Santolalla et al., 1996; Capote et al., 2002). Extension events are also recorded  
493 during the Holocene, nevertheless, the youngest erosion surface of Late Pliocene-Early  
494 Pleistocene age observed in our study area shows no tectonic-related deformation and  
495 reworking, suggesting that tectonic activity is reduced here (Gutiérrez-Elorza and Gracia,  
496 1997). This is also consistent with the relative scarcity of seismic activity observed in our study  
497 area, compared, for instance, to the Pyrenees, or to the Betics (Herraiz et al., 2000; Lacan and  
498 Ortuño, 2012). We consequently propose that local tectonic activity is not the main driver of  
499 the capture histories documented here, as most capture events postdate the cessation of tectonic  
500 activity, and occur during periods of quiescence (Gutiérrez-Santolalla et al., 1996).

501

502 The Cameros Massif is characterized by relatively high mean annual precipitation up to ~1000  
503 mm/an (Fig. 6) with high elevation (~1400-2200 m) in comparison with the surrounding areas.  
504 This contrasts with the adjacent Ebro and Duero basins where low precipitation rates, of ~400-  
505 500 mm/an (Hijmans et al., 2005), illustrate subarid climate conditions. The Cameros area is  
506 the only place in our study area where a contrast in precipitation pattern (Fig. 6) would  
507 potentially drive a migration of the divide toward the drier, Duero area. Given that the same  
508 pattern is observed everywhere, even where there isn't any precipitation difference, we suggest  
509 that the present day climatic condition is unlikely to control the general pattern of current  
510 drainage reorganization between the Ebro and Duero basins. During the Pliocene and the  
511 Pleistocene, the climatic record in the northern Iberia Peninsula is characterized by alternations  
512 between similar subarid conditions and intense glaciation. Paleoclimate proxies do not allow to  
513 highlight past precipitation differences along the divide that could explain past drainage  
514 reorganization. Moreover, there is no clear evidence of important glacier development and  
515 related erosion in our study area, especially for the Cameros basin and the Iberian Range  
516 (Ortigosa, 1994; García-Ruiz et al., 1998, 2016; Pellicer and Echeverría, 2004). This indicates  
517 that drainage evolution between the Ebro and Duero basins is unlikely to be related to climatic  
518 evolution.

519

520 4.2 Excavation of the Ebro basin as the main factor controlling divide migration and limiting  
521 incision of the Duero river

522

523 A striking morphological feature for river capture in our study area is the important contrast in  
524 the incision pattern (e.g. Fig. 1B) from one side of the divide to the other. This suggests that the  
525 incision capacity of the river network is the main driver for capture and divide migration. Both  
526 tectonic and climatic forcing does not appear to control drainage reorganization between the  
527 Ebro and Duero basins.

528 The opening of the Ebro basin toward the Mediterranean Sea during the Late Miocene led to  
529 widespread excavation (García-Castellanos et al., 2003, García-Castellanos and Larrasoña,  
530 2015), favored by more humid and seasonal climatic conditions (Calvo et al., 1993; Alonso-  
531 Zarza and Calvo, 2000). By contrast, incision related to the opening of the Duero basin toward  
532 the Atlantic Ocean is concentrated to the west in the Iberian Massif, characterized by a  
533 largescale knickzone (150 km long and 500 m high) in the Duero river long profile (Fig. 1B).  
534 This contrasts with the limited eastward propagation of incision in the Cenozoic part of the  
535 basin (Antón et al., 2012, 2014), despite climatic conditions similar to the Ebro basin. An

536 explanation resides in the fact that the resistant Iberian Massif basement rocks may have  
537 controlled and limited incision and drainage reorganization in the Cenozoic Duero basin (Antón  
538 et al., 2012). The Duero profile upstream of this major knickzone may be considered as a high  
539 elevated local base level for its tributaries there. Difference between the Ebro and Duero base-  
540 levels implies a major contrast in fluvial dynamics. We suggest the systematic and long-term  
541 trend of divide migration toward the Duero basin and fluvial capture in favor of the Ebro basin  
542 is driven by the differential incision behavior, controlled by base-level difference.

543 Our stream power analysis along the Duero river (Fig. 10) shows that the difference in drainage  
544 area of the Duero inferred from our paleo-divide map (Fig. 9) induces a noticeable decrease of  
545 stream power values of the Duero in the vicinity of the knickzone. This stream power is a  
546 minimum estimate because calculation does not take into account possible captures and divide  
547 migration in other areas along the Duero basin divide, nor the full history of the divide migration  
548 through time and the related ongoing decrease in water discharge as documented in laboratory-  
549 scale landscape experiments (Bonnet, 2009). Some contrasts of incision are also observed in  
550 the Iberian Range along the southern border of the Duero, and in the Cantabrian domain to the  
551 North. Both show more important incision than in the Duero basin, suggesting potential river  
552 captures and divide migration at the expense of the Duero basin, increasing the total of lost  
553 drainage area. Even if it gives minimal estimate, our stream power analysis suggests that  
554 drainage area reduction may have limited the erosion in the Duero basin. This provides an  
555 explanation for the preservation of the lithologic barrier to the west, along the main knickzone  
556 of the Duero considered as an intermediate, local base level (Antón et al., 2012). We propose  
557 that the reduction of the Duero drainage area caused by captures and incision in the Ebro basin,  
558 is responsible for a significant decrease of the incision capacity in the Duero basin. We infer  
559 that the ongoing drainage network growth in the Ebro basin may be responsible for the current  
560 preservation of large morphological relicts of the-endorheic stage in the Duero basin.

561 The opening of the Ebro basin toward the Mediterranean Sea resulted in a drastic base level  
562 drop. This results in the establishment of an upstream-migrating incision wave that propagates  
563 to every tributary of the Ebro network, responsible for knickpoints migration (Schumm et al.,  
564 1987; Whipple and Tucker, 1999; Yanites et al., 2013) and for drainage reorganization and  
565 divide migration. The  $\chi$ -analysis that we performed along the current Ebro-Duero divide (Fig.  
566 11) highlights areas where geomorphic disequilibrium is still ongoing, which suggests that they  
567 are areas where divide is currently mobile. The modelling study performed by Garcia-  
568 Castellanos and Larrasoña (2015) suggests that the re-opening of the Ebro basin occurred  
569 between 12.0 and 7.5 Ma. This indicates that the growth of the drainage network of the Ebro

570 basin and the establishment of new steady-state conditions is a long-lived phenomenon, which  
571 is still not achieved today.

572

## 573 **Conclusion**

574

575 In this paper we present a morphometric analysis of the landscape along the divide between the  
576 Ebro and Duero drainage basins located in the northern part of the Iberian Peninsula. This area  
577 shows numerous evidence of river captures by the Ebro drainage network resulting in a long-  
578 lasting migration of their divide, toward the Duero basin. Although these two basins record a  
579 similar geological history, with a long endorheic stage during Oligocene and Miocene times,  
580 they show a very contrasted incision and preservation state of their original endorheic  
581 morphology. Since the Late Miocene, the Ebro basin was opened to the Mediterranean Sea and  
582 record important erosion. On the opposite, the Duero was opened to the Atlantic Ocean since  
583 the Late Miocene – Early Pliocene but its longitudinal profile exhibits a pronounced knickpoint,  
584 which delimits an upstream domain of low relief and limited incision, likely representing a  
585 relict of its endorheic topography. We propose that this contrast of incision is the main driver  
586 of the migration of divide that we document. The morphological analysis of rivers across the  
587 divide highlights areas where geomorphic disequilibrium is still ongoing, which suggests that  
588 the Ebro-Duero divide is currently mobile. The quantification of the decrease of the drainage  
589 area of the Duero based on the reconstruction of a paleo-position of the Ebro-Duero divide  
590 shows that the divide migration results in a significant lowering of the stream power of the  
591 Duero river, particularly along its knickzone. We suggest that divide migration induces a  
592 decrease of the incision capacity of the Duero river, thus favoring the preservation of large  
593 relicts of the endorheic morphology in the upstream part of this basin.

594

595

## 596 **Author contributions**

597 AV undertook morphometric modeling and interpretation, and wrote the paper. SB and FM  
598 contributed to the interpretation and the writing.

599

600

## 601 **Competing interests.**

602 The authors declare that they have no conflict of interest.

603

604 Acknowledgements.

605 This study was funded by the OROGEN Project, a TOTAL-BRGM-CNRS consortium. We  
606 thank two reviewers and associated Editor Veerle Vanacker for very useful and constructive  
607 comments that greatly helped us to clarify and improve this manuscript.

608

609

610 References

611

612 Alonso-Zarza, A. M. and Calvo, J. P.: Palustrine sedimentation in an episodically subsiding  
613 basin: the Miocene of the northern Teruel Graben (Spain), *Palaeogeol., Palaeoclimatol.,*  
614 *Palaeoecol.*, 160, 1-21, 2000.

615

616 Alonso-Zarza, A. M., Armenteros, I., Braga, J. C., Muñoz, A., Pujalte, V., Ramos, E., Aguirre,  
617 J., Alonso-Gavilán, G., Arenas, C., Ignacio Baceta, J., Carballeira, J., Calvo, J. P., Corrochano,  
618 A., Fornós, J. J., González, A., Luzón, A., Martín, J. M., Pardo, G., Payros, A., Pérez, A., Pomar,  
619 L., Rodríguez, J. M., and Villena, J.: Tertiary, in: *The Geology of Spain*, Gibbons, W. and  
620 Moreno, T. (Eds.): The Geological Society, London, 293-334, 2002.

621

622 Antón, L., Rodés, A., De Vicente, G., Pallàs, R., Garcia-Castellanos, D., Stuart, F. M., Braucher,  
623 R., and Bourlès, D.: Quantification of fluvial incision in the Duero Basin (NW Iberia) from  
624 longitudinal profile analysis and terrestrial cosmogenic nuclide concentrations, *Geomorph.*,  
625 165-166, 50-61, <https://doi.org/10.1016/j.geomorph.2011.12.036>, 2012.

626

627 Antón, L., Rodés, A., De Vicente, G., and Stokes, M.: Using river long profiles and geomorphic  
628 indices to evaluate the geomorphological signature of continental scale drainage capture, Duero  
629 basin (NW Iberia), *Geomorph.*, 206, 250-261, <https://doi.org/10.1016/j.geomorph.2013.09.028>,  
630 2014.

631

632 Babault, J., Loget, N., Van Den Driessche, J., Castelltort, S., Bonnet, S., and Davy, P.: Did the  
633 Ebro basin connect to the Mediterranean before the Messinian salinity crisis ?, *Geomorph.*, 81,  
634 155-165, <https://doi.org/10.1016/j.geomorph.2006.04.004>, 2006.

635

636 Barrón, E., Postigo-Mijarra, J. M., and Casas-Gallego, M.: Late Miocene vegetation and climate  
637 of the La Cerdanya Basin (eastern Pyrenees, Spain), *Rev. Palaeobot. Palynol.*, 235, 99-119,  
638 <https://doi.org/10.1016/j.revpalbo.2016.08.007>, 2016.

639

640 Bartolomé, M., Sancho, C., Moreno, A., Oliva-Urcia, B., Belmonte, Á., Bastida, J., Cheng, H.,  
641 and Edwards, R. L.: Upper Pleistocene interstratal piping-cave speleogenesis: The Seso Cave  
642 System (Central Pyrenees, Northern Spain), *Geomorph.*, 228, 335-344,  
643 <https://doi.org/10.1016/j.geomorph.2014.09.007>, 2015.

644

645 Bessais, E. and Cravatte, J.: Les écosystèmes végétaux Pliocènes de Catalogne Méridionale.  
646 Variations latitudinales dans le domaine Nord-Ouest Méditerranéen, *Geobios*, 21, 49-63, 1988.

647

648 Bond, J.: Tectono-sedimentary evolution of the Almazan Basin, NE Spain, in: Friend, F. and  
649 Dabrio, C. (Eds.): *Tertiary Basins of Spain: the Stratigraphic Record of Crustal Kinematics,*  
650 *World and Regional Geology*, 6, Cambridge University Press, Cambridge, 203-213, 1996.

651

652 Bonnet, S.: Shrinking and splitting of drainage basins in orogenic landscapes from the migration  
653 of the main drainage divide, *Nat. Geosc.*, 90, 766-771, <https://doi.org/10.1038/NGEO666>,  
654 2009.

655

656 Brocklehurst, S. H. and Whipple, K. X.: Glacial erosion and relief production in the Eastern  
657 Sierra Nevada, California, *Geomorph.*, 42, 1-24, 2002.

658

659 Calvo, J. P., Daams, R., and Morales, J.: Up-to-date Spanish continental Neogene synthesis and  
660 paleoclimatic interpretation. *Revista de la Sociedad Geologica de España*, 6, 29-40, 1993.

661

662 Cameselle, A.J., Urgeles, R., De Mol, B., Camerlenghi, A., and Canning, J.C., Late Miocene  
663 sedimentary architecture of the Ebro Continental Margin (Western Mediterranean; Implications  
664 for the Messinian Salinity Crisis. *Int. J. Earth Sci.*, 103, 423-440, 2014.

665

666 Capote, R., Muñoz, J. A., Simón, J. L., Liesa, C. L., and Arlegui, L. E.: Alpine tectonics 1: the  
667 Alpine system north of the Betic Cordillera, in: *The Geology of Spain*, Gibbons, W. and  
668 Moreno, T. (Eds.): *The Geological Society*, London, 367-400, 2002.

669



670 Castellort, S., Goren, L., Willett, S. D., Champagnac, J. D., Herman, F., and Braun, J.: River  
671 drainage patterns in the New Zealand Alps primarily controlled by plate tectonic strain. *Nat.*  
672 *Geosci.*, 5, 744–748, <https://doi.org/10.1038/ngeo1582>, 2012.

673

674 Colomer i Busquets, M., and Santanach i Prat, P.: Estructura y evolucion del borde sur-  
675 occidental de la Fosa de Calatayud-Daroca, *Geogaceta*, 4, 29-31, 1988.

676

677 Coney, P. J., Muñoz, J. A., McClay, K. R., and Evenchick, C. A.: Syntectonic burial and post-  
678 tectonic exhumation of the southern Pyrenees foreland fold-thrust belt, *J. Geol. Soc. London*,  
679 153, 9-16, <https://doi.org/10.1144/gsjgs.153.1.0009>, 1996.

680

681 Costa, E., Garcés, M., López-Blanco, M., Beamud, E., Gómez-Paccard, M., and Larrasoaña, J.  
682 C.: Closing and continentalization of the South Pyrenean foreland basin (NE Spain):  
683 magnetochronological constraints, *Basin Res.*, 22, 904-917, <https://doi.org/10.1111/j.1365->  
684 [2117.2009.00452.x](https://doi.org/10.1111/j.1365-2117.2009.00452.x), 2010.

685

686 Delmas, M., Calvet, M., and Gunnell, Y.: Variability of Quaternary glacial erosion rates – A  
687 global perspective with special reference to the Eastern Pyrenees, *Quat. Sci. Rev.*, 28, 484-498,  
688 <https://doi.org/10.1016/j.quascirev.2008.11.006>, 2009.

689

690 Del Rio, P., Barbero, L., and Stuart, F. M.: Exhumation of the Sierra de Cameros (Iberian Range,  
691 Spain): constraints from low-temperature thermochronologie, in: Liesker, F., Ventura, B., and  
692 Glasmacher, U. A. (Eds.): *Thermochronological Methods: From Palaeotemperature Constraints*  
693 *to Landscape Evolution Models*, Geological Society, London, Special Publications, 324, 154-  
694 166, <https://doi.org/10.1144/SP324.12>, 2009.

695

696 De Vicente, G., Vegas, R., Muñoz, M. A., Silva, P. G., Andriessen, P., Cloetingh, S., González-  
697 Casado, J. M., Van Wees, J. D., Álvarez, J., Carbó, A., and Olaiz, A.: Cenozoic thick-skinned  
698 deformation and topography evolution of the Spanish Central System, *Glob. Planet. Change*,  
699 58, 335-381, <https://doi.org/10.1016/j.gloplacha.2006.11.042>, 2007.

700

701 Duval, M., Sancho, C., Calle, M., Guilarte, V., and Peña-Monné, J. L.: On the interest of using  
702 the multiple center approach in ESR dating of optically bleached quartz grains: Some examples

703 from the Early Pleistocene terraces of the Alcanadre River (Ebro basin, Spain), *Quat.*  
704 *Geochronol.*, 29, 58-69, <https://doi.org/10.1016/j.quageo.2015.06.006>, 2015.

705

706 Fillon, C. and Van der Beek, P.: Post-orogenic evolution of the southern Pyrenees: constraints  
707 from inverse thermo-kinematic modelling of low-temperature thermochronology data, *Basin*  
708 *Res.*, 23, 1-19, <https://doi.org/10.1111/j.1365-2117.2011.00533.x>, 2012.

709

710 Fillon, C., Gautheron, C., and Van der Beek, P.: Oligocene-Miocene burial and exhumation of  
711 the Southern Pyrenean foreland quantified by low-temperature thermochronology, *J. Geol. Soc.*  
712 *London*, 170, 67-77, <https://doi.org/10.1144/jgs2012-051>, 2013.

713

714 Garcia-Castellanos, D.: Long-term evolution of tectonic lakes: Climatic controls on the  
715 development of internally drained basins, *Geol. Soc. Am., Spec. Paper*, 398, 283-294,  
716 [https://doi.org/10.1130/2006.2398\(17\)](https://doi.org/10.1130/2006.2398(17)), 2006.

717

718 Garcia-Castellanos, D. and Larrasoaña, J. C.: Quantifying the post-tectonic topographic  
719 evolution of closed basins: The Ebro basin (northeast Iberia), *Geology*, 43, 663-666,  
720 <https://doi.org/10.1130/G36673.1>, 2015.

721

722 Garcia-Castellanos, D., Vergés, J., Gaspar-Escribano, J., and Cloething, S.: Interplay between  
723 tectonics, climate, and fluvial transport during the Cenozoic evolution of the Ebro Basin (NE  
724 Iberia), *J. Geophys. Res.*, 108, 2347, <https://doi.org/10.1029/2002JB002073>, 2003.

725

726 García-Ruiz, J. M., Ortigosa, L. M., Pellicer, F., and Arnáez, J.: Geomorfología glaciar del  
727 Sistema Ibérico, in: Gómez-Ortiz, A. and Pérez-Alberti, A. (Eds.): *Las huellas glaciares de las*  
728 *montañas españolas*, Universidad de Santiago de Compostela, 347-381, 1998.

729

730 García-Ruiz, J. M., Palacios, D., González-Sampériz, P., De Andrés, N., Moreno, A., Valero-  
731 Garcés, B., and Gómez-Villar, A.: Mountain glacier evolution in the Iberian Peninsula during  
732 the Younger Dryas, *Quat. Sci. Rev.*, 138, 16-30,  
733 <https://doi.org/10.1016/j.quascirev.2016.02.022>, 2016.

734

735 Goren, L., Castellort, S., and Klinger, Y.: Modes and rates of horizontal deformation from  
736 rotated river basins: Application to the Dead Sea fault system in Lebanon, *Geology*, 43, 843-  
737 846, <https://doi.org/10.1130/G36841.1>, 2015.

738

739 Gracia, F. J.: Tectonica pliocena de la Fosa de Daroca (prov. De Zaragoza), *Geogaceta*, 11, 127-  
740 129, 1992.

741

742 Gracia, F. J.: Evolucion cuaternaria del rio Jiloca (Cordillera Iberica Central), in: Fumanal, M.  
743 P. and Bernabeu, J. (Eds.): *Estudios sobre Cuaternario, Medios Sedimentarios, Cambios*  
744 *Ambientales, Habitat Humano*, Valencia, 43-51, 1993a.

745

746 Gracia, F. J.: Evolucion geomorfologica de la region de Gallocanta (Cordillera Iberica Central),  
747 *Geographicalia*, 30, 3-17, 1993b.

748

749 Gracia, F. J., Gutiérrez-Santolalla, F., and Gutiérrez-Elorza, M.: Evolucion geomorfologica del  
750 polje de Gallocanta (Cordillera Ibérica), *Revista Sociedad Geologica de España*, 12, 351-368,  
751 1999.

752

753 Gracia, F. J. and Cuchi, J. A.: Control tectonico de los travertinos fluviales del rio Jiloca  
754 (Cordillera Ibérica), in: *El Cuaternario en España y Portugal, Actas 2a Reun. Cuat. Ibérico,*  
755 *AEQUA y CTPEQ*, Madrid-1989, 2, 697-706, 1993.

756

757 Guimerà, J., Mas, R., and Alonso, Á: Intraplate deformation in the NW Iberian Chain: Mesozoic  
758 extension and Tertiary contractional inversion, *J. Geol. Soc. London*, 161, 291-303,  
759 <https://doi.org/10.1144/0016-764903-055>, 2004.

760

761 Gutiérrez-Elorza, M. and Gracia, F. J.: Environmental interpretation and evolution of the  
762 Tertiary erosion surfaces in the Iberian Range (Spain), in: Widdowson, M. (Ed.):  
763 *Palaeosurfaces: Recognition, Reconstruction and Palaeoenvironmental Interpretation,*  
764 *Geological Society Special Publication*, 120, 147-158, 1997.

765

766 Gutiérrez-Elorza, M., García-Ruiz, J. M., Goy, J. L., Gracia, F. J., Gutiérrez-Santolalla, F.,  
767 Martí, C., Martín-Serrano, A., Pérez-González, A., and Zazo, C.: Quaternary, in: *The Geology*  
768 *of Spain*, Gibbons, W. and Moreno, T. (Eds.): *The Geological Society*, London, 335-366, 2002.

769

770 Gutiérrez-Santolalla, F., Gracia, F. J., and Gutiérrez-Elorza, M.: Consideraciones sobre el final  
771 del relleno endorreico de las fossa de Calatayud y Teruel y su paso al exorreismo. Implicaciones  
772 morfoestratigráficas y estructurales, in : Grandal d'Ánglade, A. and Pagés-Valcarlos, J. (Eds.) :  
773 IV Reunion de Geomorfología, Sociedad Española de Geomorfología, O Castro (A Coruña),  
774 23-43, 1996.

775

776 Herraiz, M., De Vicente, G., Lindo-Ñaupari, R., Giner, J., Simón, J. L., González-Casado, J.  
777 M., Vadillo, O., Rodríguez-Pascua, M. A., Cicuéndez, J. I., Casas, A., Cabañas, L., Rincón, P.,  
778 Cortés, A. L., Ramírez, M., and Lucini, M.: *Tectonics*, 19, 762-786, 2000.

779

780 Hijmans, R. J., Cameron, S. E., Parra, J. L., Jones, P. G., and Jarvis, A.: Very high resolution  
781 interpolated climate surfaces for global land areas, *Int. J. Climatol.*, 25, 1965-1978,  
782 <https://doi.org/10.1002/joc.1276>, 2005.

783

784 Jiménez-Moreno, G., Fauquette, S., and Suc, J. P.: Miocene to Pliocene vegetation  
785 reconstruction and climate estimates in the Iberian Peninsula from pollen data, *Rev. Palaeobot.*  
786 *Palynol.*, 162, 403-415, <https://doi.org/10.1016/j.revpalbo.2009.08.001>, 2010.

787

788 Jiménez-Moreno, G., Burjachs, F., Expósito, I., Oms, O., Carrancho, Á., Villalaín, J. J., Agustí,  
789 J., Campeny, G., Gómez de Soler, B., and Van der Made, J.: Late Pliocene vegetation and  
790 orbital-scale climate changes from the western Mediterranean area, *Global Planet. Change*, 108,  
791 15-28, <https://doi.org/10.1016/j.gloplacha.2013.05.012>, 2013.

792

793 Jurado, M. J. and Riba, O.: The Rioja area (westernmost Ebro basin): a ramp valley with  
794 neighbouring piggybacks, in: Friend, P. and Dabrio, C. (Eds.): *Tertiary basins of Spain*, *World*  
795 *and Regional Geology*, 6, Cambridge University Press, Cambridge, 173-179, 1996.

796

797 Kirby, E. and Whipple, K. X.: Expression of active tectonics in erosional landscapes, *J. Struct.*  
798 *Geol.*, 44, 54-75, <https://doi.org/10.1016/j.jsg.2012.07.009>, 2012.

799

800 Kuhlemann, J., Frisch, W., Dunkl, I., Székely, D., and Spiegel, C.: Miocene shifts of the  
801 drainage divide in the Alps and their foreland basin, *Z. Geomorph.*, 45, 239-265, 2001.

802

803 Lacan, P. and Ortuño, M.: Active tectonics of the Pyrenees: a review, *J. Iberian Geol.*, 38, 9-30,  
804 [https://doi.org/10.5209/rev\\_JIGE.2012.v38.n1.39203](https://doi.org/10.5209/rev_JIGE.2012.v38.n1.39203), 2012.

805

806 Larrasoña, J. C., Murelaga, X., and Garcés, M.: Magnetobiochronology of Lower Miocene  
807 (Ramblian) continental sediments from the Tuleda Formation (western Ebro basin, Spain), *Ea.*  
808 *Planet. Sci. Lett.*, 243, 409-423, <https://doi.org/10.1016/j.epsl.2006.01.034>, 2006.

809

810 López-Blanco, M., Marzo, M., Burbank, D. W., Vergés, J., Roca, E., Anadón, P., and Piña, J.:  
811 Tectonic and climatic controls on the development of foreland fan deltas: Montserrat and Sant  
812 Llorenç del Munt systems (Middle Eocene, Ebro Basin, NE Spain), *Sediment. Geol.*, 138, 17-  
813 39, 2000.

814

815 López-Martínez, N., García-Moreno, E., and Álvarez-Sierra, A.: Paleontología y  
816 bioestratigrafía (micromamíferos) del Mioceno medio y superior del sector central de la cuenca  
817 del Duero, *Studia Geologica Salmanticensia*, Ediciones Universidad Salamanca, 22, 191-212,  
818 1986.

819

820 Martín-Chivelet, J., Berástegui, X., Rosales, I., Vilas, L., Vera, J. A., Caus, E., Gräfe, K. U.,  
821 Mas, R., Puig, C., Segura, M., Robles, S., Floquet, M., Quesada, S., Ruiz-Ortiz, P. A., Fregenal-  
822 Martínez, M. A., Salas, R., Arias, C., García, A., Martín-Algarra, A., Meléndez, M. N., Chacón,  
823 B., Molina, J. M., Sanz, J. L., Castro, J. M., García-Hernández, M., Carenas, B., García-  
824 Hidalgo, J., Gil, J., and Ortega, F.: Cretaceous, in: *The Geology of Spain*, Gibbons, W. and  
825 Moreno, T. (Eds.): The Geological Society, London, 255-292, 2002.

826

827 Martín-Serrano, A.: La definición y el encajamiento de la red fluvial actual sobre el macizo  
828 hesperico en el marco de su geodinamica alpina, *Rev. Soc. Geol. España*, 4, 337-351, 1991.

829

830 Mikeš, D.: The Upper Cenozoic evolution of the Duero and Ebro fluvial systems (N-Spain):  
831 Part 1. Paleogeography; Part 2. Geomorphology, *Cent. Eur. J. Geosci.*, 2, 320-332,  
832 <https://doi.org/10.2478/v10085-010-0017-4>, 2010.

833

834 Montgomery, D. R., Balco, G., and Willett, S. D.: Climate, tectonics, and the morphology of  
835 the Andes, *Geology*, 29, 579-582, 2001.

836

837 Moreno, D., Falguères, C., Pérez-González, A., Duval, M., Voinchet, P., Benito-Calvo, A.,  
838 Ortega, A. I., Bahain, J. J., Sala, R., Carbonell, E., Bermúdez de Castro, J. M., and Arsuaga, J.  
839 L.: ESR chronology of alluvial deposits in the Arlanzon valley (Atapuerca, Spain):  
840 Contemporaneity with Atapuerca Gran Dolina site, *Quat. Geochronol.*, 10, 418-423,  
841 <https://doi.org/10.1016/j.quageo.2012.04.018>, 2012.

842

843 Moreno, D., Belmonte, A., Bartolomé, M., Sancho, C., Oliva, C., Stoll, H., Edwards, L. R.,  
844 Cheng, H., and Hellstrom, J.: Formacion de espeleotemas en el noreste peninsular y su relacion  
845 con las condiciones climaticas durante los ultimos ciclos glaciares, *Cuadernos de Investigacion*  
846 *Geografica*, 39, 25-47, 2013.

847

848 Mudd, S., Attal, M., Milodowski, D. T., Grieve, S. W. D., and Valters, D. A.: A statistical  
849 framework to quantify spatial variation in channel gradients using the integral method of  
850 channel profile analysis, *J. Geophys. Res.- Earth Surf.*, 119, 138-152,  
851 <https://doi.org/10.1002/2013JF002981>, 2014.

852

853 Muñoz-Jiménez, A. and Casas-Sainz, A. M.: The Rioja Trough (N Spain): tectonosedimentary  
854 evolution of a symmetric foreland basin, *Basin Res.*, 9, 65-85, 1997.

855

856 Nivière, B., Lacan, P., Regard, V., Delmas, M., Calvet, M., Huyghe, D., and Roddaz, B.:  
857 Evolution of the Late Pleistocene Aspe River (Western Pyrenees, France). Signature of climatic  
858 events and active tectonics, *Comptes Rendus Geosci.*, 348, 203-212, <https://doi.org/10.1016/j.crte.2015.07.003>, 2016.

859

860

861 Ortigosa, L. M.: Las grandes unidades des relieve, *Geografia de la Rioja*, 1, 62-71, 1994.

862

863 Palacios, D., De Marcos, J., and Vásquez-Selem, L.: Last Glacial Maximum and deglaciation  
864 of the Sierra de Gredos, central Iberian Peninsula, *Quat. Int.*, 233, 16-26,  
865 <https://doi.org/10.1016/j.quaint.2010.04.029>, 2011.

866

867 Palacios, D., Andrés, N., De Marcos, J., and Vásquez-Selem, L.: Maximum glacial advance and  
868 deglaciation of the Pinar Valley (Sierra de Gredos, Central Spain) and its significance in the  
869 Mediterranean context, *Geomorph.*, 177-178, 51-61,  
870 <https://doi.org/10.1016/j.geomorph.2012.07.013>, 2012.

871

872 Pellicer, F. and Echeverría, M. T.: El modelado glaciar y periglacial en el macizo del moncayo,  
873 in: Peña, J. L., Longares, L. A., and Sánchez, M. (Eds.): Geografía Física de Aragón, Aspectos  
874 generals y tematicos, Universidad de Zaragoza e Institucion Fernando el Catolico, Zaragoza,  
875 173-185, 2004.

876

877 Pérez-Rivarés, F. J., Garcés, M., Arenas, C., and Pardo, G.: Magnetocronologia de la sucesion  
878 Miocena de la Sierra de Alcubierre (sector central de la cuenca del Ebro), Rev. Soc. Geol.  
879 España, 15, 217-231, 2002.

880

881 Pérez-Rivarés, F. J., Garcés, M., Arenas, C., and Pardo, G.: Magnetostratigraphy of the Miocene  
882 continental deposits of the Montes de Castejon (central Ebro basin, Spain): geochronological  
883 and paleoenvironmental implications, Geologica Acta, 2, 221-234, 2004.

884

885 Perron, J. T. and Royden, L.: An integral approach to bedrock river profile analysis. Earth Surf.  
886 Process. Landforms, 38, 570–576, <https://doi.org/10.1002/esp.3302>, 2012.

887

888 Pineda Velasco, A.: Montorio. Mapa geologico de España; escala 1:50.000; Segunda serie.  
889 Instituto Geologico y Minero de España (IGME), Madrid, pp. 110, 1997.

890

891 Prince, P. S., Spotila, J. A., and Henika, W. S.: Stream capture as driver of transient landscape  
892 evolution in a tectonically quiescent setting, Geology, 39, 823–826,  
893 <https://doi.org/10.1130/G32008.1>, 2011.

894

895 Puigdefàbregas, C., Muñoz, J. A., and Vergés, J.: Thrusting and foreland basin evolution in the  
896 Southern Pyrenees, in: Thrust Tectonics, McClay, K.R. (Ed.): Chapman & Hall, London, 247-  
897 254, 1992.

898

899 Pulgar, J. A., Alonso, J. L., Espina, R. G., and Marín, J. A.: La deformacion alpine en el  
900 basamento varisco de la Zona Cantabrica, 283-294, 1999.

901

902 Riba, O., Reguant, S., and Villena, J.: Ensayo de sintesis estratigrafica y evolutiva de la Cuenca  
903 terciaria del Ebro, in: Comba, J. A. (Ed.): Geologia de España, 2, Libro Jubila J. M. Rios,  
904 Instituto Geologico y Minero de España, Madrid, 131-159, 1983.

905

906 Rivas-Carballo, M. R., Alonso-Gavilán, G., Valle, M. F., and Civis, J.: Miocene Palynology of  
907 the central sector of the Duero Basin (Spain) in relation to palaeogeography and  
908 palaeoenvironment, *Rev. Palaeobot. Palynol.*, 82, 251-264, 1994.

909

910 Salas, R., Guimerà, J., Mas, R., Martín-Closas, C., Meléndez, A., and Alonso, A.: Evolution of  
911 the Mesozoic Central Iberian Rift System and its Cainozoic inversion (Iberian Chain), in:  
912 Ziegler, P. A., Cavazza, W., Robertson, A. F. H., and Crasquin-Soleau, S. (Eds.): Peri-Tethys  
913 Memoir 6: Peri-Tethyan Rift/Wrench Basins and Passive Margins. *Mémoires du Muséum  
914 national d'Histoire naturelle*, 186, 145-185, 2001.

915

916 Sancho, C., Calle, M., Peña-Monné, J. L., Duval, M., Oliva-Urcia, B., Pueyo, E. L., Benito, G.,  
917 and Moreno, A.: Dating the Earliest Pleistocene alluvial terrace of the Alcanadre River (Ebro  
918 Basin, NE Spain): Insights into the landscape evolution and involved processes, *Quat. Int.*, 407,  
919 86-95, <https://doi.org/10.1016/j.quaint.2015.10.050>, 2016.

920

921 Schumm, S. A., Mosley, M. P., and Weaver, W. E.: *Experimental fluvial geomorphology*, John  
922 Wiley and Sons, New York, pp. 413, 1987.

923

924 Schwanghart, W. and Scherler, D.: TopoToolbolx 2 a MATLAB-based software for topographic  
925 analysis and modeling in Earth surface sciences, *Earth Surf. Dynamics*, 2, 1-7,  
926 <https://doi.org/10.5194/esurf-2-1-2014>, 2014.

927

928 Serrano, E., González-Trueba, J. J., Pellitero, R., González-García, M., and Gómez-Lende, M.:  
929 Quaternary glacial evolution in the Central Cantabrian Mountains (Northern Spain),  
930 *Geomorph.*, 196, 65-82, <https://doi.org/10.1016/j.geomorph.2012.05.001>, 2013.

931

932 Serrano, E., González-Trueba, J. J., Pellitero, R., Gómez-Lende, M.: Quaternary glacial history  
933 of the Cantabrian Mountains of northern Spain: a new synthesis, in: Hughes, P. D. and  
934 Woodward, J. C. (Eds.): *Quaternary Glaciation in the Mediterranean Mountains*, Geological  
935 Society, London, Special Publications, 433, <https://doi.org/10.1144/SP433.8>, 2016.

936



937 Sobel, E. R. and Strecker, M. R.: Uplift, exhumation and precipitation: tectonic and climatic  
938 control of Late Cenozoic landscape evolution in the northern Sierras Pampeanas, Argentina,  
939 Basin Res., 15, 431-451, <https://doi.org/10.1046/j.1365-2117.2003.00214.x>, 2003.  
940

941 Sobel, E. R., Hilley, G. E., and Strecker, M. R.: Formation of internally drained contractional  
942 basins by aridity-limited bedrock incision, J. Geophys. Res., 108, 2344,  
943 <https://doi.org/10.1029/2002JB001883>, 2003.  
944

945 Stange, K. M., Van Balen, R. T., Garcia-Castellanos, D., and Cloething, S.: Numerical  
946 modelling of Quaternary terrace staircase formation in the Ebro foreland basin, southern  
947 Pyrenees, NE Iberia, Basin Res., 1-23, <https://doi.org/10.1111/bre.12103>, 2014.  
948

949 Suc, J. P. and Popescu, S. M.: Pollen records and climatic cycles in the Mediterranean region  
950 since 2.7 Ma, in: Head, M. J. and Gibbard, P. L. (Eds.): Early-Middle Pleistocene Transitions,  
951 the Land-Ocean Evidence, Geological Society, London, Special Publications, 247, 147-158,  
952 <https://doi.org/10.1144/GSL.SP.2005.247.01.08>, 2005.  
953

954 Urgeles, R., Camerlenghi, A., Garcia-Castellanos, D., De Mol, B., Garcés, M., Vergés, J.,  
955 Haslam, I., and Hardman, M.: New constraints on the Messinian sealevel drawdown from 3D  
956 seismic data of the Ebro Margin, western Mediterranean, Basin Res., 23, 123-145,  
957 <https://doi.org/10.1111/j.1365-2117.2010.00477.x>, 2010.  
958

959 Van der Beek, P., Litty, C., Baudin, M., Mercier, J., Robert, X., and Hardwick, E.: Contrasting  
960 tectonically driven exhumation and incision patterns, Western versus central Nepal Himalaya,  
961 Geology, 44, 327-330, <https://doi.org/10.1130/G37579.1>, 2016.  
962

963 Vázquez-Urbez, M., Arenas, C., Pardo, G., and Pérez-Rivarés, J.: The effect of drainage  
964 reorganization and climate on the sedimentologic evolution of intermontane lake systems: the  
965 final fill stage of the Tertiary Ebro Basin (Spain), J. Sediment. Res., 83, 562-590,  
966 <https://doi.org/10.2110/jsr.2013.47>, 2013.  
967

968 Villena, J., Pardo, G., Pérez, A., Muñoz, A., and González, A.: The Tertiary of the Iberian margin  
969 of the Ebro basin: palaeogeography and tectonic control, in: Friend, P. and Dabrio, C. (Eds.):

970 Tertiary basins of Spain, *World and Regional Geology*, 6, Cambridge University Press,  
971 Cambridge, 83-88, 1996.

972

973 Whipple, K.: The influence of climate on the tectonic evolution of mountain belts, *Nature*  
974 *Geosci.*, 2, 97-104, <https://doi.org/10.1038/ngeo638>, 2009.

975

976 Whipple, K. X. and Tucker, G. E.: Dynamics of the stream-power river incision model:  
977 Implications for height limits of mountain ranges, landscape response timescales, and research  
978 needs, *J. Geophys. Res.*, 104, 17661-17674, 1999.

979

980 Whipple, K. X., Forte, A. M., DiBiase, R. A., Gasparini, N. M., Ouimet, W. B.: Timescales of  
981 landscape response to divide migration and drainage capture: implications for the role of divide  
982 mobility in landscape evolution, *J. Geophys. Res.- Ea. Surf.*, 122, 248-273,  
983 <https://doi.org/10.1002/2016JF003973>, 2017.

984

985 Whitfield, E. and Harvey, A. M.: Interaction between the controls on fluvial system  
986 development: tectonics, climate, base level and river capture – Rio Alias, Southeast Spain, *Earth*  
987 *Surf. Process. Landforms*, 37, 1387-1397, <https://doi.org/10.1002/esp.3247>, 2012.

988

989 Willett, S. D.: Orogeny and orography: The effects of erosion on the structure of mountain belts,  
990 *J. Geophys. Res.*, 104, 28957-28981, 1999.

991

992 Willett, S. D., McCoy, S. W., Perron, J. T., Goren, L., and Chen, C. Y.: Dynamic reorganization  
993 of river basins, *Science*, 343, 1248765, <https://doi.org/10.1126/science.1248765>, 2014.

994

995 Yanites, B. J., Elhers, T. A., Becker, J. K., Schnellmann, M., and Heuberger, S.: High magnitude  
996 and rapid incision from river capture: Rhine River, Switzerland, *J. Geophys. Res.- Ea. Surf.*,  
997 118, 1060-1084, <https://doi.org/10.1002/jgrf.20056>, 2013.

998

999

1000

1001

1002

1003

1004

1005

1006

1007

1008

Figure captions:

Figure 1: A) Topographic map of the Duero and Ebro basins and surrounding belts. B) Averaged topographic section throughout the Duero and Ebro basins showing important incision contrast between the two basins. The Duero basin recorded low incision, especially in its upper part, whereas the Ebro basin is highly excavated.

Figure 2: Simplified geological map of the study area.

Figure 3: Topographic map of the study area with all the rivers considered in this study. The red lines represent drainage divides between main hydrographic basins.

Figure 4: Zoom in the geological map of the Iberian Range showing the location of the Jalon river tributaries. The river long profiles of these streams and the location of knickpoints are shown to the left.

Figure 5: A) Zoom in the geological map of the Bureba sector. B) Zoom in the Homino river (Ebro tributary) capturing the upper reach of the Jordan river (Duero tributary). C) Schematic representation of this capture using river long profiles and map orientation, showing the associated knickpoint and wind gap.

Figure 6: Mean annual precipitation map for the study area (data from Hijmans et al., 2005).

Figure 7: A) 3D view of the DEM of the Bureba sector showing important contrast of incision between the Ebro and Duero basins across their divide (red dashed line) and river capture evidence (elbows of capture, knickpoints and wind gaps). B) Google Earth image around the locality of Hontomin where the Homino river is capturing the upper reach of the Jordan river. C) and D) Wind gaps cut into the Bureba anticline (see location on Fig. 7A). Pictures have been taken from the north of this structure toward the south. E) Possible three steps evolution of the southwestward divide retreat through multiple river captures witnessed in the area.

Figure 8: River long profiles for all the streams described in the Bureba area showing evidence of river capture. Colors are given to rivers that are linked in these capture processes.

Figure 9: Topographic map showing the location of all the knickpoints and low relief surfaces that may be associated to river capture. The black dashed line represents a possible paleodrainage divide between the Ebro and Duero basins. The area between this dashed line and the present-day location of the divide in red may have belonged the Duero basin before being captured by the Ebro basin.

Figure 10: Duero river long profile (black line) and difference in the specific stream power of the river (grey) calculated by considering the paleo and present-day position of its divide. Positive values suggest a significant diminution of the incision capacity of the Duero river, particularly along the knickzone of its longitudinal profile. Details on calculation are available in the Supplement (Section S1).

Figure 11: Topographic map with  $\chi$  values calculated on different opposite streams in the vicinity of the Ebro/Duero drainage divide. This map shows significant contrasting values between the Ebro and Duero drainage networks.

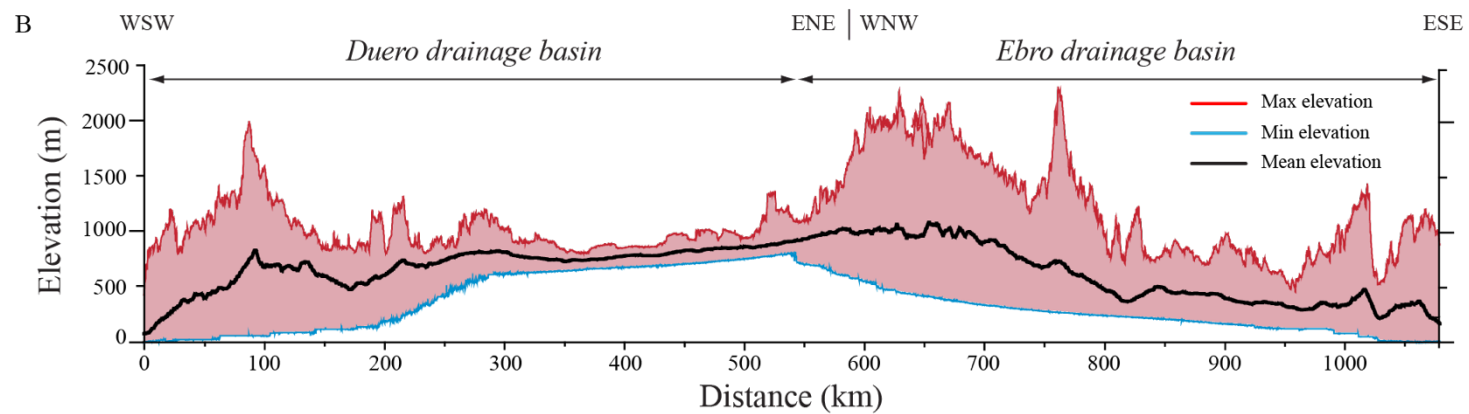
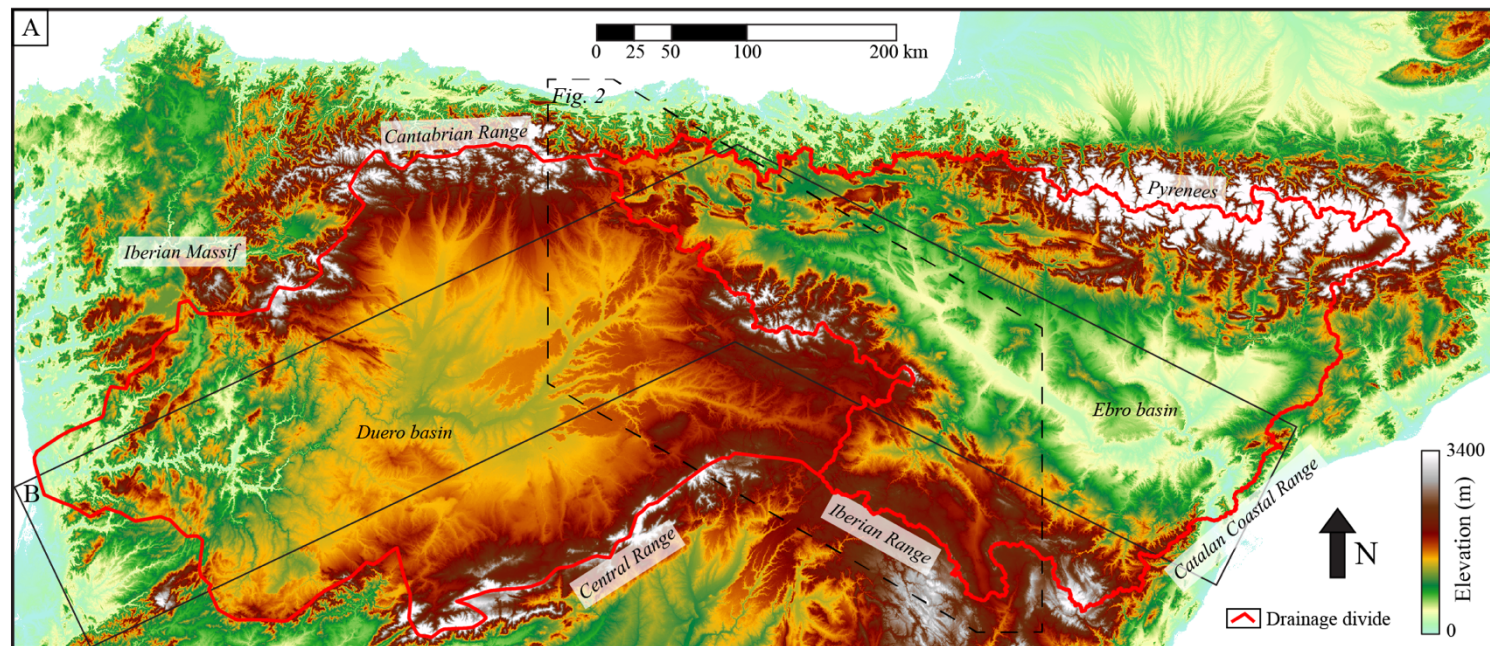


Figure 1

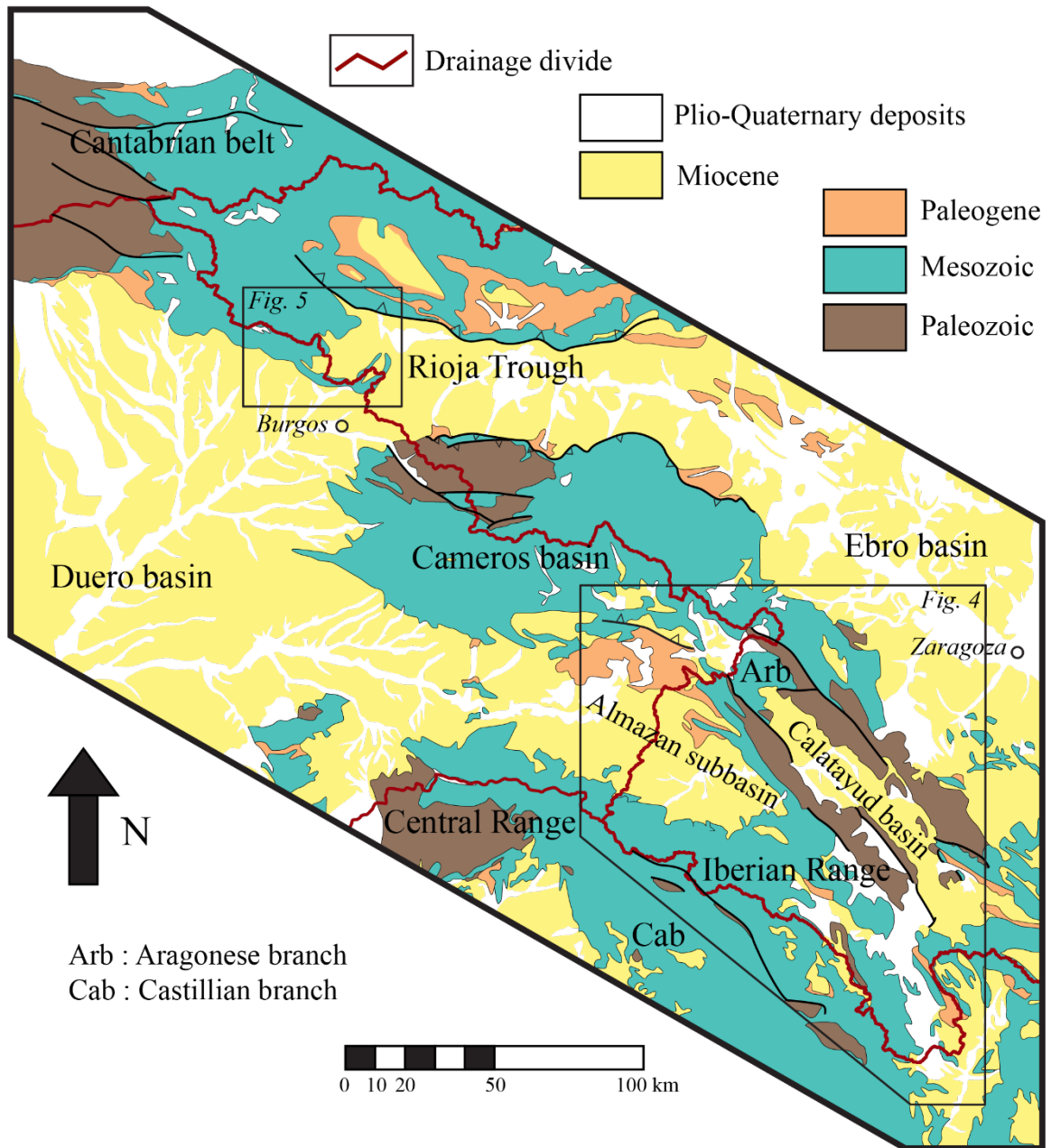


Figure 2



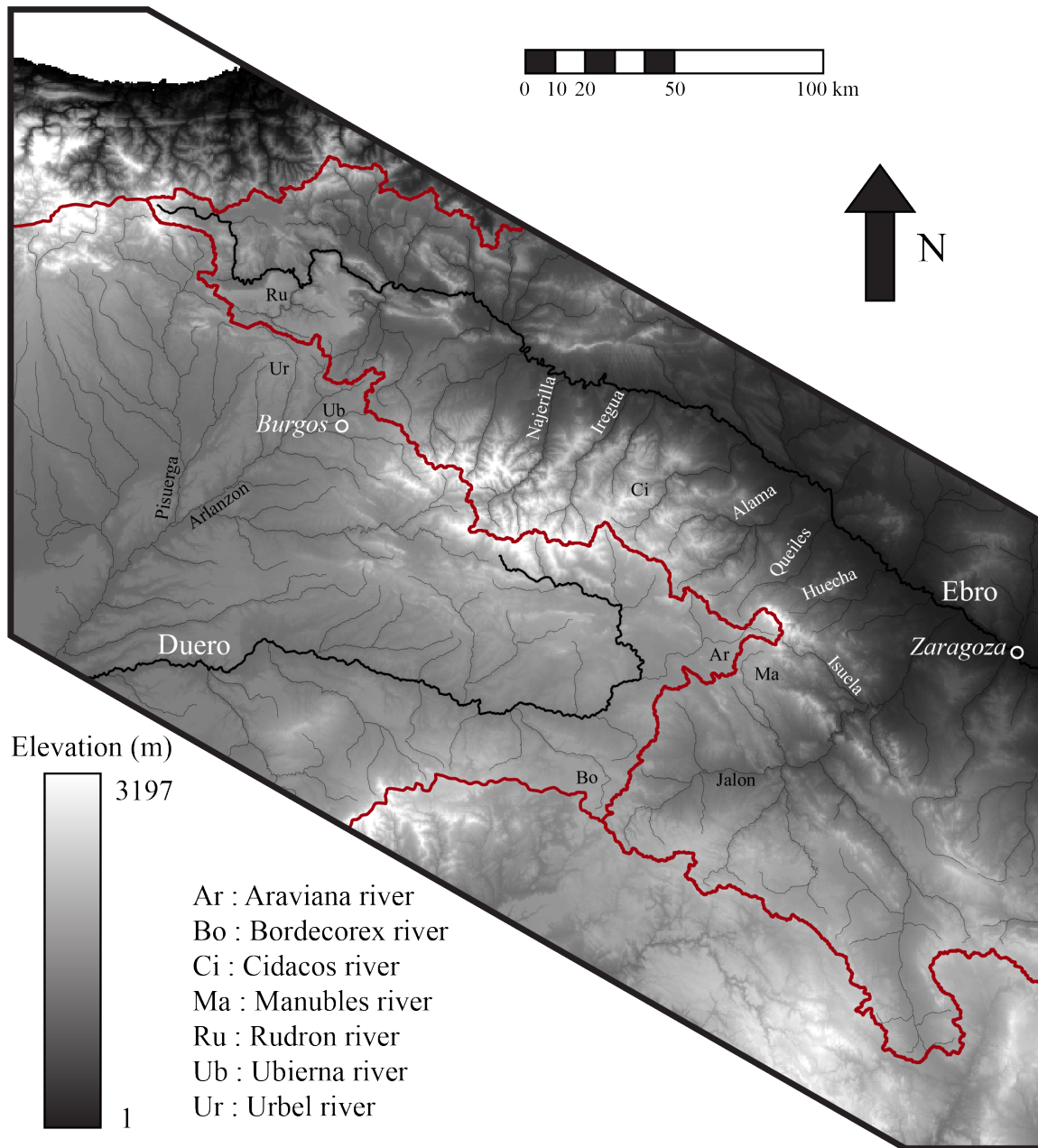


Figure 3



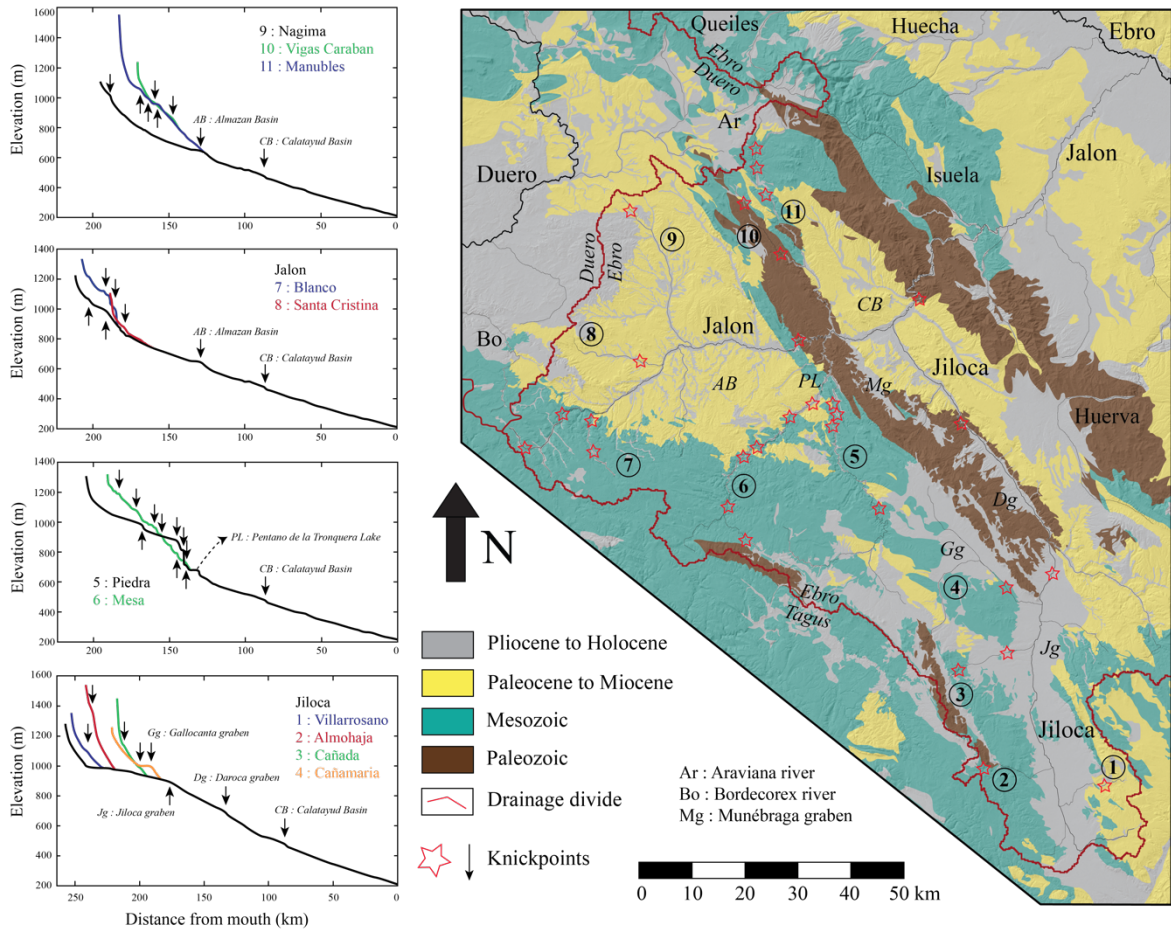


Figure 4

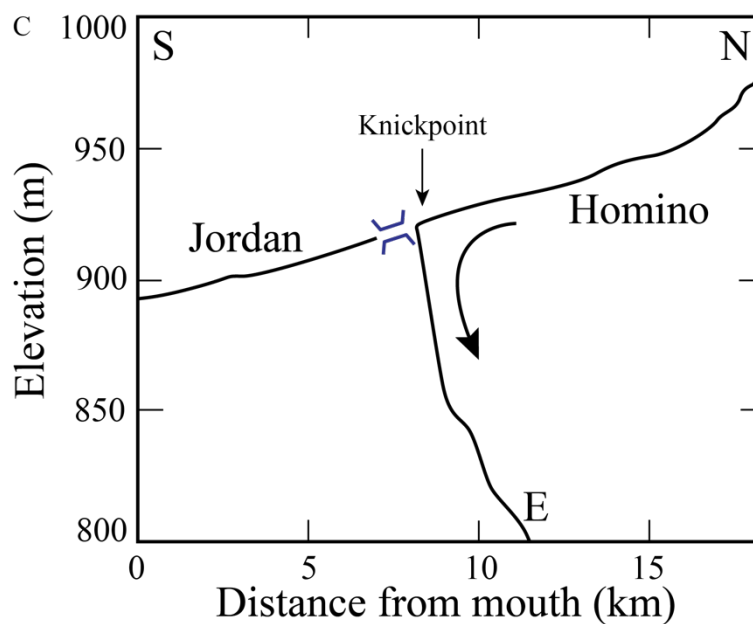
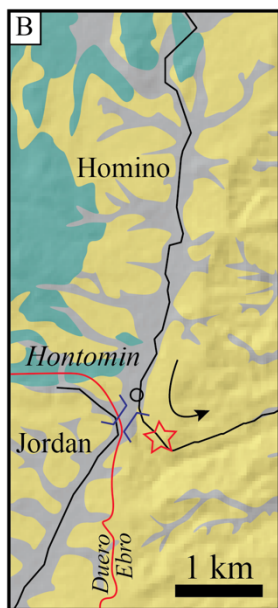
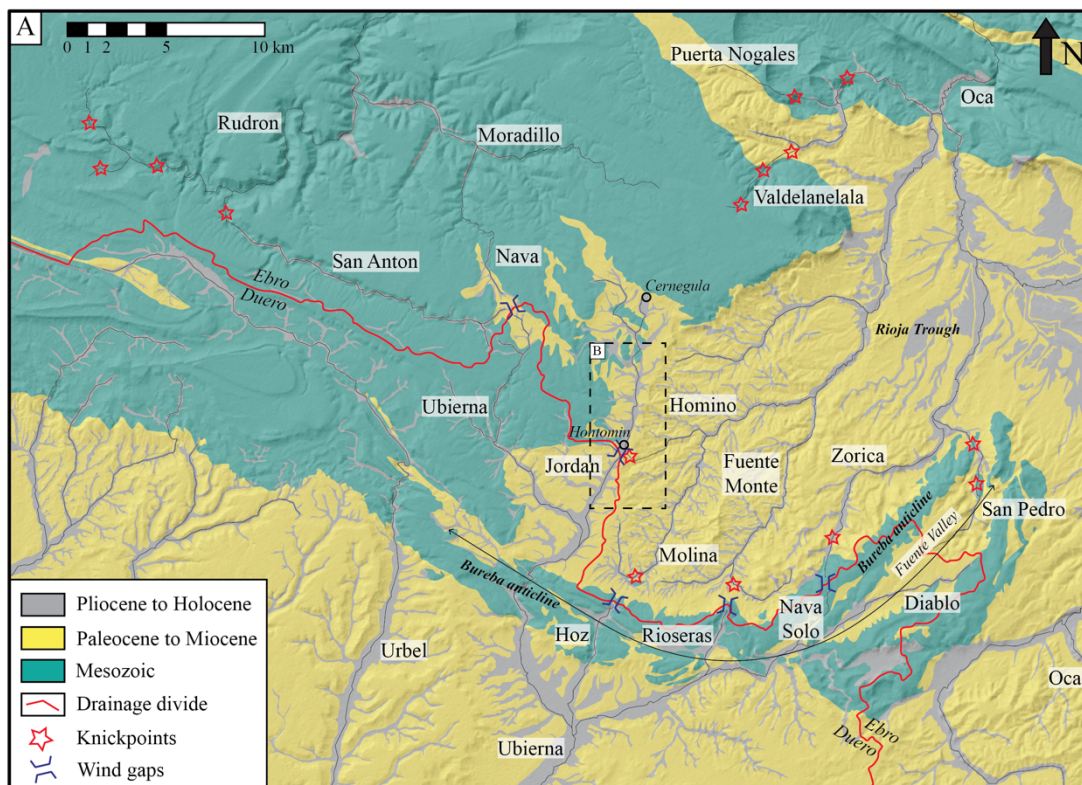


Figure 5

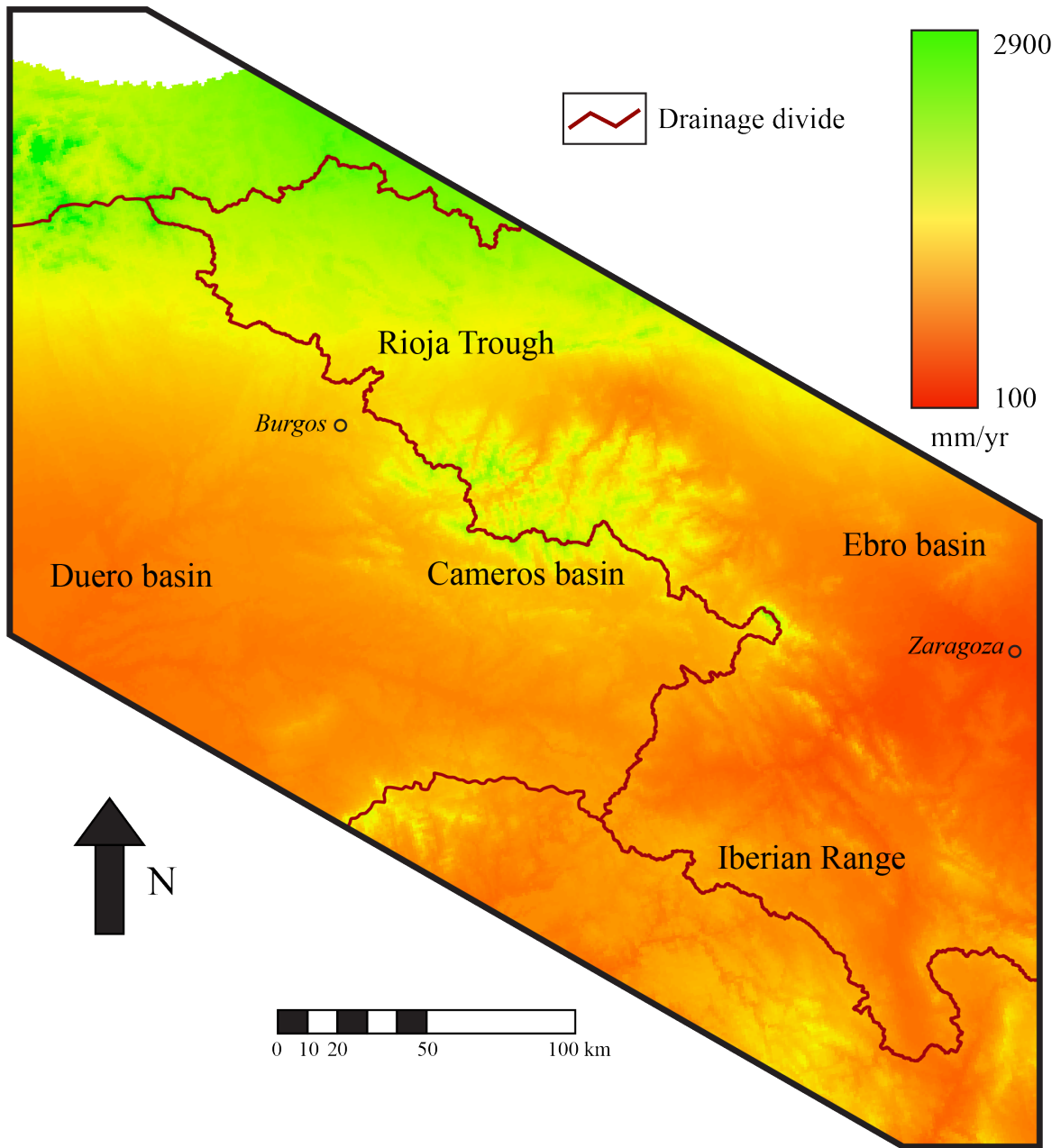
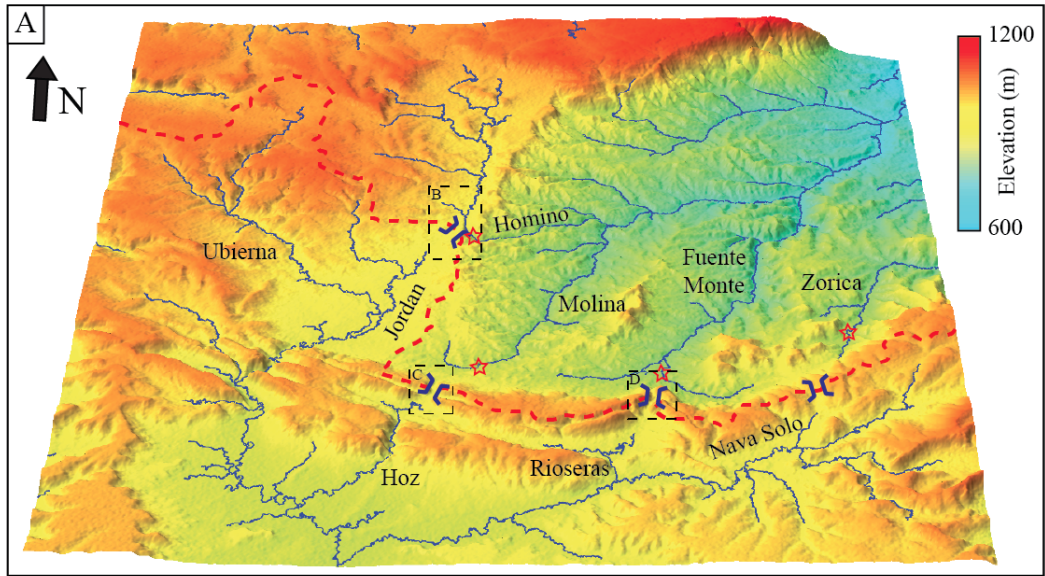


Figure 6





- Drainage divide
- Knickpoints
- Wind gaps
- Mesozoic relief
- Cenozoic incision

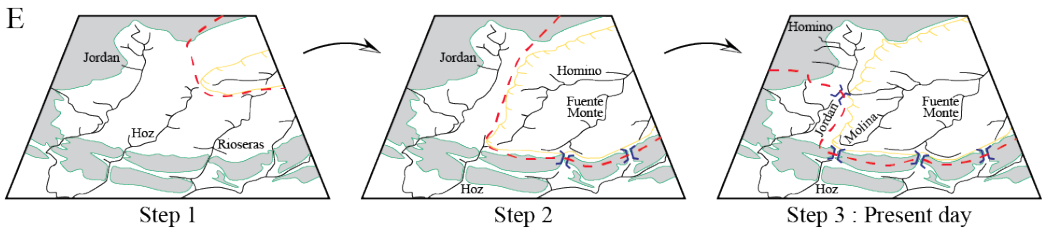
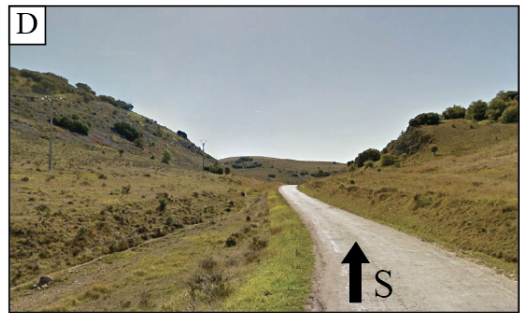
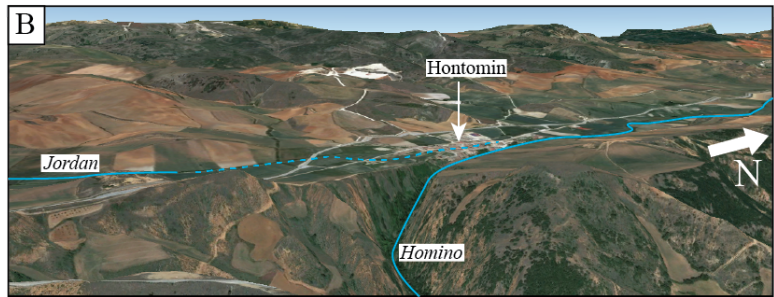


Figure 7

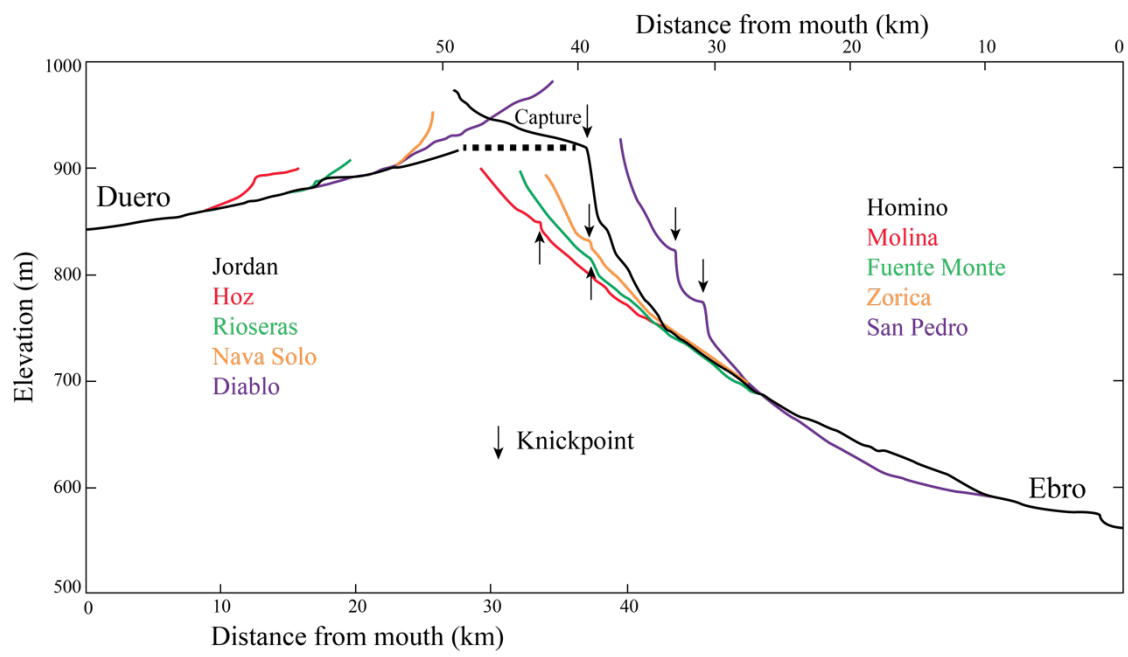


Figure 8

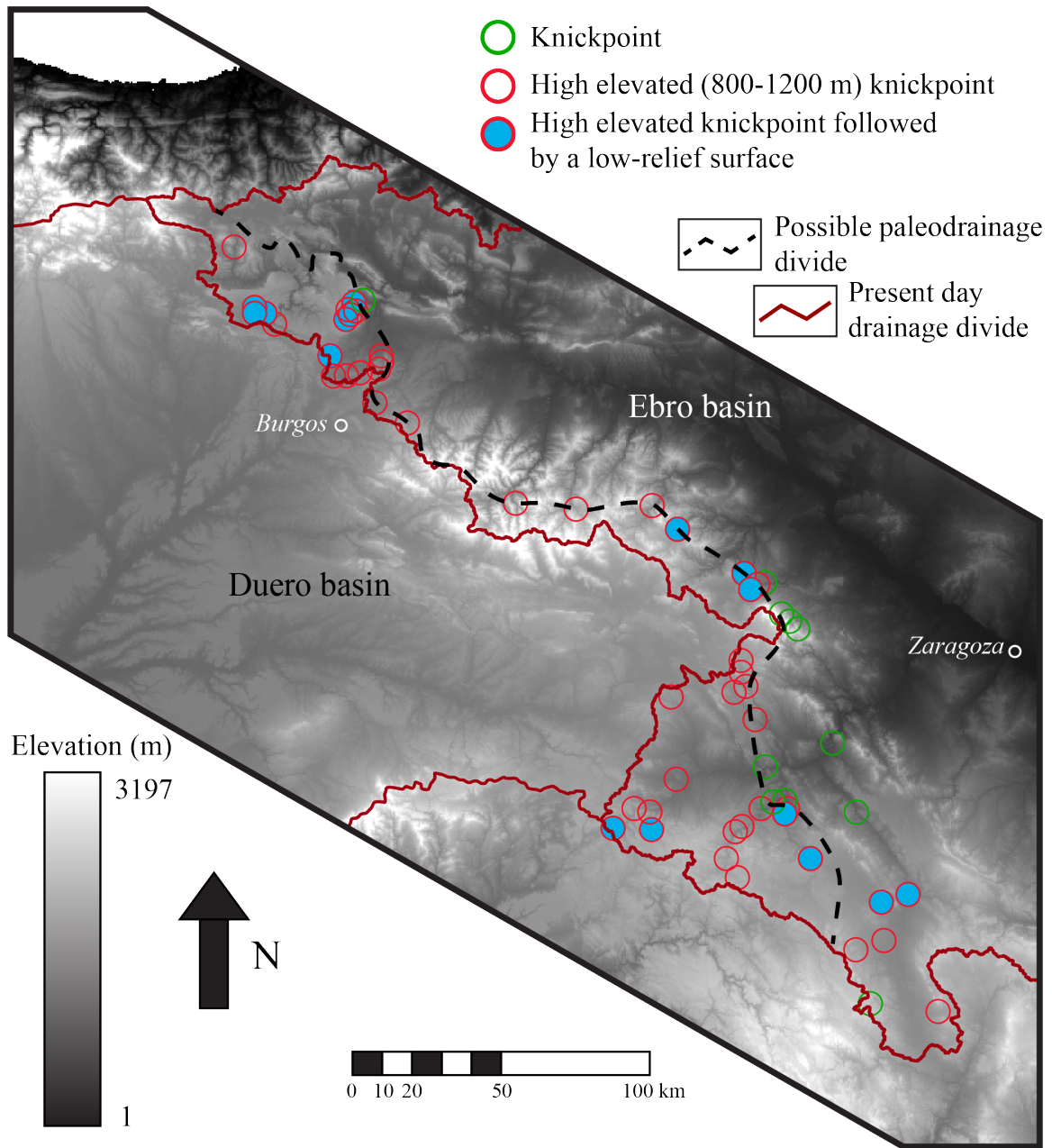


Figure 9

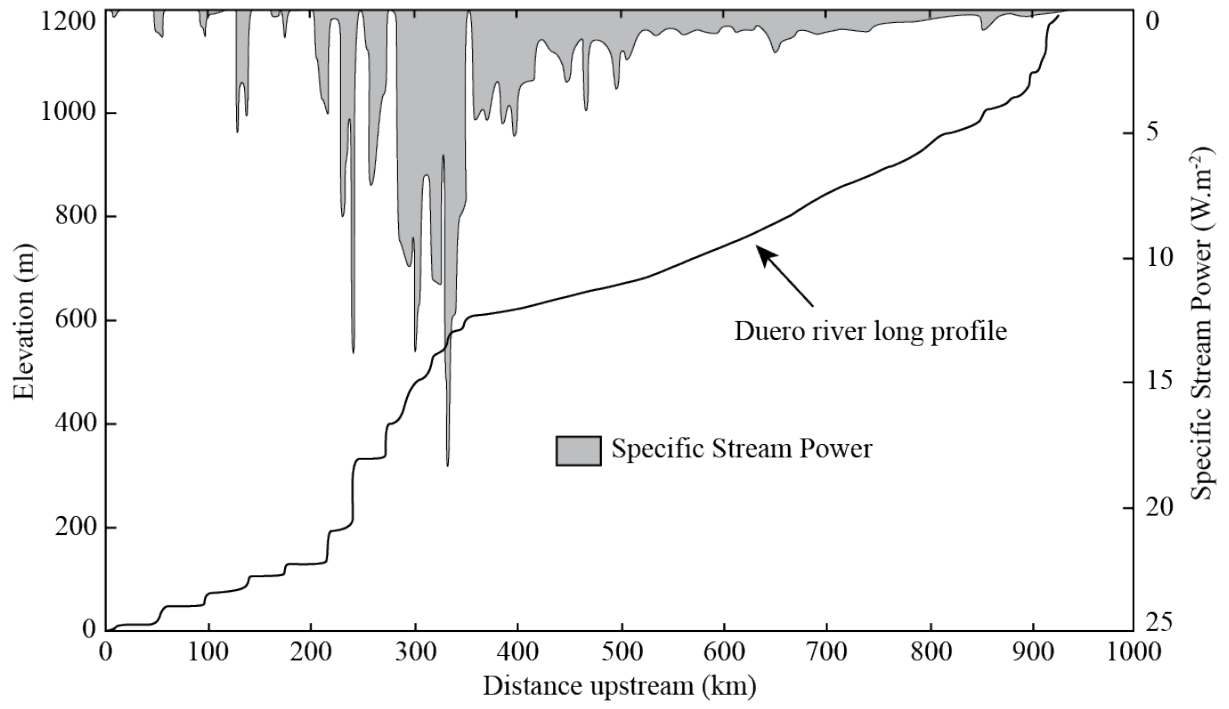


Figure 10

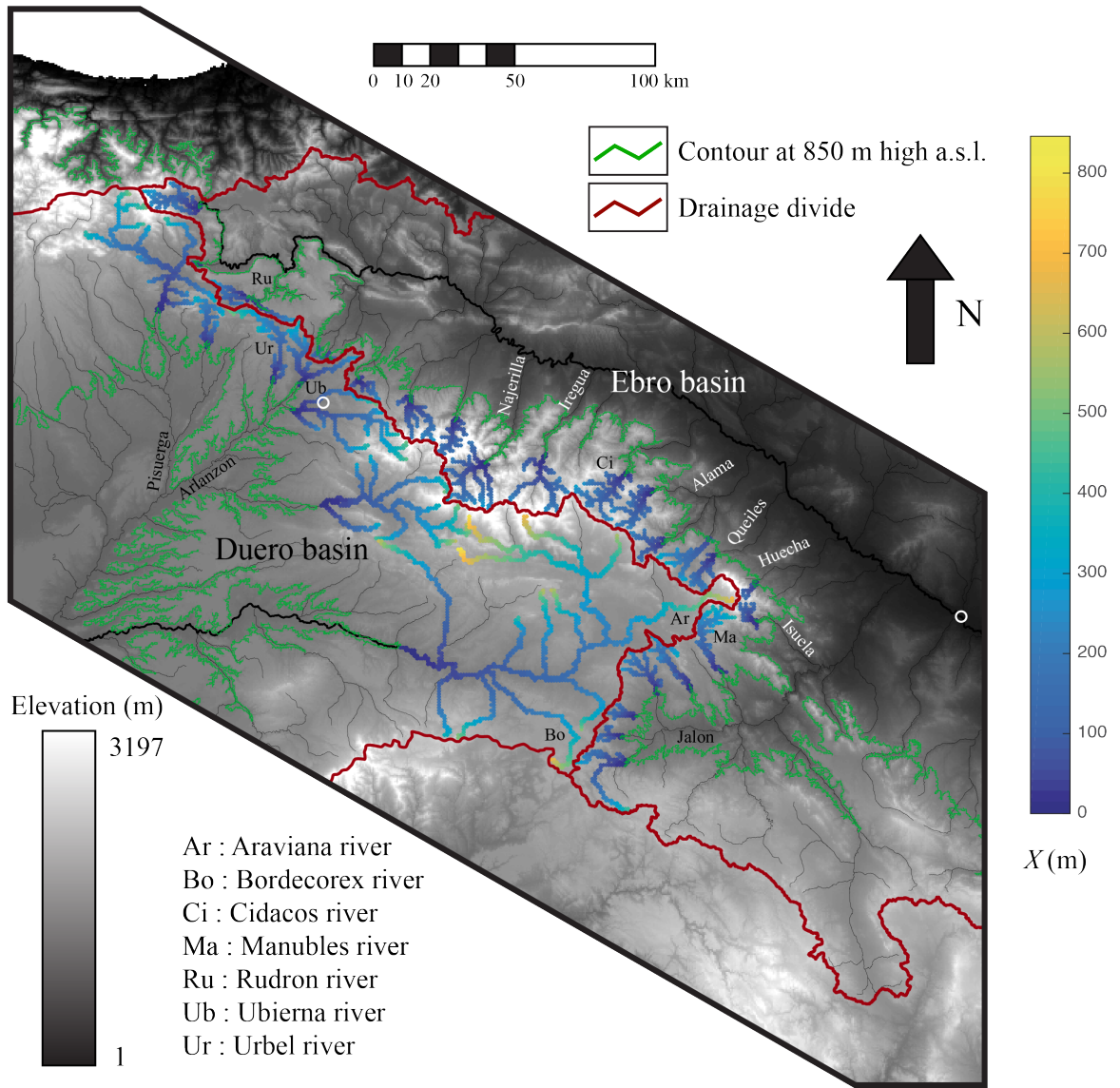


Figure 11



1 **Drainage reorganization and divide migration induced by the excavation of the Ebro**  
2 **basin (NE Spain)**

3

4 Arnaud Vacherat <sup>1</sup>, Stéphane Bonnet <sup>1</sup>, Frédéric Mouthereau <sup>1</sup>

5

6 <sup>1</sup>Géosciences Environnement Toulouse (GET), Université de Toulouse, CNRS, IRD, UPS,  
7 (Toulouse), France

8

9 *Correspondance to:* Stéphane Bonnet (stephane.bonnet@get.omp.eu)

10

11 **Abstract**

12

13 Intracontinental endorheic basins are key elements of source-to-sink systems as they preserve  
14 sediments eroded from the surrounding catchments. Drainage reorganization in such a basin in  
15 response to changing boundary conditions has strong implications on the sediment routing  
16 system and on landscape evolution. The Ebro and Duero basins represent two foreland basins,  
17 which developed in response to the growth of surrounding compressional orogens, the Pyrenees  
18 and the Cantabrian mountains to the north, the Iberian Ranges to the south, and the Catalan  
19 Coastal Range to the east. They were once connected as endorheic basins in the early Oligocene.  
20 By the end of the Miocene, new post-orogenic conditions led to the current setting in which the  
21 Ebro and Duero basins are flowing in opposite directions, towards the Mediterranean Sea and  
22 the Atlantic Ocean. Although these two hydrographic basins recorded a similar history, they are  
23 characterized by very different morphologic features. The Ebro basin is highly excavated,  
24 whereas relicts of the endorheic stage are very well preserved in the Duero basin. The  
25 contrasting morphological preservation of the endorheic stage represents an ideal natural  
26 laboratory to study the drivers (internal / external) of post-orogenic drainage divide mobility,  
27 drainage network and landscape evolution. To that aim, we use field and map observations and  
28 we apply the  $\chi$ -analysis of river profiles along the divide between the Ebro and Duero drainage  
29 basins. We show here that the contrasting excavation of the Ebro and Duero basins drives a  
30 reorganization of their drainage network through a series of captures, which resulted in the  
31 southwestward migration of their main drainage divide. Fluvial captures have strong impact on  
32 drainage areas, fluxes, and so on their respective incision capacity. We conclude that drainage  
33 reorganization driven by the capture of the Duero rivers by the Ebro drainage system explains

34 the first-order preservation of endorheic stage remnants in the Duero basin, due to drainage area  
35 loss, independently from tectonics and climate.

36

## 37 **1. Introduction**

38

39 Landscapes subjected to contrasted erosion rates between adjacent drainage basins show a  
40 migration of their drainage divide toward the area of lower erosion rates (Bonnet, 2009; Willett  
41 et al., 2014). This is the case for mountain ranges characterized by gradients in precipitation  
42 rates due to orography, once landscapes are in a transient state and are not adjusted to  
43 precipitation differences (Bonnet, 2009). It also occurs when drainage reorganized in response  
44 to capture (Yanites et al., 2013; Willett et al., 2014). River capture actually drives a drop in the  
45 spatial position location of drainage divide (Prince et al. 2011) but also produces a wave of  
46 erosion in the captured reach (Yanites et al., 2013) that may impact divide position. Historically,  
47 migration of divides has been inferred by changes in the provenance of sediments stored in  
48 sedimentary basins (*e.g.* Kuhlemann et al., 2001). It is however a process that is generally very  
49 difficult to document in erosional landscapes. Recent developments have provided models and  
50 analytical approaches to identify divide migration in the landscape (Bonnet, 2009; Castelltort  
51 et al., 2012; Willett et al., 2014; Whipple et al., 2017). Among them the recently-developed  $\chi$ -  
52 analysis of longitudinal profiles of rivers (Perron and Royden, 2012) is based on the recognition  
53 of disequilibrium along river profiles, disequilibrium being defined by the departure from an  
54 ideal equilibrium shape. The application of this method to both natural and numerically-  
55 simulated landscapes, has allowed to demonstrate contrasts in the equilibrium state of rivers  
56 across divide and then to infer their migration (Willett et al., 2014). The applicability of this  
57 method is however limited to settings where the response time of rivers is larger compared to  
58 the rate of divide migration, so they can actually show disequilibrium in their longitudinal  
59 profiles (Whipple et al., 2017).

60

61 The Ebro and Duero drainage basins in the Northern Iberian Peninsula show geological and  
62 geomorphological evidence of very contrasted erosional histories during the Neogene. They  
63 initially recorded a long endorheic stage from the Early Oligocene to the Late Miocene (Riba  
64 et al., 1983; Garcia-Castellanos et al., 2003). Since then, both basins opened toward the Atlantic  
65 Ocean (Duero) or the Mediterranean Sea (Ebro). The Ebro basin's opening is reflected in the  
66 landscape by evidence of river incision (Garcia-Castellanos et al., 2003), whereas the Duero  
67 Basin does not show significant incision in its upstream part as a large relict of its endorheic

68 morphology is preserved (Antón et al., 2012). The Duero river long profile actually shows a  
69 pronounced knickpoint (knickzone) defining an upstream domain of high mean elevation (~800  
70 m) and low relief where the sediments deposited during the endorheic stage are relatively well  
71 preserved. Then, these two adjacent basins are characterized by differences in incision and in  
72 the preservation of their endorheic stages. They thus represent an ideal natural laboratory to  
73 evaluate divide migration in response to differential post-orogenic incision. Following a  
74 presentation of the geological context, we first compile evidence of fluvial captures along the  
75 Ebro-Duero divide, based on previous studies and our own investigations, and we map the  
76 location of knickpoints and relict portions of the drainage network. We use all these  
77 observations to reconstruct a paleo-divide position and to estimate the impact of divide  
78 migration in terms of drainage area and stream power. We complement this dataset by providing  
79 a map of  $\chi$  across divide (Willett et al., 2014) to highlight potential disequilibrium state between  
80 rivers of the Ebro and Duero catchments.

81

## 82 **2. Geological setting**

83

### 84 2.1 The Ebro and Duero basins

85

86 The Ebro and Duero basins represent two hydrographic basins located in the northern part of  
87 the Iberian Peninsula (Fig. 1). The bedrock of the Ebro and Duero drainage basins mainly  
88 consists of Cenozoic deposits, and Mesozoic and Paleozoic rocks in their headwaters (Fig. 2).  
89 They formed once a unique foreland basin during the Cenozoic controlled by the flexural  
90 loading by the surrounding mountain belts: the Pyrenees and the Cantabrian mountains to the  
91 north (Pulgar et al., 1999), the Iberian and Central Ranges to the south (Guimerà et al., 2004;  
92 De Vicente et al., 2007), and the Catalan Coastal Range (CCR) to the east (López-Blanco et al.,  
93 2000 ; Salas et al., 2001), during collision between Iberia and Europe since the Late Cretaceous.

94

95 From the Late Cretaceous, the Ebro and Duero basins were essentially filled by clastic deposits,  
96 and opened toward the Atlantic Ocean in the Bay of Biscay (Alonso-Zarza et al., 2002). During  
97 the Late Eocene – Early Oligocene, the uplift in the Western Pyrenees (Puigdefàbregas et al.,  
98 1992) led to the closure of the Ebro and Duero basins as attested by the Ebro basin  
99 continentalization dated at ~36 Ma (Costa et al., 2010). The center of these two basins became  
100 long-lived lakes filled with lacustrine, sandy, and evaporitic deposits from the Oligocene to the  
101 Miocene (Riba et al., 1983; Alonso-Zarza et al., 2002; Pérez-Rivarés et al., 2002, 2004; Garcia-

102 Castellanos et al, 2003; Garcia-Castellanos, 2006; Larrasoña et al., 2006; Vázquez-Urbez et  
103 al., 2013). The opening of the Ebro basin through the Catalan Coastal Range toward the  
104 Mediterranean Sea occurred during the Late Miocene, leading to kilometer-scale excavation  
105 throughout the basin (Fillon and Van der Beek, 2012; Fillon et al., 2013; Garcia-Castellanos  
106 and Larrasoña, 2015). The exact timing and processes driving the opening, as well as the  
107 role of the Messinian Salinity Crisis, have long been debated (Coney et al., 1996 (post-  
108 Messinian); Garcia-Castellanos et al., 2003 (13-8.5 Ma); Babault et al., 2006 (post-Messinian);  
109 Urgeles et al., 2010; Cameselle et al. (2014) (Serravallian-Tortonian); Garcia-Castellanos and  
110 Larrasoña, 2015 (12-7.5 Ma)). In contrast with the Ebro basin, incision in the upper Duero  
111 basin appears much less significant. The Duero basin is characterized by a low relief topography  
112 (Fig. 1) in its upstream part, at 700-800 m above sea level to the west, and at 1000-1100 m a.s.l.  
113 to the north, northeast, and to the east in the Almazan subbasin, close to the divide with the  
114 Ebro basin. The connection of the Duero River with the Atlantic Ocean occurred from the Late  
115 Miocene-Early Pliocene to the Late Pliocene-Early Pleistocene (Martín-Serrano, 1991). The  
116 current Ebro and Duero drainage networks are separated by a divide running from the  
117 Cantabrian belt to the NW, toward the SE in the Iberian Range (Figs. 1, 2, 3). In the following,  
118 we review the geological evolution of the different domains that constitute this drainage divide  
119 between the Ebro and Duero drainage basins.

120

## 121 2.2 The Iberian Range

122

123 The Iberian Range (Figs. 2, 4) is a double vergent fold-and-thrust belt resulting from Late  
124 Cretaceous inversion of Late Jurassic-Early Cretaceous rift basins during Iberia – Europe  
125 convergence (Salas et al., 2001; Guimerà et al., 2004; Martín-Chivelet et al., 2002). It is divided  
126 into two NW-SE directed branches, the Aragonese and the Castilian branches, separated by the  
127 Tertiary Almazan subbasin (Bond, 1996). The Almazan subbasin is connected to the Duero  
128 basin since the Early Miocene (Alonso-Zarza et al., 2002).

129 The Iberian Range is essentially made of marine carbonates and continental clastic sediments  
130 ranging from Late Permian to Albian, overlying a Hercynian basement. The Cameros subbasin  
131 to the NW represents a late Jurassic-Early Cretaceous trough almost exclusively filled by  
132 continental siliciclastic deposits (Martín-Chivelet et al., 2002 and references therein; Del Rio  
133 et al., 2009). Shortening in the Iberian Range occurred from the Late Cretaceous to the Early  
134 Miocene, along inherited Hercynian NW-SE structures (Gutiérrez-Elorza and Gracia, 1997;  
135 Guimerà et al., 2004; Gutiérrez-Elorza et al., 2002). The opening of the Calatayud basin in the

136 Aragonese branch occurred during the Early Miocene in response to right-lateral transpression  
137 on the southern margin of the Iberian Range (Daroca area) (Colomer and Santanach, 1988). It  
138 is followed during the Pliocene and the Pleistocene, by pulses of extension reactivating faults  
139 in the Calatayud basin, and the formation of grabens such as the Daroca, Munébrega,  
140 Gallocanta, and Jiloca grabens (Fig. 4; Colomer and Santanach, 1988; Gutiérrez-Elorza et al.,  
141 2002; Capote et al., 2002). This is also outlined by the occurrence of Late Pliocene to Early  
142 Pleistocene breccias and glacis levels in the Daroca and Jiloca grabens (Gracia, 1992, 1993a;  
143 Gracia and Cuchi, 1993; Gutiérrez-Santolalla et al., 1996). These Neogene troughs are filled by  
144 continental deposits and pediments, up to the Quaternary (Fig. 4). The Neogene tectonic pulses  
145 in the Iberian are interrupted by periods of quiescence during which erosion surfaces developed  
146 (Gutiérrez-Elorza and Gracia, 1997).

147 Deformation and uplift of the Iberian Range and Cameros basin resulted in the development of  
148 a new drainage divide between the Duero and Ebro basins and in the isolation of the Almazan  
149 subbasin (Alonso-Zarza et al., 2002). In contrast, the connection between the Duero the Ebro  
150 basins has not been affected by significant deformation and uplift in the proto-Rioja trough  
151 (Mikes, 2010).

152

### 153 2.3 The Rioja trough and Bureba high

154

155 The Rioja trough (Figs. 2, 5) recorded important subsidence, especially during the Cenozoic (>  
156 5 km), related to compression and thrusting on its borders (Jurado and Riba, 1996). As thrusting  
157 initiated in the Pyrenean-Cantabrian belt and in the Iberian Range and Cameros basin, the Rioja  
158 trough became domain of important synorogenic sediment transfer between the Ebro and Duero  
159 basins. During the Paleocene, the Rioja trough was a marine depositional environment. With  
160 the increase of sediment fluxes that originated from the exhumation of surrounding mountain  
161 belts, sedimentation became essentially continental in the Eocene. Thrusting continued during  
162 the Oligocene resulting in the formation of an anticline connecting the Cantabrian domain and  
163 the Cameros inverted basin. This morphologic high (the Bureba anticline, Fig. 5) located in the  
164 center of the area is supposed to have triggered the disconnection between the Duero and Ebro  
165 basins (Mikes, 2010), as suggested by the repartition of alluvial fans on both sides of this  
166 structure (Muñoz-Jiménez and Casas-Sainz, 1997; Villena et al., 1996). During the Miocene,  
167 deformation ceased as evidenced by the deposition of undeformed middle Miocene to Holocene  
168 strata. The Bureba anticline is cored by Albian strata and topped by Santonian limestones and

169 Oligocene conglomerates controlling the location of the current main drainage divide between  
170 the Ebro and Duero river networks (Fig. 5).

171

## 172 2.4 Climate evolution

173

174 Climate exerts a major control on valley incision, sediment discharge, and on the evolution of  
175 drainage networks (Willet, 1999; Garcia-Castellanos, 2006; Bonnet, 2009; Whipple, 2009;  
176 Whitfield and Harvey, 2012; Stange et al., 2014). The mean annual precipitation map for the  
177 North Iberian Peninsula (Hijmans et al., 2005) shows a similar pattern for both the Ebro and  
178 Duero basins as they record very low precipitation, associated with global subarid conditions,  
179 with the exception of the Cameros basin that record a slightly higher precipitation rate (Fig. 6).  
180 There is a strong contrast to the north, toward the Mediterranean Sea and the most elevated  
181 areas in the Cantabrian and Pyrenean belts, where precipitation drastically increases.

182 The paleoclimatic evolution from the Late Cretaceous to the Neogene is linked both with the  
183 effects of surrounding mountains uplift, and with the latitudinal variation drift of Iberia from  
184 30°N in the Cretaceous to ~40°N during Late Neogene times. The hot-humid tropical climate  
185 of the Late Cretaceous became drier and arid from the Paleocene to the Middle Miocene (López-  
186 Martínez et al., 1986), favouring the development of endorheic lakes (Garcia-Castellanos,  
187 2006). During the Middle-Late Miocene and Early Pliocene, the northern Iberia recorded more  
188 humid and seasonal conditions (Calvo et al., 1993; Alonso-Zarza and Calvo, 2000) with  
189 alternations of cold-wet and hot-dry periods (Bessais and Cravatte, 1988; Rivas-Carballo et al.,  
190 1994; Jiménez-Moreno et al., 2010). More humid and colder conditions took place in the Late  
191 Pliocene, characterized by dry glacial periods and humid interglacials (Suc and Popescu, 2005;  
192 Jiménez-Moreno et al., 2013). Climatic contrasts increased, triggering intense glaciers  
193 fluctuations in the surrounding mountain ranges during the Lower-Middle Pleistocene transition  
194 (1.4-0.8 Ma) (Moreno et al., 2012; Duval et al., 2015; Sancho et al., 2016), and throughout the  
195 Late Pleistocene period, which record glacial / interglacial oscillations, as evidenced by pollen  
196 identification (Suc and Popescu, 2005; Jiménez-Moreno et al., 2010, 2013; Barrón et al., 2016;  
197 García-Ruiz et al., 2016) and speleothem studies (Moreno et al., 2013; Bartolomé et al., 2015).  
198 Glaciers are considered as very efficient erosion tool in continental environment. They are  
199 likely to influence drainage divide migration (Brocklehurst and Whipple, 2002). There is large  
200 evidence of glaciers development especially for the Late Pleistocene in the Pyrenees (Delmas  
201 et al., 2009; Nivière et al., 2016; García-Ruiz et al., 2016), in the Cantabrian belt (Serrano et  
202 al., 2013, 2016; García-Ruiz et al., 2016), and in the Central Range (Palacios et al., 2011, 2012;

203 García-Ruiz et al., 2016). However, although numerous moraines have been mapped throughout  
204 the Iberian Range (Ortigosa, 1994; García-Ruiz et al., 1998; Pellicer and Echeverría, 2004),  
205 there is no evidence of U-shaped valleys and because of the lack of very high elevated massifs  
206 (>2500 m), the occurrence of active ice tongues are considered as limited, if not precluded  
207 (García-Ruiz et al., 2016).

208

### 209 **3. Evidence of divide mobility between the Duero and Ebro catchments**

210

211 The easternmost part of the Duero river is opposed to the Ebro tributaries that are the Jalon,  
212 Huecha, Queiles, Alama, Cidacos, Iregua, and Najerilla rivers, whereas the Arlanzon and  
213 Pisuerga rivers (Duero tributaries) are opposed to the Najerilla, Tiron, Oca, and Rudron rivers,  
214 and to the westernmost part of the Ebro river (Fig. 3). The northeastern part of the Duero basin  
215 (the easternmost Duero river, the Arlanzon and Pisuerga rivers) mainly consists of broad flat  
216 valleys characterized by low incision depth and low-gradient streams with concave longitudinal  
217 profiles (Antón et al., 2012, 2014). By contrast, the western part of the Ebro basin is  
218 characterized by more incised valleys, especially in the Cantabrian and in the Cameros – Iberian  
219 Range domains, with more complex longitudinal profiles (knickpoints, remnants of high  
220 elevated surfaces). Previous studies (Gutiérrez-Santolalla et al., 1996; Pineda, 1997; Mikes,  
221 2010) already shown that the Jalon and Homino rivers, which belong to the Ebro basin, have  
222 recently captured parts of the Duero basin in the Iberian Range and in the Rioja trough,  
223 respectively. Such evolution has been recorded by the occurrence of geomorphological markers  
224 as wind gaps and elbows of captures, as well as by the presence of knickpoints and/or remnants  
225 of high elevated surfaces in river long profiles. To highlight this dynamic evolution, we  
226 performed a morphometric analysis of rivers all around the divide separating the Ebro basin  
227 from the Duero basin, with particular attention given to the Aragonese branch of the Iberian  
228 Range (Fig. 4) and to the Rioja Trough (Fig. 5), where captures have already been described.  
229 The studied basins were digitally mapped using high-resolution (~30 meters) digital elevation  
230 models (DEMs) from SRTM 1 Arc-Second Global elevation data available at the U.S.  
231 Geological Survey ([www.usgs.gov](http://www.usgs.gov)). The different DEMs were assembled using the ENVI  
232 software. We also used 1:50,000 geological maps from the Instituto Geológico y Minero de  
233 España ([www.igme.es](http://www.igme.es)). We used the TopoToolbox, a MATLAB-based software developed by  
234 Schwanghart and Scherler (2014), to extract the river network and longitudinal profiles and the  
235  $\chi$ -analysis Tool developed by Mudd et al. (2014).

236

### 237 3.1 Fluvial captures and related knickpoints in the Iberian Range

238

239 Neogene tectonics in the Iberian range controlled the uplift of topographic ranges and the  
240 formation of several basins whose connection with the Ebro or the Duero has occasionally  
241 changed through time. Nowadays, the western part of the Almazan subbasin (Figs. 2, 4) belongs  
242 to the Duero catchment, its eastern part being drained by the Ebro drainage network and  
243 especially by the Jalon river and its tributaries (Fig. 4). Gutiérrez-Santolalla et al. (1996)  
244 proposed that the Jalon river captured this domain after cutting into the Mesozoic and Neogene  
245 strata and the two Paleozoic ridges of the Aragonese branch of the Iberian Range. They used  
246 chronostratigraphic evidence to build a relative chronology of capture events in the Jalon area.  
247 First, the incision of the northern Paleozoic ridge and capture of the Calatayud basin by the  
248 Jalon river is attributed to a post-Messinian age. The Jiloca river, the easternmost main Jalon  
249 tributary, is then thought to capture the Daroca graben area to the east during the Late Pliocene  
250 – Early Pleistocene. This is followed from the Early to Late Pleistocene by the capture of the  
251 Jiloca graben to the southeast and finally by the capture of the Munébraga graben to the  
252 southwest, by the Jalon river (Gutiérrez-Santolalla et al., 1996), toward the easternmost part of  
253 the Almazan subbasin.

254 The Jalon river and tributaries show knickpoints in their longitudinal profiles (Fig. 4), at  
255 locations that are consistent with the events of captures proposed by Gutiérrez-Santolalla et al.  
256 (1996), suggesting that these captures are actually witnessed by knickpoints. The capture of the  
257 Jiloca graben corresponds to a major knickpoint in the Jiloca river profile that appears very  
258 smoothed, and that is followed by an upstream ~50 km long flat domain preserved at ~1000 m  
259 high above sea level. This imparts a convex shape to the Jiloca profile (Fig. 4). Due to the short  
260 period of time between the formation of the Jiloca graben (the earliest glacial deposits are  
261 attributed to the Middle Pliocene) and its capture (Early Pleistocene; Gutiérrez-Santolalla et al.,  
262 1996), we suggest this upstream domain was a short-lived endorheic domain that has never  
263 been externally drained before being captured by the Ebro network. In the northwestern part of  
264 the Jiloca graben, the Cañamaria river, a tributary of the Jiloca river, heads to the northwest,  
265 reaching the Gallocanta basin, also considered as a former graben (Gracia, 1993b; Gracia et al.,  
266 1999; Gutiérrez-Elorza et al., 2002). The upstream part of its river long profile is characterized  
267 by a sharper knickpoint at the entrance of the basin, and is followed by a ~15 km long flat  
268 domain (Fig. 4). Similarly to the Jiloca graben, the Gallocanta basin appears to be a short-lived  
269 endorheic domain that has been more recently captured by the Jiloca river network.



270 According to Gutiérrez-Santolalla et al. (1996), the Jalon river reached the southern Paleozoic  
271 ridge of the Aragonese branch, to the southwest of the Calatayud basin, captured the Munébrega  
272 graben and the Almazan subbasin (also characterized by a pronounced knickpoint) during the  
273 Pleistocene-Holocene, slightly after the capture of the Jiloca graben by the Jiloca river. This is  
274 coherent with morphological analysis of longitudinal profiles, as the major knickpoint related  
275 to the capture of the Jiloca graben appears very smoothed, whereas knickpoints observed in the  
276 west are sharper, suggesting they are younger. However we cannot ruled out some local  
277 influence of the lithology on the shape of these knickpoints.

278 Finally, the Piedra river (Jalon tributary) long profile shows major sharp knickpoints and two  
279 successive ~30 km long almost flat domains in the Almazan subbasin, at ~900-1000 m above  
280 sea level (Fig. 4). In addition, the upper reach of the river long profiles of the Jalon river, and  
281 of its tributary the Blanco river, are characterized by major sharp knickpoints, and by a ~15 km  
282 long flat domain at ~1000-1100 m above sea level, in the Mesozoic Castilian branch of the  
283 Iberian Range (Fig. 4).

284

### 285 3.2 Fluvial captures and related knickpoints in the Rioja trough area

286

287 In the Rioja trough area, the position of the Ebro-Duero divide is partly controlled by the Bureba  
288 anticline. It consists of folded Middle Cretaceous to Early Miocene series, covered by  
289 undeformed Middle Miocene to Holocene deposits (Fig. 5). The anticline is orientated E-W to  
290 the west and NE-SW to the east. The western part of the Rioja trough to the west of the NE-SW  
291 directed branch of the Bureba anticline (Fig. 5), used to be drained toward the Duero basin since  
292 the Oligocene (Pineda, 1997; Mikes, 2010). The westward migration of the divide to its current  
293 location is thought to have occurred in several steps of captures as shown by the occurrence of  
294 remnants of escarpments during the Late Miocene - Pliocene (Mikes, 2010). Once the eastern  
295 branch of the Bureba anticline has been incised, the Ebro tributaries captured the western part  
296 of the Rioja trough, up to the E-W branch of the Bureba anticline to the southwest, from the  
297 Late Miocene to the Pliocene. The western part of the anticline forms a topographic ridge that  
298 is incised by Jordan river (Fig. 5) in a place where the divide between the Ebro and Duero river  
299 networks is located to the north of the ridge. To the East of this location however, the  
300 topographic ridge formed by the Bureba anticline controls the current location of the main  
301 drainage divide (Fig. 5). Here, the ridge exhibits several wind gaps, located on the northward  
302 prolongation of the Hoz, Rioseras, and Nava Solo rivers (Figs. 5, 7). Further east, the Diabolo  
303 river does not incise the ridge and its headwater is located in the core of the eastern branch of

304 the Bureba anticline, the Fuente Valley (Fig. 5). These last streams are tributaries of the Ubierna  
305 river, which is a tributary of the Arlanzon river and so, of the Duero river. To the north, the Ebro  
306 river system is represented, from west to east, by the Homino river (a tributary of the Oca river)  
307 and its four tributaries, the Molina, the Fuente Monte, the Zorica, and the San Pedro rivers (Figs.  
308 5, 7). All these streams are outlined by Late Pleistocene to Holocene alluvial series that are  
309 deposited at the bottom of their respective valleys. Valleys from the Duero side appears larger  
310 than those from the Ebro side, which are significantly more incised.

311 The Jordan river's headwater is located north of the ridge formed by the Bureba anticline. We  
312 can continuously follow its valley deposits northward along a broadly gentle slope, up to the  
313 locality of Coraegula (Fig. 5). However, the current course of the Jordan river is cut ~8 km  
314 south, in the vicinity of Hontomin, by the Homino (Ebro) river (Figs. 5B, C, 7). This fluvial  
315 capture is characterized by a well-defined and highly incised elbow of capture, already  
316 described by Pineda (1997) and Mikes (2010). The longitudinal profile of the Homino river  
317 shows a sharp knickpoint located on Hontomin (Fig. 7C). Finally, there is a small wind gap on  
318 the divide between the two opposite rivers (Figs. 5, 7).

319 To the southeast, the headwater of the Hoz river is located to the south of a wind gap cut into  
320 the Bureba ridge (Fig. 7C). To the north, in the exact prolongation of the Hoz river, the Molina  
321 river shows a bend similar to the elbow of capture previously described for the Homino river  
322 (Fig. 7) and there is a minor knickpoint located on this elbow, according to the extracted river  
323 long profile. Thus, it is likely that the Molina river used to represent the former upper reach of  
324 the Hoz river, in a period when the Ebro-Duero divide was located northward, before being  
325 captured by the Ebro network.

326 To the east, the Rioseras and the Nava Solo rivers have also their headwater located to the South  
327 of wind gaps in the Bureba ridge (Fig. 7). Similarly, in their exact prolongations, the Fuente  
328 Monte and the Zorica rivers show important elbows of capture with minor knickpoints. They  
329 may also represent former upper reaches of Duero streams that have been captured by the Ebro  
330 network (Figs. 5, 7, 8).

331 Further east, the headwater of the Diablo river is located on the depression represented by the  
332 core of the eastern branch of the Bureba anticline, the Fuente valley. In its prolongation to the  
333 northeast, the San Pedro river incises the northeastern termination of the anticline from the  
334 north before entering the valley, leading to a southward retreat of the divide (Fig. 5). Capture is  
335 again evidenced by important incision contrast between Ebro and Duero systems, and by sharp  
336 knickpoints on the upper reach of the San Pedro river long profile when crossing the Santonian  
337 dolomites (Fig. 8). According to this whole set of observations, and in agreement with previous

338 findings of Pineda (1997) and Mikes (2010), we propose that the western part of the Rioja  
339 trough, in the Bureba area has been recently captured by the Ebro drainage network leading to  
340 a sequence of southwestward retreat of the main drainage divide, toward the Duero basin (Fig.  
341 7E).

342

343 A similar capture pattern can be observed further west in the continuity of the Bureba anticline  
344 (Fig. 5). The San Anton river shows a well-defined elbow of capture accompanied by a  
345 smoothed knickpoint (See Fig. S1 in the Supplement) at its junction with the Rudron river (Ebro  
346 tributary). The river course is highly incised toward the east, along the northern flank of the  
347 WNW – ESE anticline, almost connecting to the upper reach of the Ubierna river. Valley  
348 deposits are also observed in the continuity of the Ubierna valley, which former route is  
349 suggested by a wind gap (Fig. 5). However, this domain is no longer connected to its network  
350 as it is now wandered from the North by the Nava river, a tributary of the Moradillo river, which  
351 is a tributary of the Rudron river. This domain clearly records captures leading to divide  
352 migration toward the Duero, also in favor of the Ebro basin.

353

### 354 3.3 Past position of the Ebro-Duero divide and implication for stream-power of the Duero River

355

356 We used all observations that support divide migration in the Iberian Range and Rioja trough  
357 to estimate a paleo-position of the drainage divide between the Duero and Ebro drainage basins  
358 (Fig. 9). For this purpose, we considered the location of major knickpoint along the rivers where  
359 fluvial captures are defined. Both the Ebro river and several tributaries show high elevated ~10-  
360 20 km long flat domains at ~800 – 1200 m a.s.l. and major knickpoints in the upper reach of  
361 their long profiles as the Rudron, Queiles, and Alama rivers, as well as the Homino river and  
362 its tributaries: the Puerta Nogales and Valdelanelala rivers (Figs. 5, 8; Fig. S1). All these flat  
363 domains may not be related to surface uplift as they are not clearly associated with active  
364 tectonic features. The Duero basin being characterized by a high mean elevation (~1000 m) and  
365 by a very limited incision in the vicinity of the Ebro/Duero drainage divide, a sudden divide  
366 migration toward the Duero basin is then expected to isolate such high elevated and relatively  
367 preserved surfaces. We suggest these flat domains have been recently captured by Ebro  
368 tributaries, and represent remnants of Duero drainage areas, integrated into the Ebro catchment  
369 from divide retreat toward the Duero basin. Overall, we consider a paleodrainage divide  
370 delimited by these high-elevated knickpoints and flat domains, except for the Jiloca graben area  
371 to the southeast, characterized by the occurrence of short-lived endorheic domains (Fig. 9).

372 Incision in the Ebro basin leads to the capture of new drainage areas, whereas the Duero basin  
373 recorded important loss of its own surface. The present day drainage area of the Cenozoic Duero  
374 basin, upstream of the major knickzone observed to the west in the Iberian Massif is ~63000  
375 km<sup>2</sup>. We used the paleo-divide position shown in Figure 9 to define a « recent » captured area  
376 that used to belong to the Duero basin. This area represents ~7700 km<sup>2</sup>, which corresponds to  
377 ~12% of the present-day Cenozoic Duero basin drainage area. Such a reduction of the drainage  
378 area could have strong implications on the evolution of the Duero basin, as important lowering  
379 of water and sediment fluxes, and so of incision throughout the basin. To better resolve the  
380 impact of such drainage area reduction on incision capacity, we perform a stream power analysis  
381 of the Duero river. We consider the specific stream power,  $\omega$ , defined as  $\omega = \rho g Q S / W$ , where  
382  $\rho$  is water density,  $g$  is gravitational acceleration,  $Q$  is discharge,  $S$  is local river gradient, and  
383  $W$  is river width (see the Supplement for details of the calculation). We calculate  $\omega$  for the  
384 present-day Duero river, and for a restored ancient Duero river that drained this 12% of lost  
385 area. We plot the difference (ancient – present day) between the two curves in Figure 10, with  
386 the Duero river long profile. Calculated difference in specific stream power values are relatively  
387 low ( $< 2 \text{ W m}^{-2}$ ) for the upstream part of the basin, but increase to  $\sim 5 \text{ W m}^{-2}$  when approaching  
388 the major knickzone at a distance of  $\sim 350 \text{ km}$  from the river mouth. The knickzone is  
389 characterized by peak values exceeding  $10 \text{ W m}^{-2}$ , which rapidly decrease to  $\sim 0 \text{ W m}^{-2}$  at the  
390 base of the knickzone ( $\sim 200 \text{ km}$ ) and up to the river mouth (Fig. 10). Some alternating peak  
391 and null values are observed in the lower reach of the river and may be related to the occurrence  
392 of numerous dams along the river. Overall, the specific stream power calculated for the ancient  
393 Duero river show higher values than for the present day from the base of the knickzone to the  
394 uppermost reach of the river (Fig. 10). This implies a general decrease of the Duero river's  
395 incision capacity between this ancient state to the present day, magnified on the knickzone.

396

### 397 3.4 $\chi$ map

398

399 The comparison of the shape of longitudinal profiles of rivers across divide is a way that has  
400 been proposed recently to infer disequilibrium between rivers and the potential migration of  
401 their divide (Willett et al., 2014). The  $\chi$ -analysis of river profiles (Perron and Royden, 2012) is  
402 a powerful tool to evidence differences in the equilibrium state of rivers across divide, and then  
403 to infer their migration (Willett et al., 2014). This method is based on a coordinate  
404 transformation allowing linearizing river profiles (Perron and Royden, 2012). Considering

405 constant uplift rate (U) and erodibility (K) in time and space the  $\chi$ -transformed profile of a river  
406 is defined by the following equation (Perron and Royden, 2012; Mudd et al., 2014):

407

$$408 \quad z(x) = z_b(x_b) + \left(\frac{U}{KA_0^m}\right)^{1/n} \chi$$

409

410 with

$$411 \quad \chi = \int_{x_b}^x \left(\frac{A_0}{A(x)}\right)^{\frac{m}{n}} dx$$

412 where  $z(x)$  is the elevation of the channel,  $x$  is the longitudinal distance,  $z_b$  is the elevation at  
413 the river's base level (distance  $x_b$ ),  $A$  is the drainage area,  $A_0$  is a reference drainage area, and  
414 exponents  $m$  and  $n$  are empirical constants.

415

416 When using the  $\chi$  variable instead of the distance for plotting the elevation  $z$  along channel, ( $\chi$ -  
417 plot), the longitudinal profile of a steady-state channel is shown as a straight line (Perron and  
418 Royden, 2012). Any channel pulled away from this line is in disequilibrium and is then expected  
419 to attempt to reach equilibrium. Mapping  $\chi$  on several watersheds and comparing  $\chi$  across  
420 drainage divides is then a potential way to high disequilibrium between rivers across divide and  
421 to elucidate divide migration and drainage reorganization through captures (Willett et al., 2014).  
422 We used the  $\chi$ -analysis Tool developed by Mudd et al. (2014) to select the best  $m/n$  ratio by  
423 iteration (Perron and Royden, 2012) and to calculate  $\chi$  for rivers throughout the divide between  
424 the Ebro and Duero basins from a similar base level at 850 m a.s.l. The best mean  $m/n$  ratio for  
425 all our streams is 0.425, which falls in the typical range of values observed for rivers ( $\sim 0.4 -$   
426  $0.6$ : e.g. Kirby and Whipple, 2012). The resulting map (Fig. 11) shows  $\chi$  values calculated on  
427 different opposite streams in the vicinity of the Ebro/Duero drainage divide. Similar values on  
428 both sides of the divide suggest the two opposite streams are at equilibrium, whereas strong  
429 contrasted  $\chi$  values imply disequilibrium leading to divide migration, continuously or through  
430 fluvial capture, toward the high  $\chi$  values (Willett et al., 2014). The map of  $\chi$  values actually  
431 shows significant contrasting values across the Ebro/Duero divide. We comment here these  
432 contrasts along the divide from the SE to the NW of the area considered (Fig. 11).

433 There is a strong contrast in  $\chi$  values between the headwater of the Jalon river (Fig. 11),  
434 characterized by low values ( $\sim 300$  m), and the closest part from the divide of the Bordecorex  
435 river (Fig. 4), a tributary of the Duero river ( $\sim 500$  m). Such a disequilibrium implies divide  
436 migration toward the Duero basin, predicting the capture of the uppermost reach of the

437 Bordecorex river by the Jalon river. To the north, tributaries of the Jalon river show slightly  
438 lower  $\chi$  values than the tributaries of the Duero river. This suggests a relative stable situation  
439 although small captures may occur toward the Duero basin. A higher contrast is observed  
440 around the easternmost part of the Duero basin, which is surrounded by the Ebro basin. The  
441 Araviana river (tributary of the Duero river) seems to be taken in a bottleneck between the  
442 Manubles river to the south and the Queiles river to the north (Fig. 4), which both show lower  
443  $\chi$  values (Fig. 11). Toward the east, there is a strongest  $\chi$  values contrast between headwaters  
444 of the Araviana river (>700 m) and of the Isuela (Jalon tributary) and Huecha rivers (<100 m).  
445 This domain appears clearly in disequilibrium and is expected to be captured by the Ebro  
446 drainage network. Such high  $\chi$  values differences appear also to the northwest (Fig. 11), in the  
447 southern part of the Cameros basin where the Duero river and its tributaries' headwaters show  
448  $\chi$  values >500-700 m, whereas the facing rivers (Alama, Cidacos, Iregua, and Najerilla) are all  
449 characterized by low  $\chi$  values <100 m. This predicts important disequilibrium and divide  
450 migration and fluvial captures toward the south. Northwestward,  $\chi$  values between Duero and  
451 Ebro network are more similar indicating that the divide is relatively more stable here, up to the  
452 westernmost part of the Ebro basin (Fig. 11). However, there are some slight localized  $\chi$  value  
453 contrasts (~200 / ~450 m) as observed between the Tiron and the Arlanzon rivers, between the  
454 Rudron and the Ubierna and Urbel rivers, and between the Ebro and the Pisuerga rivers (Fig.  
455 11). It suggests minor local captures toward the Duero basin.

456

457 To sum up,  $\chi$  values calculated in the vicinity of the drainage divide between the Ebro and  
458 Duero river networks show a general disequilibrium (Fig. 11) as the Ebro network is  
459 characterized by low  $\chi$  values (up to ~200-300 m) compared to those for the Duero network  
460 (up to ~450-700 m). In complement with all the evidence of divide displacements induced by  
461 captures described previously this allows predicting a general divide migration toward the  
462 Duero basin through headwater retreat, in favor of the Ebro tributaries, especially around the  
463 Almazan subbasin, which is expected to be entirely captured by the Ebro basin.

464

## 465 **4. Discussion**

466

### 467 4.1 Long term trend of divide migration

468

469 The oldest capture evidence in our study area corresponds to the incision of the northern part  
470 of the Iberian Range by the Jalon river and by the capture of the Calatayud basin, attributed to  
471 the post-Messinian (Gutiérrez-Santolalla et al. 1996). We propose, based on morphological  
472 evidence (Fig. 4) and in agreement with stratigraphic data (Gutiérrez-Santolalla et al. 1996),  
473 that the Jalon river system captured the Jiloca graben to the east since the Early Pleistocene,  
474 before progressively capturing the Almazan subbasin toward the west in the Holocene  
475 (Gutiérrez-Santolalla et al. 1996). From  $\chi$ -analysis (Fig. 11), we deduce that the eastern part of  
476 the Duero basin, the Almazan subbasin, is being actively captured by Ebro tributaries that  
477 drained the Iberian Range and the Cameros basin. Despite low contrasts in  $\chi$  values, local  
478 captures are also suggested in the vicinity of the Ebro / Duero drainage divide toward the  
479 northwest. Capture is further implied by the occurrence of numerous high elevated (~1000 m)  
480 knickpoints and low-relief surfaces (Figs. 5, 8, 9, 11).

481 Thus, there is a good correlation between  $\chi$  evidence and morphological and stratigraphic data  
482 implying long-lasting captures and divide migration during Pliocene, Pleistocene, and  
483 Holocene times in favor of the Ebro basin.

484

485 The pursuit of such a long-term capture trend may be driven by tectonic and/or climatic forcing  
486 (Willett, 1999; Montgomery et al., 2001; Sobel et al., 2003; Sobel and Strecker, 2003; Bonnet,  
487 2009; Whipple, 2009; Castelltort et al., 2012; Kirby and Whipple, 2012; Goren et al., 2015; Van  
488 der Beek et al., 2016). However, such long-term trend in drainage reorganization may also occur  
489 in tectonically quiescent domains, independently of external forcing (Prince et al., 2011). Here,  
490 the Iberian Range and the Cameros basin recorded extension pulses from the Late Miocene to  
491 the Early Pleistocene, responsible for the formation of several grabens as previously described  
492 (Gutiérrez-Santolalla et al., 1996; Capote et al., 2002). Extension events are also recorded  
493 during the Holocene, nevertheless, the youngest erosion surface of Late Pliocene-Early  
494 Pleistocene age observed in our study area shows no tectonic-related deformation and  
495 reworking, suggesting that tectonic activity is reduced here (Gutiérrez-Elorza and Gracia,  
496 1997). This is also consistent with the relative scarcity of seismic activity observed in our study  
497 area, compared, for instance, to the Pyrenees, or to the Betics (Herraiz et al., 2000; Lacan and  
498 Ortuño, 2012). We consequently propose that local tectonic activity is not the main driver of  
499 the capture histories documented here, as most capture events postdate the cessation of tectonic  
500 activity, and occur during periods of quiescence (Gutiérrez-Santolalla et al., 1996).

501

502 The Cameros Massif is characterized by relatively high mean annual precipitation up to ~1000  
503 mm/an (Fig. 6) with high elevation (~1400-2200 m) in comparison with the surrounding areas.  
504 This contrasts with the adjacent Ebro and Duero basins where low precipitation rates, of ~400-  
505 500 mm/an (Hijmans et al., 2005), illustrate subarid climate conditions. The Cameros area is  
506 the only place in our study area where a contrast in precipitation pattern (Fig. 6) would  
507 potentially drive a migration of the divide toward the drier, Duero area. Given that the same  
508 pattern is observed everywhere, even where there isn't any precipitation difference, we suggest  
509 that the present day climatic condition is unlikely to control the general pattern of current  
510 drainage reorganization between the Ebro and Duero basins. During the Pliocene and the  
511 Pleistocene, the climatic record in the northern Iberian Peninsula is characterized by alternations  
512 between similar subarid conditions and intense glaciation. Paleoclimate proxies do not allow to  
513 highlight past precipitation differences along the divide that could explain past drainage  
514 reorganization. Moreover, there is no clear evidence of important glacier development and  
515 related erosion in our study area, especially for the Cameros basin and the Iberian Range  
516 (Ortigosa, 1994; García-Ruiz et al., 1998, 2016; Pellicer and Echeverría, 2004). This indicates  
517 that drainage evolution between the Ebro and Duero basins is unlikely to be related to climatic  
518 evolution.

519

520 4.2 Excavation of the Ebro basin as the main factor controlling divide migration and limiting  
521 incision of the Duero river

522

523 A striking morphological feature for river capture in our study area is the important contrast in  
524 the incision pattern (e.g. Fig. 1B) from one side of the divide to the other. This suggests that the  
525 incision capacity of the river network is the main driver for capture and divide migration. Both  
526 tectonic and climatic forcing does not appear to control drainage reorganization between the  
527 Ebro and Duero basins.

528 The opening of the Ebro basin toward the Mediterranean Sea during the Late Miocene led to  
529 widespread excavation (García-Castellanos et al., 2003, García-Castellanos and Larrasoña,  
530 2015), favored by more humid and seasonal climatic conditions (Calvo et al., 1993; Alonso-  
531 Zarza and Calvo, 2000). By contrast, incision related to the opening of the Duero basin toward  
532 the Atlantic Ocean is concentrated to the west in the Iberian Massif, characterized by a  
533 largescale knickzone (150 km long and 500 m high) in the Duero river long profile (Fig. 1B).  
534 This contrasts with the limited eastward propagation of incision in the Cenozoic part of the  
535 basin (Antón et al., 2012, 2014), despite climatic conditions similar to the Ebro basin. An



536 explanation resides in the fact that the resistant Iberian Massif basement rocks may have  
537 controlled and limited incision and drainage reorganization in the Cenozoic Duero basin (Antón  
538 et al., 2012). The Duero profile upstream of this major knickzone may be considered as a high  
539 elevated local base level for its tributaries there. Difference between the Ebro and Duero base-  
540 levels implies a major contrast in fluvial dynamics. We suggest the systematic and long-term  
541 trend of divide migration toward the Duero basin and fluvial capture in favor of the Ebro basin  
542 is driven by the differential incision behavior, controlled by base-level difference.

543 Our stream power analysis along the Duero river (Fig. 10) shows that the difference in drainage  
544 area of the Duero inferred from our paleo-divide map (Fig. 9) induces a noticeable decrease of  
545 stream power values of the Duero in the vicinity of the knickzone. This stream power is a  
546 minimum estimate because calculation does not take into account possible captures and divide  
547 migration in other areas along the Duero basin divide, nor the full history of the divide migration  
548 through time and the related ongoing decrease in water discharge as documented in laboratory-  
549 scale landscape experiments (Bonnet, 2009). Some contrasts of incision are also observed in  
550 the Iberian Range along the southern border of the Duero, and in the Cantabrian domain to the  
551 North. Both show more important incision than in the Duero basin, suggesting potential river  
552 captures and divide migration at the expense of the Duero basin, increasing the total of lost  
553 drainage area. Even if it gives minimal estimate, our stream power analysis suggests that  
554 drainage area reduction may have limited the erosion in the Duero basin. This provides an  
555 explanation for the preservation of the lithologic barrier to the west, along the main knickzone  
556 of the Duero considered as an intermediate, local base level (Antón et al., 2012). We propose  
557 that the reduction of the Duero drainage area caused by captures and incision in the Ebro basin,  
558 is responsible for a significant decrease of the incision capacity in the Duero basin. We infer  
559 that the ongoing drainage network growth in the Ebro basin may be responsible for the current  
560 preservation of large morphological relicts of the-endorheic stage in the Duero basin.

561 The opening of the Ebro basin toward the Mediterranean Sea resulted in a drastic base level  
562 drop. This results in the establishment of an upstream-migrating incision wave that propagates  
563 to every tributary of the Ebro network, responsible for knickpoints migration (Schumm et al.,  
564 1987; Whipple and Tucker, 1999; Yanites et al., 2013) and for drainage reorganization and  
565 divide migration. The  $\chi$ -analysis that we performed along the current Ebro-Duero divide (Fig.  
566 11) highlights areas where geomorphic disequilibrium is still ongoing, which suggests that they  
567 are areas where divide is currently mobile. The modelling study performed by Garcia-  
568 Castellanos and Larrasoña (2015) suggests that the re-opening of the Ebro basin occurred  
569 between 12.0 and 7.5 Ma. This indicates that the growth of the drainage network of the Ebro

570 basin and the establishment of new steady-state conditions is a long-lived phenomenon, which  
571 is still not achieved today.

572

## 573 **Conclusion**

574

575 In this paper we present a morphometric analysis of the landscape along the divide between the  
576 Ebro and Duero drainage basins located in the northern part of the Iberian Peninsula. This area  
577 shows numerous evidence of river captures by the Ebro drainage network resulting in a long-  
578 lasting migration of their divide, toward the Duero basin. Although these two basins record a  
579 similar geological history, with a long endorheic stage during Oligocene and Miocene times,  
580 they show a very contrasted incision and preservation state of their original endorheic  
581 morphology. Since the Late Miocene, the Ebro basin was opened to the Mediterranean Sea and  
582 record important erosion. On the opposite, the Duero was opened to the Atlantic Ocean since  
583 the Late Miocene – Early Pliocene but its longitudinal profile exhibits a pronounced knickpoint,  
584 which delimits an upstream domain of low relief and limited incision, likely representing a  
585 relict of its endorheic topography. We propose that this contrast of incision is the main driver  
586 of the migration of divide that we document. The morphological analysis of rivers across the  
587 divide highlights areas where geomorphic disequilibrium is still ongoing, which suggests that  
588 the Ebro-Duero divide is currently mobile. The quantification of the decrease of the drainage  
589 area of the Duero based on the reconstruction of a paleo-position of the Ebro-Duero divide  
590 shows that the divide migration results in a significant lowering of the stream power of the  
591 Duero river, particularly along its knickzone. We suggest that divide migration induces a  
592 decrease of the incision capacity of the Duero river, thus favoring the preservation of large  
593 relicts of the endorheic morphology in the upstream part of this basin.

594

595

## 596 Author contributions

597 AV undertook morphometric modeling and interpretation, and wrote the paper. SB and FM  
598 contributed to the interpretation and the writing.

599

600

## 601 Competing interests.

602 The authors declare that they have no conflict of interest.

603

604 Acknowledgements.

605 This study was funded by the OROGEN Project, a TOTAL-BRGM-CNRS consortium. We  
606 thank two reviewers and associated Editor Veerle Vanacker for very useful and constructive  
607 comments that greatly helped us to clarify and improve this manuscript.

608

609

610 References

611

612 Alonso-Zarza, A. M. and Calvo, J. P.: Palustrine sedimentation in an episodically subsiding  
613 basin: the Miocene of the northern Teruel Graben (Spain), *Palaeogeog., Palaeoclimatol.,*  
614 *Palaeoecol.*, 160, 1-21, 2000.

615

616 Alonso-Zarza, A. M., Armenteros, I., Braga, J. C., Muñoz, A., Pujalte, V., Ramos, E., Aguirre,  
617 J., Alonso-Gavilán, G., Arenas, C., Ignacio Baceta, J., Carballeira, J., Calvo, J. P., Corrochano,  
618 A., Fornós, J. J., González, A., Luzón, A., Martín, J. M., Pardo, G., Payros, A., Pérez, A., Pomar,  
619 L., Rodríguez, J. M., and Villena, J.: Tertiary, in: *The Geology of Spain*, Gibbons, W. and  
620 Moreno, T. (Eds.): The Geological Society, London, 293-334, 2002.

621

622 Antón, L., Rodés, A., De Vicente, G., Pallàs, R., Garcia-Castellanos, D., Stuart, F. M., Braucher,  
623 R., and Bourlès, D.: Quantification of fluvial incision in the Duero Basin (NW Iberia) from  
624 longitudinal profile analysis and terrestrial cosmogenic nuclide concentrations, *Geomorph.*,  
625 165-166, 50-61, <https://doi.org/10.1016/j.geomorph.2011.12.036>, 2012.

626

627 Antón, L., Rodés, A., De Vicente, G., and Stokes, M.: Using river long profiles and geomorphic  
628 indices to evaluate the geomorphological signature of continental scale drainage capture, Duero  
629 basin (NW Iberia), *Geomorph.*, 206, 250-261, <https://doi.org/10.1016/j.geomorph.2013.09.028>,  
630 2014.

631

632 Babault, J., Loget, N., Van Den Driessche, J., Castelltort, S., Bonnet, S., and Davy, P.: Did the  
633 Ebro basin connect to the Mediterranean before the Messinian salinity crisis ?, *Geomorph.*, 81,  
634 155-165, <https://doi.org/10.1016/j.geomorph.2006.04.004>, 2006.

635

636 Barrón, E., Postigo-Mijarra, J. M., and Casas-Gallego, M.: Late Miocene vegetation and climate  
637 of the La Cerdanya Basin (eastern Pyrenees, Spain), *Rev. Palaeobot. Palynol.*, 235, 99-119,  
638 <https://doi.org/10.1016/j.revpalbo.2016.08.007>, 2016.

639

640 Bartolomé, M., Sancho, C., Moreno, A., Oliva-Urcia, B., Belmonte, Á., Bastida, J., Cheng, H.,  
641 and Edwards, R. L.: Upper Pleistocene interstratal piping-cave speleogenesis: The Seso Cave  
642 System (Central Pyrenees, Northern Spain), *Geomorph.*, 228, 335-344,  
643 <https://doi.org/10.1016/j.geomorph.2014.09.007>, 2015.

644

645 Bessais, E. and Cravatte, J.: Les écosystèmes végétaux Pliocènes de Catalogne Méridionale.  
646 Variations latitudinales dans le domaine Nord-Ouest Méditerranéen, *Geobios*, 21, 49-63, 1988.

647

648 Bond, J.: Tectono-sedimentary evolution of the Almazan Basin, NE Spain, in: Friend, F. and  
649 Dabrio, C. (Eds.): *Tertiary Basins of Spain: the Stratigraphic Record of Crustal Kinematics,*  
650 *World and Regional Geology*, 6, Cambridge University Press, Cambridge, 203-213, 1996.

651

652 Bonnet, S.: Shrinking and splitting of drainage basins in orogenic landscapes from the migration  
653 of the main drainage divide, *Nat. Geosc.*, 90, 766-771, <https://doi.org/10.1038/NGEO666>,  
654 2009.

655

656 Brocklehurst, S. H. and Whipple, K. X.: Glacial erosion and relief production in the Eastern  
657 Sierra Nevada, California, *Geomorph.*, 42, 1-24, 2002.

658

659 Calvo, J. P., Daams, R., and Morales, J.: Up-to-date Spanish continental Neogene synthesis and  
660 paleoclimatic interpretation. *Revista de la Sociedad Geologica de España*, 6, 29-40, 1993.

661

662 Cameselle, A.J., Urgeles, R., De Mol, B., Camerlenghi, A., and Canning, J.C., Late Miocene  
663 sedimentary architecture of the Ebro Continental Margin (Western Mediterranean; Implications  
664 for the Messinian Salinity Crisis. *Int. J. Earth Sci.*, 103, 423-440, 2014.

665

666 Capote, R., Muñoz, J. A., Simón, J. L., Liesa, C. L., and Arlegui, L. E.: Alpine tectonics 1: the  
667 Alpine system north of the Betic Cordillera, in: *The Geology of Spain*, Gibbons, W. and  
668 Moreno, T. (Eds.): *The Geological Society*, London, 367-400, 2002.

669

670 Castellort, S., Goren, L., Willett, S. D., Champagnac, J. D., Herman, F., and Braun, J.: River  
671 drainage patterns in the New Zealand Alps primarily controlled by plate tectonic strain. *Nat.*  
672 *Geosci.*, 5, 744–748, <https://doi.org/10.1038/ngeo1582>, 2012.

673

674 Colomer i Busquets, M., and Santanach i Prat, P.: Estructura y evolucion del borde sur-  
675 occidental de la Fosa de Calatayud-Daroca, *Geogaceta*, 4, 29-31, 1988.

676

677 Coney, P. J., Muñoz, J. A., McClay, K. R., and Evenchick, C. A.: Syntectonic burial and post-  
678 tectonic exhumation of the southern Pyrenees foreland fold-thrust belt, *J. Geol. Soc. London*,  
679 153, 9-16, <https://doi.org/10.1144/gsjgs.153.1.0009>, 1996.

680

681 Costa, E., Garcés, M., López-Blanco, M., Beamud, E., Gómez-Paccard, M., and Larrasoaña, J.  
682 C.: Closing and continentalization of the South Pyrenean foreland basin (NE Spain):  
683 magnetochronological constraints, *Basin Res.*, 22, 904-917, <https://doi.org/10.1111/j.1365->  
684 [2117.2009.00452.x](https://doi.org/10.1111/j.1365-2117.2009.00452.x), 2010.

685

686 Delmas, M., Calvet, M., and Gunnell, Y.: Variability of Quaternary glacial erosion rates – A  
687 global perspective with special reference to the Eastern Pyrenees, *Quat. Sci. Rev.*, 28, 484-498,  
688 <https://doi.org/10.1016/j.quascirev.2008.11.006>, 2009.

689

690 Del Rio, P., Barbero, L., and Stuart, F. M.: Exhumation of the Sierra de Cameros (Iberian Range,  
691 Spain): constraints from low-temperature thermochronologie, in: Liesker, F., Ventura, B., and  
692 Glasmacher, U. A. (Eds.): *Thermochronological Methods: From Palaeotemperature Constraints*  
693 *to Landscape Evolution Models*, Geological Society, London, Special Publications, 324, 154-  
694 166, <https://doi.org/10.1144/SP324.12>, 2009.

695

696 De Vicente, G., Vegas, R., Muñoz, M. A., Silva, P. G., Andriessen, P., Cloetingh, S., González-  
697 Casado, J. M., Van Wees, J. D., Álvarez, J., Carbó, A., and Olaiz, A.: Cenozoic thick-skinned  
698 deformation and topography evolution of the Spanish Central System, *Glob. Planet. Change*,  
699 58, 335-381, <https://doi.org/10.1016/j.gloplacha.2006.11.042>, 2007.

700

701 Duval, M., Sancho, C., Calle, M., Guilarte, V., and Peña-Monné, J. L.: On the interest of using  
702 the multiple center approach in ESR dating of optically bleached quartz grains: Some examples

703 from the Early Pleistocene terraces of the Alcanadre River (Ebro basin, Spain), *Quat.*  
704 *Geochronol.*, 29, 58-69, <https://doi.org/10.1016/j.quageo.2015.06.006>, 2015.

705

706 Fillon, C. and Van der Beek, P.: Post-orogenic evolution of the southern Pyrenees: constraints  
707 from inverse thermo-kinematic modelling of low-temperature thermochronology data, *Basin*  
708 *Res.*, 23, 1-19, <https://doi.org/10.1111/j.1365-2117.2011.00533.x>, 2012.

709

710 Fillon, C., Gautheron, C., and Van der Beek, P.: Oligocene-Miocene burial and exhumation of  
711 the Southern Pyrenean foreland quantified by low-temperature thermochronology, *J. Geol. Soc.*  
712 *London*, 170, 67-77, <https://doi.org/10.1144/jgs2012-051>, 2013.

713

714 Garcia-Castellanos, D.: Long-term evolution of tectonic lakes: Climatic controls on the  
715 development of internally drained basins, *Geol. Soc. Am., Spec. Paper*, 398, 283-294,  
716 [https://doi.org/10.1130/2006.2398\(17\)](https://doi.org/10.1130/2006.2398(17)), 2006.

717

718 Garcia-Castellanos, D. and Larrasoaña, J. C.: Quantifying the post-tectonic topographic  
719 evolution of closed basins: The Ebro basin (northeast Iberia), *Geology*, 43, 663-666,  
720 <https://doi.org/10.1130/G36673.1>, 2015.

721

722 Garcia-Castellanos, D., Vergés, J., Gaspar-Escribano, J., and Cloething, S.: Interplay between  
723 tectonics, climate, and fluvial transport during the Cenozoic evolution of the Ebro Basin (NE  
724 Iberia), *J. Geophys. Res.*, 108, 2347, <https://doi.org/10.1029/2002JB002073>, 2003.

725

726 García-Ruiz, J. M., Ortigosa, L. M., Pellicer, F., and Arnáez, J.: Geomorfología glaciar del  
727 Sistema Ibérico, in: Gómez-Ortiz, A. and Pérez-Alberti, A. (Eds.): *Las huellas glaciares de las*  
728 *montañas españolas*, Universidad de Santiago de Compostela, 347-381, 1998.

729

730 García-Ruiz, J. M., Palacios, D., González-Sampériz, P., De Andrés, N., Moreno, A., Valero-  
731 Garcés, B., and Gómez-Villar, A.: Mountain glacier evolution in the Iberian Peninsula during  
732 the Younger Dryas, *Quat. Sci. Rev.*, 138, 16-30,  
733 <https://doi.org/10.1016/j.quascirev.2016.02.022>, 2016.

734

735 Goren, L., Castelltort, S., and Klinger, Y.: Modes and rates of horizontal deformation from  
736 rotated river basins: Application to the Dead Sea fault system in Lebanon, *Geology*, 43, 843-  
737 846, <https://doi.org/10.1130/G36841.1>, 2015.

738

739 Gracia, F. J.: Tectonica pliocena de la Fosa de Daroca (prov. De Zaragoza), *Geogaceta*, 11, 127-  
740 129, 1992.

741

742 Gracia, F. J.: Evolucion cuaternaria del rio Jiloca (Cordillera Iberica Central), in: Fumanal, M.  
743 P. and Bernabeu, J. (Eds.): *Estudios sobre Cuaternario, Medios Sedimentarios, Cambios*  
744 *Ambientales, Habitat Humano*, Valencia, 43-51, 1993a.

745

746 Gracia, F. J.: Evolucion geomorfologica de la region de Gallocanta (Cordillera Iberica Central),  
747 *Geographicalia*, 30, 3-17, 1993b.

748

749 Gracia, F. J., Gutiérrez-Santolalla, F., and Gutiérrez-Elorza, M.: Evolucion geomorfologica del  
750 polje de Gallocanta (Cordillera Ibérica), *Revista Sociedad Geologica de España*, 12, 351-368,  
751 1999.

752

753 Gracia, F. J. and Cuchi, J. A.: Control tectonico de los travertinos fluviales del rio Jiloca  
754 (Cordillera Ibérica), in: *El Cuaternario en España y Portugal, Actas 2a Reun. Cuat. Ibérico,*  
755 *AEQUA y CTPEQ*, Madrid-1989, 2, 697-706, 1993.

756

757 Guimerà, J., Mas, R., and Alonso, Á: Intraplate deformation in the NW Iberian Chain: Mesozoic  
758 extension and Tertiary contractional inversion, *J. Geol. Soc. London*, 161, 291-303,  
759 <https://doi.org/10.1144/0016-764903-055>, 2004.

760

761 Gutiérrez-Elorza, M. and Gracia, F. J.: Environmental interpretation and evolution of the  
762 Tertiary erosion surfaces in the Iberian Range (Spain), in: Widdowson, M. (Ed.):  
763 *Palaeosurfaces: Recognition, Reconstruction and Palaeoenvironmental Interpretation,*  
764 *Geological Society Special Publication*, 120, 147-158, 1997.

765

766 Gutiérrez-Elorza, M., García-Ruiz, J. M., Goy, J. L., Gracia, F. J., Gutiérrez-Santolalla, F.,  
767 Martí, C., Martín-Serrano, A., Pérez-González, A., and Zazo, C.: Quaternary, in: *The Geology*  
768 *of Spain*, Gibbons, W. and Moreno, T. (Eds.): *The Geological Society*, London, 335-366, 2002.

769

770 Gutiérrez-Santolalla, F., Gracia, F. J., and Gutiérrez-Elorza, M.: Consideraciones sobre el final  
771 del relleno endorreico de las fossa de Calatayud y Teruel y su paso al exorreismo. Implicaciones  
772 morfoestratigráficas y estructurales, in : Grandal d'Ánglade, A. and Pagés-Valcarlos, J. (Eds.) :  
773 IV Reunion de Geomorfología, Sociedad Española de Geomorfología, O Castro (A Coruña),  
774 23-43, 1996.

775

776 Herraiz, M., De Vicente, G., Lindo-Ñaupari, R., Giner, J., Simón, J. L., González-Casado, J.  
777 M., Vadillo, O., Rodríguez-Pascua, M. A., Cicuéndez, J. I., Casas, A., Cabañas, L., Rincón, P.,  
778 Cortés, A. L., Ramírez, M., and Lucini, M.: *Tectonics*, 19, 762-786, 2000.

779

780 Hijmans, R. J., Cameron, S. E., Parra, J. L., Jones, P. G., and Jarvis, A.: Very high resolution  
781 interpolated climate surfaces for global land areas, *Int. J. Climatol.*, 25, 1965-1978,  
782 <https://doi.org/10.1002/joc.1276>, 2005.

783

784 Jiménez-Moreno, G., Fauquette, S., and Suc, J. P.: Miocene to Pliocene vegetation  
785 reconstruction and climate estimates in the Iberian Peninsula from pollen data, *Rev. Palaeobot.*  
786 *Palynol.*, 162, 403-415, <https://doi.org/10.1016/j.revpalbo.2009.08.001>, 2010.

787

788 Jiménez-Moreno, G., Burjachs, F., Expósito, I., Oms, O., Carrancho, Á., Villalaín, J. J., Agustí,  
789 J., Campeny, G., Gómez de Soler, B., and Van der Made, J.: Late Pliocene vegetation and  
790 orbital-scale climate changes from the western Mediterranean area, *Global Planet. Change*, 108,  
791 15-28, <https://doi.org/10.1016/j.gloplacha.2013.05.012>, 2013.

792

793 Jurado, M. J. and Riba, O.: The Rioja area (westernmost Ebro basin): a ramp valley with  
794 neighbouring piggybacks, in: Friend, P. and Dabrio, C. (Eds.): *Tertiary basins of Spain*, *World*  
795 *and Regional Geology*, 6, Cambridge University Press, Cambridge, 173-179, 1996.

796

797 Kirby, E. and Whipple, K. X.: Expression of active tectonics in erosional landscapes, *J. Struct.*  
798 *Geol.*, 44, 54-75, <https://doi.org/10.1016/j.jsg.2012.07.009>, 2012.

799

800 Kuhlemann, J., Frisch, W., Dunkl, I., Székely, D., and Spiegel, C.: Miocene shifts of the  
801 drainage divide in the Alps and their foreland basin, *Z. Geomorph.*, 45, 239-265, 2001.

802



803 Lacan, P. and Ortuño, M.: Active tectonics of the Pyrenees: a review, *J. Iberian Geol.*, 38, 9-30,  
804 [https://doi.org/10.5209/rev\\_JIGE.2012.v38.n1.39203](https://doi.org/10.5209/rev_JIGE.2012.v38.n1.39203), 2012.

805

806 Larrasoaña, J. C., Murelaga, X., and Garcés, M.: Magnetobiochronology of Lower Miocene  
807 (Ramblian) continental sediments from the Tuleda Formation (western Ebro basin, Spain), *Ea.*  
808 *Planet. Sci. Lett.*, 243, 409-423, <https://doi.org/10.1016/j.epsl.2006.01.034>, 2006.

809

810 López-Blanco, M., Marzo, M., Burbank, D. W., Vergés, J., Roca, E., Anadón, P., and Piña, J.:  
811 Tectonic and climatic controls on the development of foreland fan deltas: Montserrat and Sant  
812 Llorenç del Munt systems (Middle Eocene, Ebro Basin, NE Spain), *Sediment. Geol.*, 138, 17-  
813 39, 2000.

814

815 López-Martínez, N., García-Moreno, E., and Álvarez-Sierra, A.: Paleontología y  
816 bioestratigrafía (micromamíferos) del Mioceno medio y superior del sector central de la cuenca  
817 del Duero, *Studia Geologica Salmanticensia*, Ediciones Universidad Salamanca, 22, 191-212,  
818 1986.

819

820 Martín-Chivelet, J., Berástegui, X., Rosales, I., Vilas, L., Vera, J. A., Caus, E., Gräfe, K. U.,  
821 Mas, R., Puig, C., Segura, M., Robles, S., Floquet, M., Quesada, S., Ruiz-Ortiz, P. A., Fregenal-  
822 Martínez, M. A., Salas, R., Arias, C., García, A., Martín-Algarra, A., Meléndez, M. N., Chacón,  
823 B., Molina, J. M., Sanz, J. L., Castro, J. M., García-Hernández, M., Carenas, B., García-  
824 Hidalgo, J., Gil, J., and Ortega, F.: Cretaceous, in: *The Geology of Spain*, Gibbons, W. and  
825 Moreno, T. (Eds.): The Geological Society, London, 255-292, 2002.

826

827 Martín-Serrano, A.: La definición y el encajamiento de la red fluvial actual sobre el macizo  
828 hesperico en el marco de su geodinamica alpina, *Rev. Soc. Geol. España*, 4, 337-351, 1991.

829

830 Mikeš, D.: The Upper Cenozoic evolution of the Duero and Ebro fluvial systems (N-Spain):  
831 Part 1. Paleogeography; Part 2. Geomorphology, *Cent. Eur. J. Geosci.*, 2, 320-332,  
832 <https://doi.org/10.2478/v10085-010-0017-4>, 2010.

833

834 Montgomery, D. R., Balco, G., and Willett, S. D.: Climate, tectonics, and the morphology of  
835 the Andes, *Geology*, 29, 579-582, 2001.

836

837 Moreno, D., Falguères, C., Pérez-González, A., Duval, M., Voinchet, P., Benito-Calvo, A.,  
838 Ortega, A. I., Bahain, J. J., Sala, R., Carbonell, E., Bermúdez de Castro, J. M., and Arsuaga, J.  
839 L.: ESR chronology of alluvial deposits in the Arlanzon valley (Atapuerca, Spain):  
840 Contemporaneity with Atapuerca Gran Dolina site, *Quat. Geochronol.*, 10, 418-423,  
841 <https://doi.org/10.1016/j.quageo.2012.04.018>, 2012.

842

843 Moreno, D., Belmonte, A., Bartolomé, M., Sancho, C., Oliva, C., Stoll, H., Edwards, L. R.,  
844 Cheng, H., and Hellstrom, J.: Formacion de espeleotemas en el noreste peninsular y su relacion  
845 con las condiciones climaticas durante los ultimos ciclos glaciares, *Cuadernos de Investigacion*  
846 *Geografica*, 39, 25-47, 2013.

847

848 Mudd, S., Attal, M., Milodowski, D. T., Grieve, S. W. D., and Valters, D. A.: A statistical  
849 framework to quantify spatial variation in channel gradients using the integral method of  
850 channel profile analysis, *J. Geophys. Res.- Earth Surf.*, 119, 138-152,  
851 <https://doi.org/10.1002/2013JF002981>, 2014.

852

853 Muñoz-Jiménez, A. and Casas-Sainz, A. M.: The Rioja Trough (N Spain): tectonosedimentary  
854 evolution of a symmetric foreland basin, *Basin Res.*, 9, 65-85, 1997.

855

856 Nivière, B., Lacan, P., Regard, V., Delmas, M., Calvet, M., Huyghe, D., and Roddaz, B.:  
857 Evolution of the Late Pleistocene Aspe River (Western Pyrenees, France). Signature of climatic  
858 events and active tectonics, *Comptes Rendus Geosci.*, 348, 203-212, <https://doi.org/10.1016/j.crte.2015.07.003>, 2016.

859 <https://doi.org/10.1016/j.crte.2015.07.003>, 2016.

860

861 Ortigosa, L. M.: Las grandes unidades des relieve, *Geografia de la Rioja*, 1, 62-71, 1994.

862

863 Palacios, D., De Marcos, J., and Vásquez-Selem, L.: Last Glacial Maximum and deglaciation  
864 of the Sierra de Gredos, central Iberian Peninsula, *Quat. Int.*, 233, 16-26,  
865 <https://doi.org/10.1016/j.quaint.2010.04.029>, 2011.

866

867 Palacios, D., Andrés, N., De Marcos, J., and Vásquez-Selem, L.: Maximum glacial advance and  
868 deglaciation of the Pinar Valley (Sierra de Gredos, Central Spain) and its significance in the  
869 Mediterranean context, *Geomorph.*, 177-178, 51-61,  
870 <https://doi.org/10.1016/j.geomorph.2012.07.013>, 2012.

871

872 Pellicer, F. and Echeverría, M. T.: El modelado glaciar y periglacial en el macizo del moncayo,  
873 in: Peña, J. L., Longares, L. A., and Sánchez, M. (Eds.): Geografía Física de Aragón, Aspectos  
874 generales y temáticos, Universidad de Zaragoza e Institución Fernando el Católico, Zaragoza,  
875 173-185, 2004.

876

877 Pérez-Rivarés, F. J., Garcés, M., Arenas, C., and Pardo, G.: Magnetocronología de la sucesión  
878 Miocena de la Sierra de Alcubierre (sector central de la cuenca del Ebro), *Rev. Soc. Geol.*  
879 *España*, 15, 217-231, 2002.

880

881 Pérez-Rivarés, F. J., Garcés, M., Arenas, C., and Pardo, G.: Magnetostratigraphy of the Miocene  
882 continental deposits of the Montes de Castejón (central Ebro basin, Spain): geochronological  
883 and paleoenvironmental implications, *Geologica Acta*, 2, 221-234, 2004.

884

885 Perron, J. T. and Royden, L.: An integral approach to bedrock river profile analysis. *Earth Surf.*  
886 *Process. Landforms*, 38, 570–576, <https://doi.org/10.1002/esp.3302>, 2012.

887

888 Pineda Velasco, A.: Montorio. Mapa geológico de España; escala 1:50.000; Segunda serie.  
889 Instituto Geológico y Minero de España (IGME), Madrid, pp. 110, 1997.

890

891 Prince, P. S., Spotila, J. A., and Henika, W. S.: Stream capture as driver of transient landscape  
892 evolution in a tectonically quiescent setting, *Geology*, 39, 823–826,  
893 <https://doi.org/10.1130/G32008.1>, 2011.

894

895 Puigdefàbregas, C., Muñoz, J. A., and Vergés, J.: Thrusting and foreland basin evolution in the  
896 Southern Pyrenees, in: *Thrust Tectonics*, McClay, K.R. (Ed.): Chapman & Hall, London, 247-  
897 254, 1992.

898

899 Pulgar, J. A., Alonso, J. L., Espina, R. G., and Marín, J. A.: La deformación alpina en el  
900 basamento varisco de la Zona Cantábrica, 283-294, 1999.

901

902 Riba, O., Reguant, S., and Villena, J.: Ensayo de síntesis estratigráfica y evolutiva de la Cuenca  
903 terciaria del Ebro, in: Comba, J. A. (Ed.): *Geología de España*, 2, Libro Jubila J. M. Rios,  
904 Instituto Geológico y Minero de España, Madrid, 131-159, 1983.

905

906 Rivas-Carballo, M. R., Alonso-Gavilán, G., Valle, M. F., and Civis, J.: Miocene Palynology of  
907 the central sector of the Duero Basin (Spain) in relation to palaeogeography and  
908 palaeoenvironment, *Rev. Palaeobot. Palynol.*, 82, 251-264, 1994.

909

910 Salas, R., Guimerà, J., Mas, R., Martín-Closas, C., Meléndez, A., and Alonso, A.: Evolution of  
911 the Mesozoic Central Iberian Rift System and its Cainozoic inversion (Iberian Chain), in:  
912 Ziegler, P. A., Cavazza, W., Robertson, A. F. H., and Crasquin-Soleau, S. (Eds.): Peri-Tethys  
913 Memoir 6: Peri-Tethyan Rift/Wrench Basins and Passive Margins. *Mémoires du Muséum  
914 national d'Histoire naturelle*, 186, 145-185, 2001.

915

916 Sancho, C., Calle, M., Peña-Monné, J. L., Duval, M., Oliva-Urcia, B., Pueyo, E. L., Benito, G.,  
917 and Moreno, A.: Dating the Earliest Pleistocene alluvial terrace of the Alcanadre River (Ebro  
918 Basin, NE Spain): Insights into the landscape evolution and involved processes, *Quat. Int.*, 407,  
919 86-95, <https://doi.org/10.1016/j.quaint.2015.10.050>, 2016.

920

921 Schumm, S. A., Mosley, M. P., and Weaver, W. E.: *Experimental fluvial geomorphology*, John  
922 Wiley and Sons, New York, pp. 413, 1987.

923

924 Schwanghart, W. and Scherler, D.: TopoToolbolx 2 a MATLAB-based software for topographic  
925 analysis and modeling in Earth surface sciences, *Earth Surf. Dynamics*, 2, 1-7,  
926 <https://doi.org/10.5194/esurf-2-1-2014>, 2014.

927

928 Serrano, E., González-Trueba, J. J., Pellitero, R., González-García, M., and Gómez-Lende, M.:  
929 Quaternary glacial evolution in the Central Cantabrian Mountains (Northern Spain),  
930 *Geomorph.*, 196, 65-82, <https://doi.org/10.1016/j.geomorph.2012.05.001>, 2013.

931

932 Serrano, E., González-Trueba, J. J., Pellitero, R., Gómez-Lende, M.: Quaternary glacial history  
933 of the Cantabrian Mountains of northern Spain: a new synthesis, in: Hughes, P. D. and  
934 Woodward, J. C. (Eds.): *Quaternary Glaciation in the Mediterranean Mountains*, Geological  
935 Society, London, Special Publications, 433, <https://doi.org/10.1144/SP433.8>, 2016.

936

937 Sobel, E. R. and Strecker, M. R.: Uplift, exhumation and precipitation: tectonic and climatic  
938 control of Late Cenozoic landscape evolution in the northern Sierras Pampeanas, Argentina,  
939 Basin Res., 15, 431-451, <https://doi.org/10.1046/j.1365-2117.2003.00214.x>, 2003.  
940

941 Sobel, E. R., Hilley, G. E., and Strecker, M. R.: Formation of internally drained contractional  
942 basins by aridity-limited bedrock incision, J. Geophys. Res., 108, 2344,  
943 <https://doi.org/10.1029/2002JB001883>, 2003.  
944

945 Stange, K. M., Van Balen, R. T., Garcia-Castellanos, D., and Cloething, S.: Numerical  
946 modelling of Quaternary terrace staircase formation in the Ebro foreland basin, southern  
947 Pyrenees, NE Iberia, Basin Res., 1-23, <https://doi.org/10.1111/bre.12103>, 2014.  
948

949 Suc, J. P. and Popescu, S. M.: Pollen records and climatic cycles in the Mediterranean region  
950 since 2.7 Ma, in: Head, M. J. and Gibbard, P. L. (Eds.): Early-Middle Pleistocene Transitions,  
951 the Land-Ocean Evidence, Geological Society, London, Special Publications, 247, 147-158,  
952 <https://doi.org/10.1144/GSL.SP.2005.247.01.08>, 2005.  
953

954 Urgeles, R., Camerlenghi, A., Garcia-Castellanos, D., De Mol, B., Garcés, M., Vergés, J.,  
955 Haslam, I., and Hardman, M.: New constraints on the Messinian sealevel drawdown from 3D  
956 seismic data of the Ebro Margin, western Mediterranean, Basin Res., 23, 123-145,  
957 <https://doi.org/10.1111/j.1365-2117.2010.00477.x>, 2010.  
958

959 Van der Beek, P., Litty, C., Baudin, M., Mercier, J., Robert, X., and Hardwick, E.: Contrasting  
960 tectonically driven exhumation and incision patterns, Western versus central Nepal Himalaya,  
961 Geology, 44, 327-330, <https://doi.org/10.1130/G37579.1>, 2016.  
962

963 Vázquez-Urbez, M., Arenas, C., Pardo, G., and Pérez-Rivarés, J.: The effect of drainage  
964 reorganization and climate on the sedimentologic evolution of intermontane lake systems: the  
965 final fill stage of the Tertiary Ebro Basin (Spain), J. Sediment. Res., 83, 562-590,  
966 <https://doi.org/10.2110/jsr.2013.47>, 2013.  
967

968 Villena, J., Pardo, G., Pérez, A., Muñoz, A., and González, A.: The Tertiary of the Iberian margin  
969 of the Ebro basin: palaeogeography and tectonic control, in: Friend, P. and Dabrio, C. (Eds.):

970 Tertiary basins of Spain, *World and Regional Geology*, 6, Cambridge University Press,  
971 Cambridge, 83-88, 1996.

972

973 Whipple, K.: The influence of climate on the tectonic evolution of mountain belts, *Nature*  
974 *Geosci.*, 2, 97-104, <https://doi.org/10.1038/ngeo638>, 2009.

975

976 Whipple, K. X. and Tucker, G. E.: Dynamics of the stream-power river incision model:  
977 Implications for height limits of mountain ranges, landscape response timescales, and research  
978 needs, *J. Geophys. Res.*, 104, 17661-17674, 1999.

979

980 Whipple, K. X., Forte, A. M., DiBiase, R. A., Gasparini, N. M., Ouimet, W. B.: Timescales of  
981 landscape response to divide migration and drainage capture: implications for the role of divide  
982 mobility in landscape evolution, *J. Geophys. Res.- Ea. Surf.*, 122, 248-273,  
983 <https://doi.org/10.1002/2016JF003973>, 2017.

984

985 Whitfield, E. and Harvey, A. M.: Interaction between the controls on fluvial system  
986 development: tectonics, climate, base level and river capture – Rio Alias, Southeast Spain, *Earth*  
987 *Surf. Process. Landforms*, 37, 1387-1397, <https://doi.org/10.1002/esp.3247>, 2012.

988

989 Willett, S. D.: Orogeny and orography: The effects of erosion on the structure of mountain belts,  
990 *J. Geophys. Res.*, 104, 28957-28981, 1999.

991

992 Willett, S. D., McCoy, S. W., Perron, J. T., Goren, L., and Chen, C. Y.: Dynamic reorganization  
993 of river basins, *Science*, 343, 1248765, <https://doi.org/10.1126/science.1248765>, 2014.

994

995 Yanites, B. J., Elhers, T. A., Becker, J. K., Schnellmann, M., and Heuberger, S.: High magnitude  
996 and rapid incision from river capture: Rhine River, Switzerland, *J. Geophys. Res.- Ea. Surf.*,  
997 118, 1060-1084, <https://doi.org/10.1002/jgrf.20056>, 2013.

998

999

1000

1001

1002

Figure captions:

Figure 1: A) Topographic map of the Duero and Ebro basins and surrounding belts. B) Averaged topographic section throughout the Duero and Ebro basins showing important incision contrast between the two basins. The Duero basin recorded low incision, especially in its upper part, whereas the Ebro basin is highly excavated.

Figure 2: Simplified geological map of the study area.

Figure 3: Topographic map of the study area with all the rivers considered in this study. The red lines represent drainage divides between main hydrographic basins.

Figure 4: Zoom in the geological map of the Iberian Range showing the location of the Jalon river tributaries. The river long profiles of these streams and the location of knickpoints are shown to the left.

Figure 5: A) Zoom in the geological map of the Bureba sector. B) Zoom in the Homino river (Ebro tributary) capturing the upper reach of the Jordan river (Duero tributary). C) Schematic representation of this capture using river long profiles and map orientation, showing the associated knickpoint and wind gap.

Figure 6: Mean annual precipitation map for the study area (data from Hijmans et al., 2005).

Figure 7: A) 3D view of the DEM of the Bureba sector showing important contrast of incision between the Ebro and Duero basins across their divide (red dashed line) and river capture evidence (elbows of capture, knickpoints and wind gaps). B) Google Earth image around the locality of Hontomin where the Homino river is capturing the upper reach of the Jordan river. C) and D) Wind gaps cut into the Bureba anticline (see location on Fig. 7A). Pictures have been taken from the north of this structure toward the south. E) Possible three steps evolution of the southwestward divide retreat through multiple river captures witnessed in the area.

Figure 8: River long profiles for all the streams described in the Bureba area showing evidence of river capture. Colors are given to rivers that are linked in these capture processes.

Figure 9: Topographic map showing the location of all the knickpoints and low relief surfaces that may be associated to river capture. The black dashed line represents a possible paleodrainage divide between the Ebro and Duero basins. The area between this dashed line and the present-day location of the divide in red may have belonged the Duero basin before being captured by the Ebro basin.

Figure 10: Duero river long profile (black line) and difference in the specific stream power of the river (grey) calculated by considering the paleo and present-day position of its divide. Positive values suggest a significant diminution of the incision capacity of the Duero river, particularly along the knickzone of its longitudinal profile. Details on calculation are available in the Supplement (Section S1).

Figure 11: Topographic map with  $\chi$  values calculated on different opposite streams in the vicinity of the Ebro/Duero drainage divide. This map shows significant contrasting values between the Ebro and Duero drainage networks.



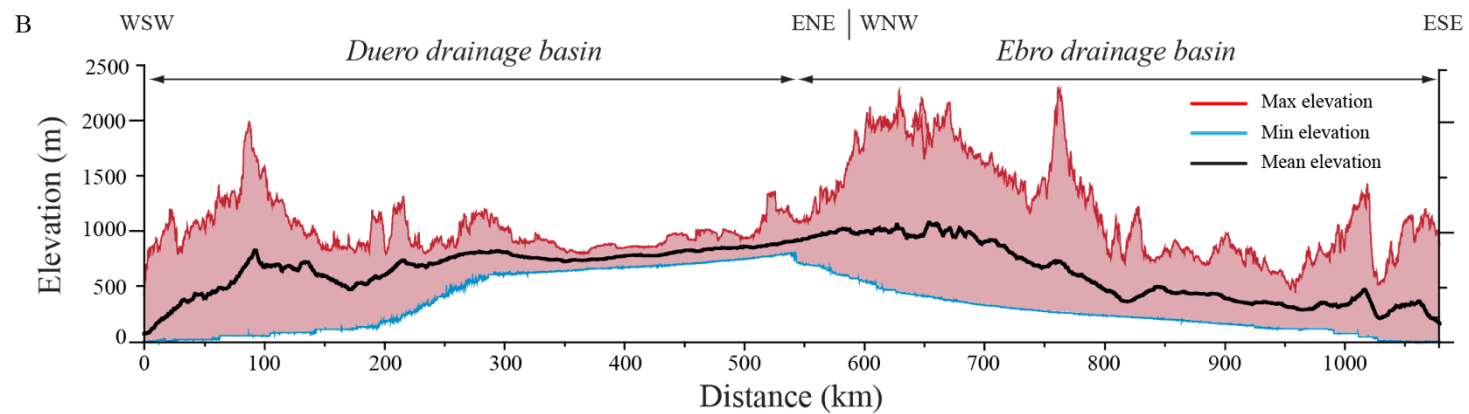
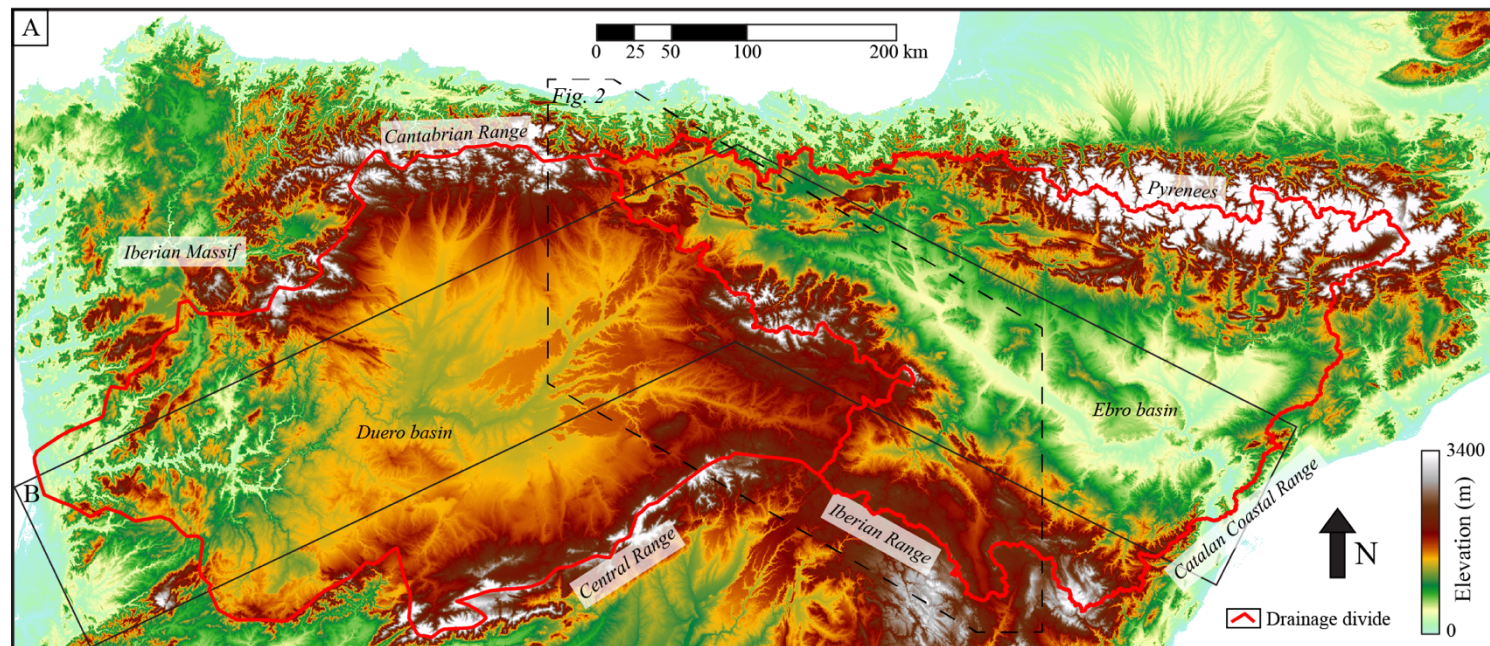


Figure 1

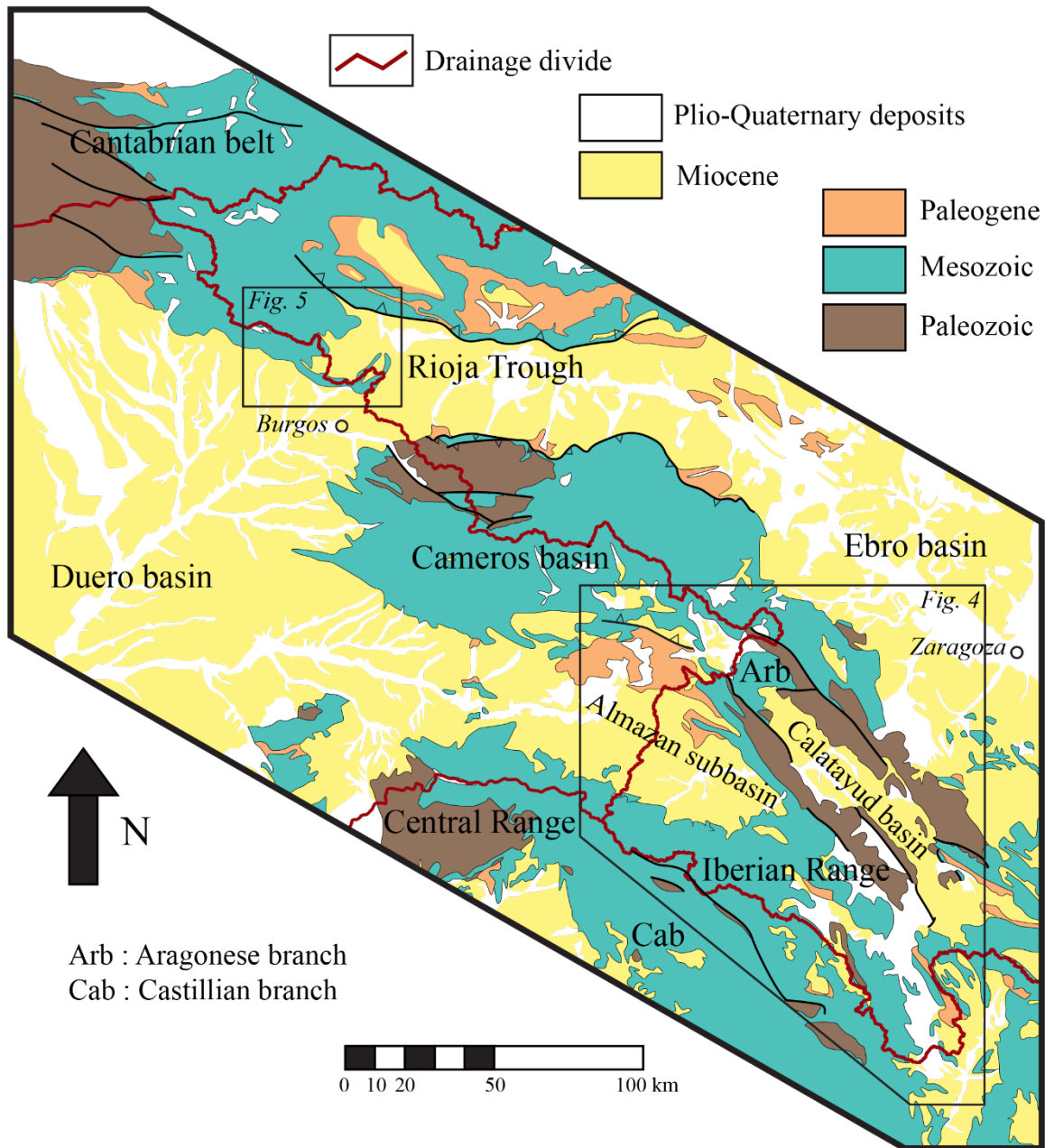


Figure 2

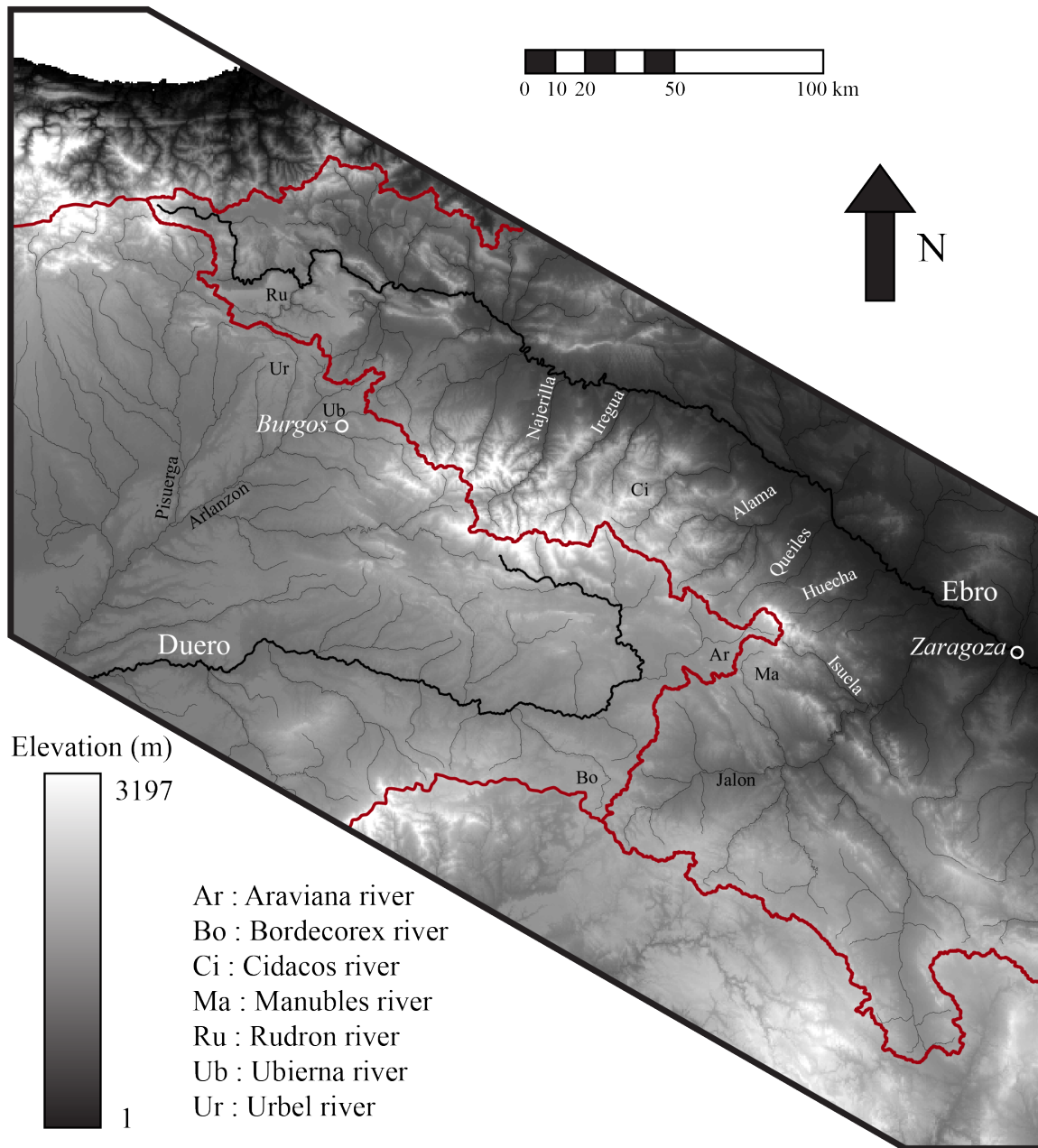


Figure 3



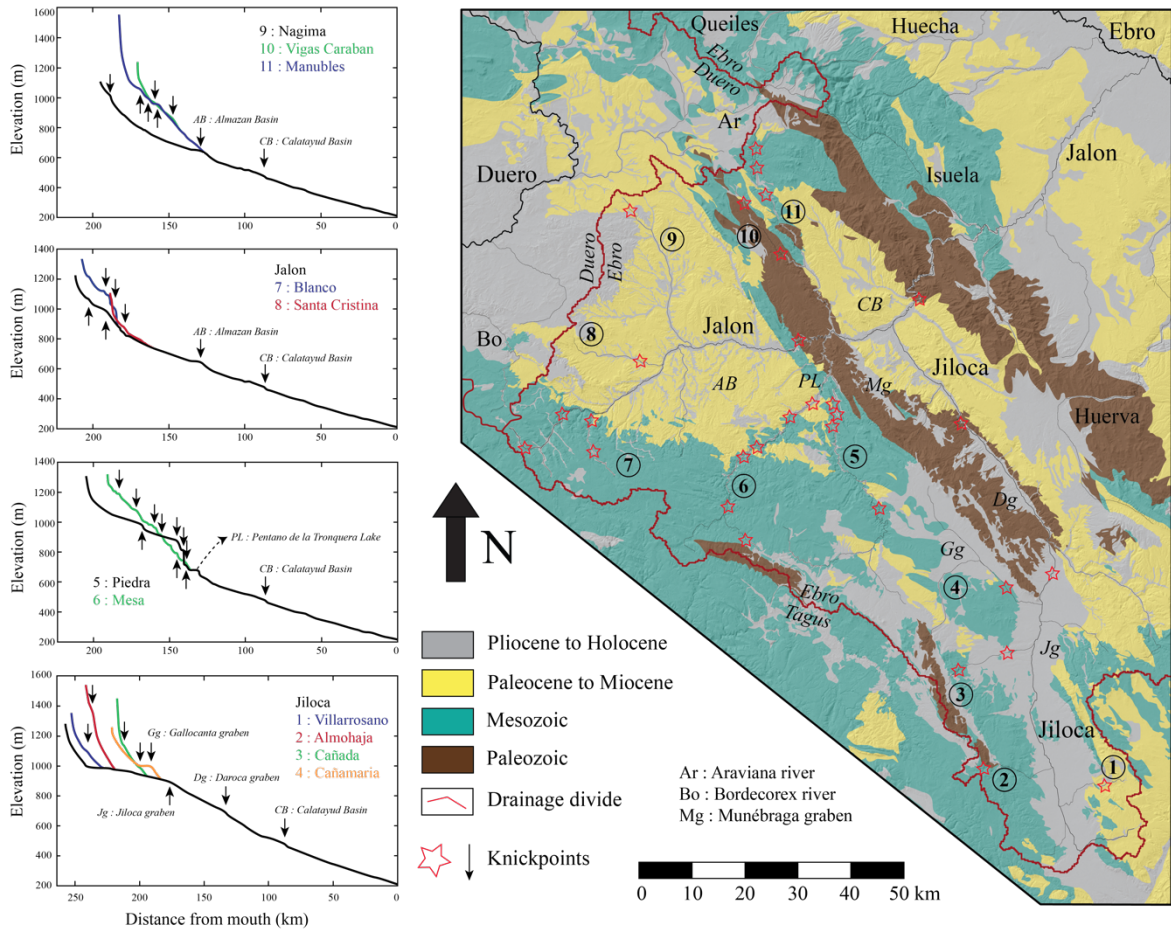


Figure 4

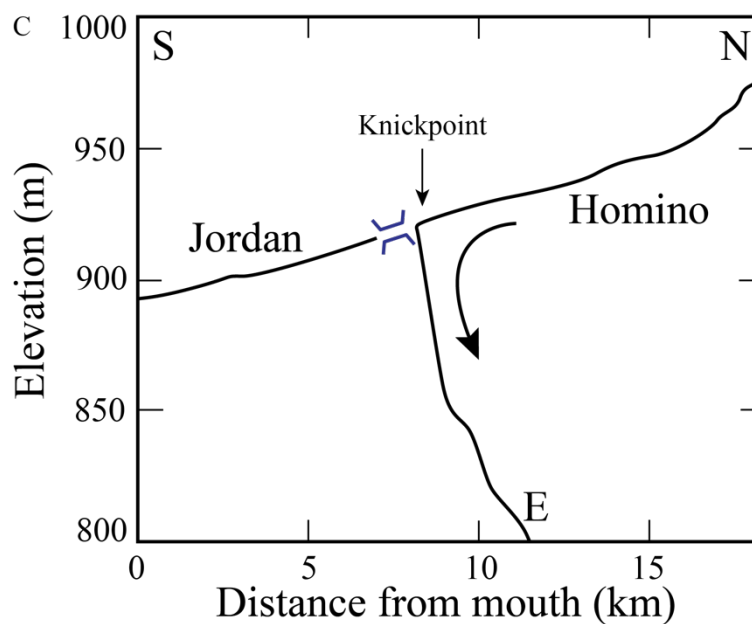
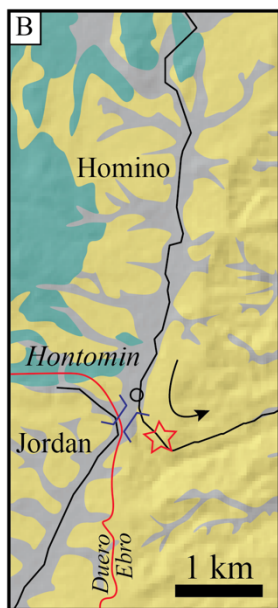
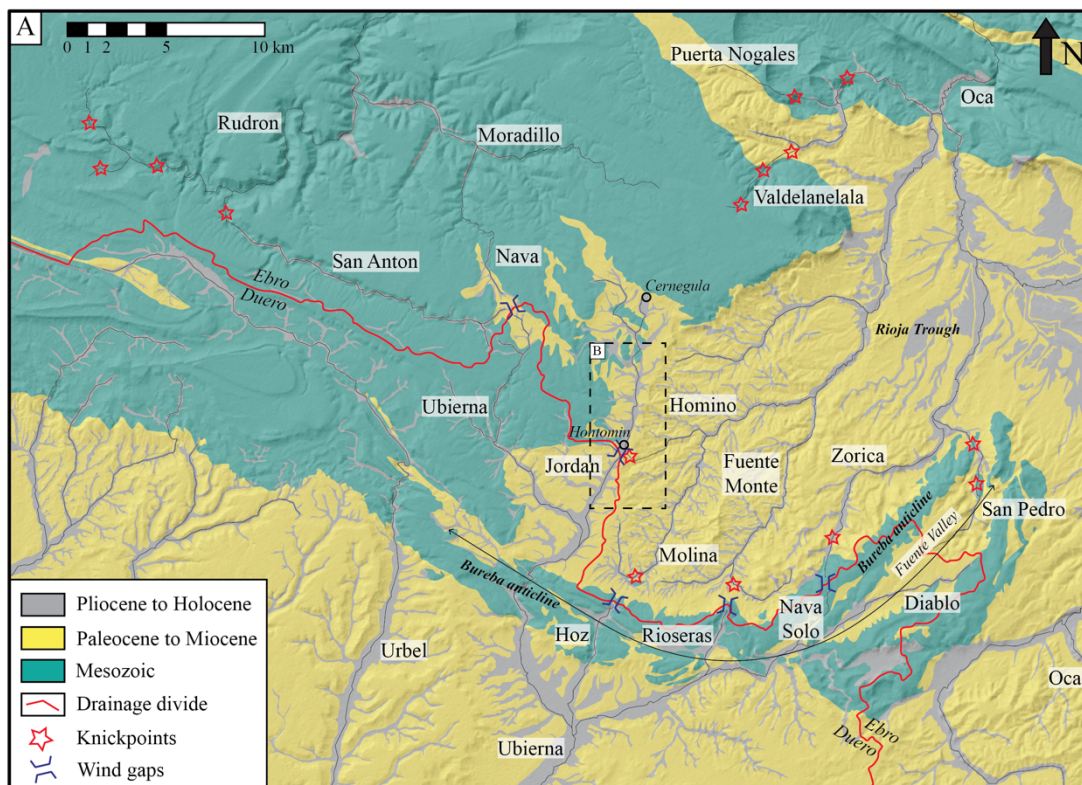


Figure 5

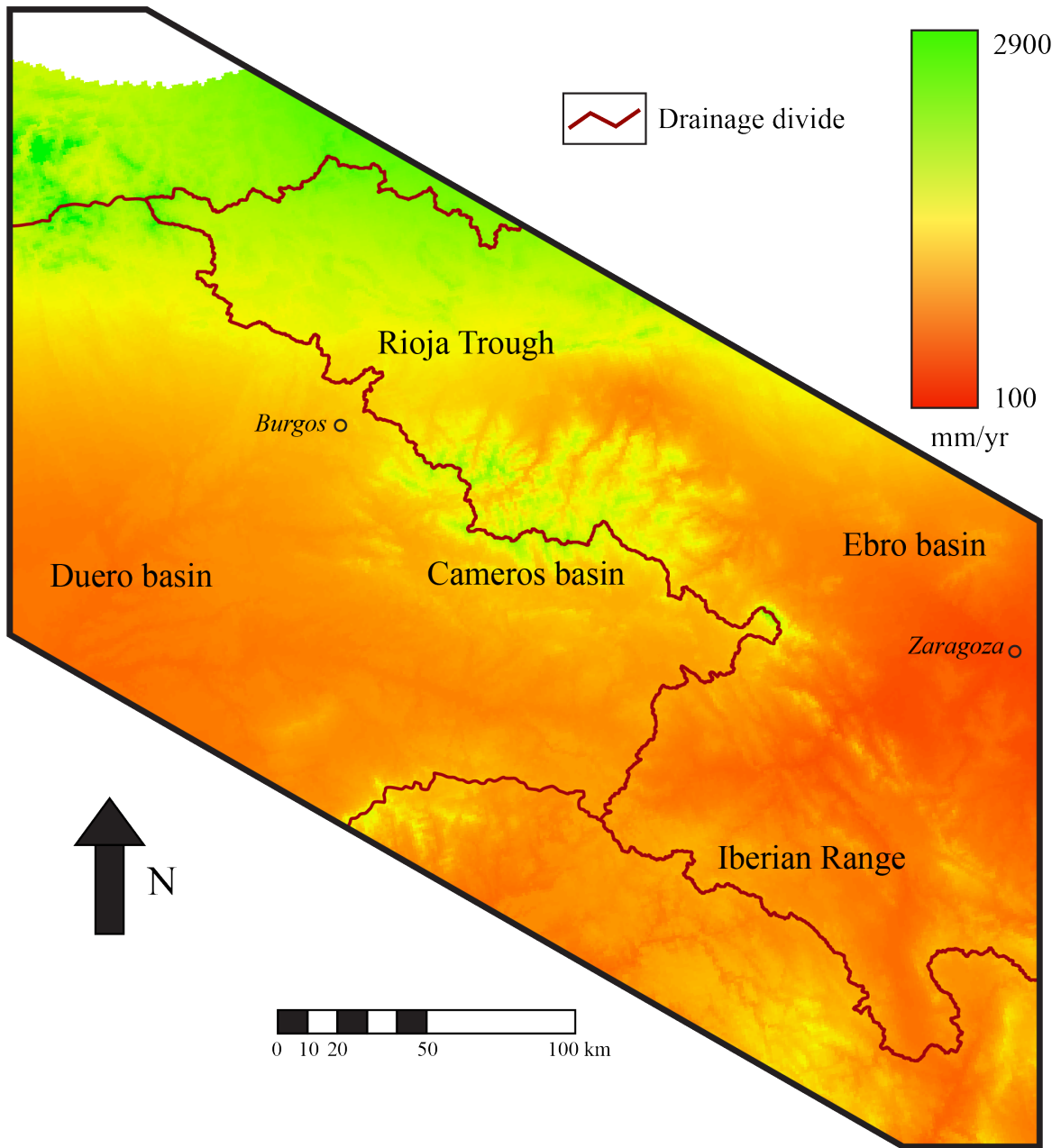
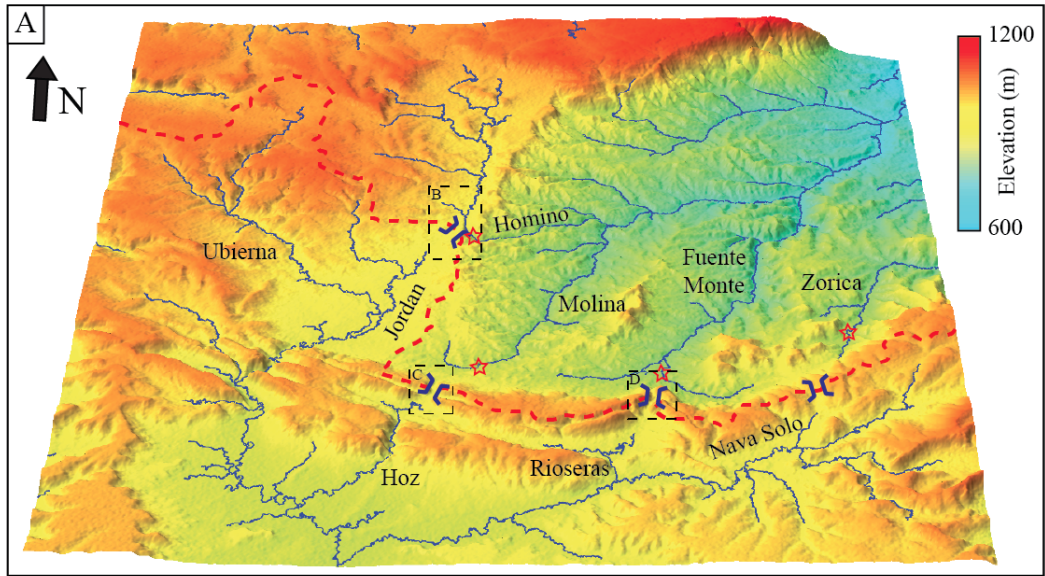


Figure 6





- Drainage divide
- Knickpoints
- Wind gaps
- Mesozoic relief
- Cenozoic incision

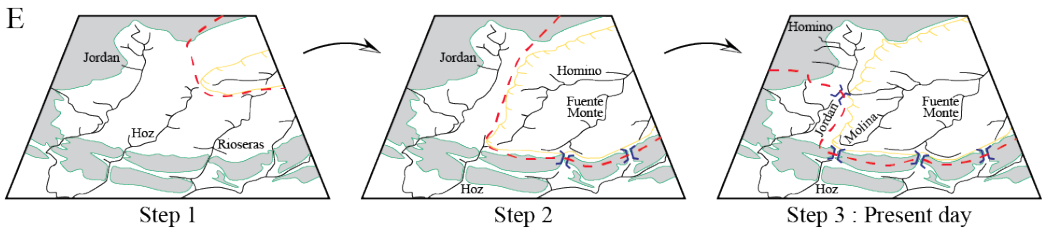
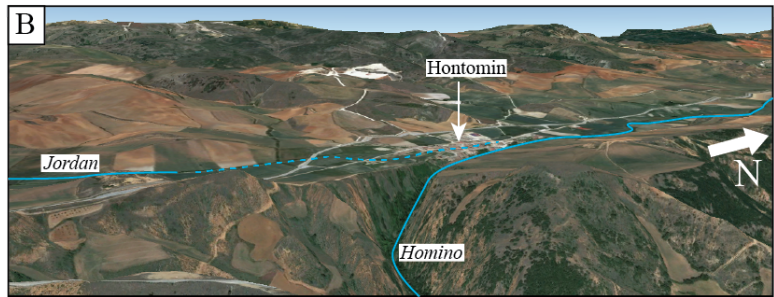


Figure 7

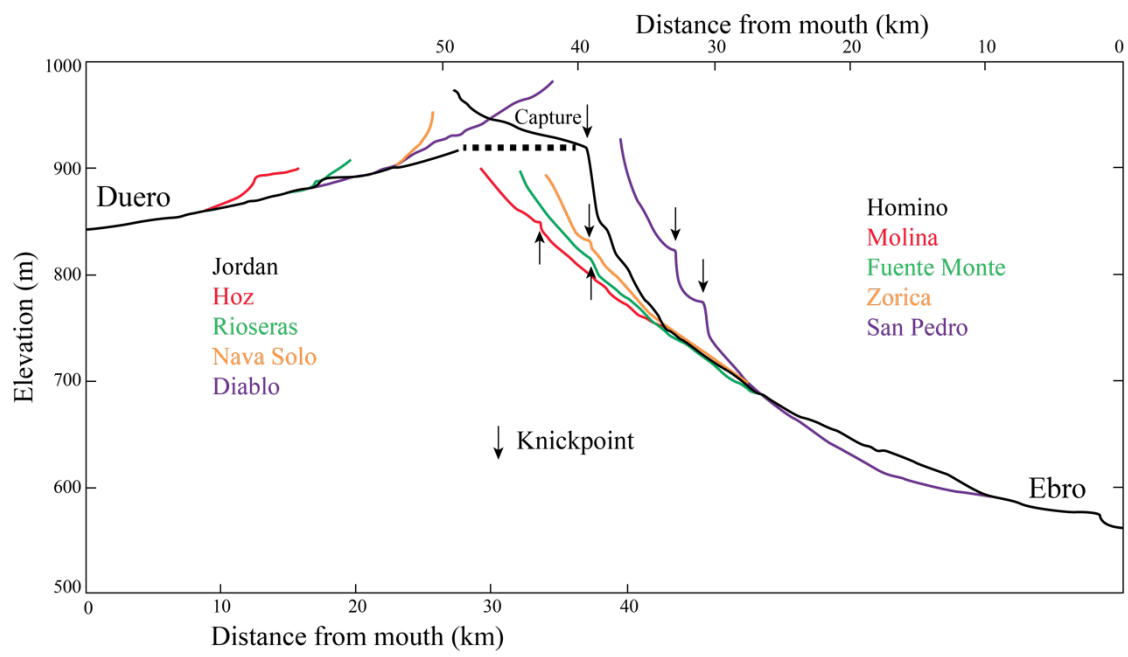


Figure 8



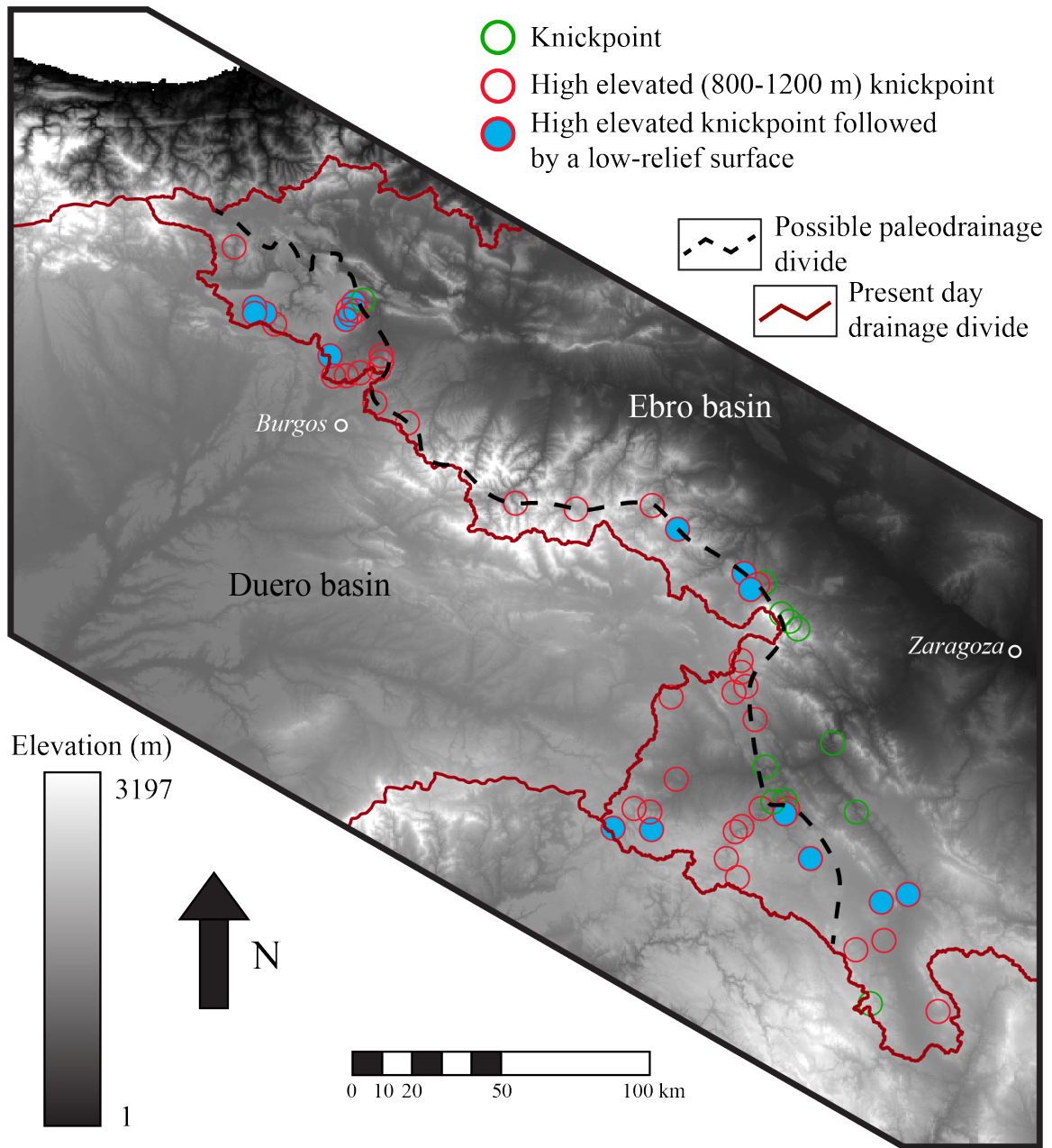


Figure 9

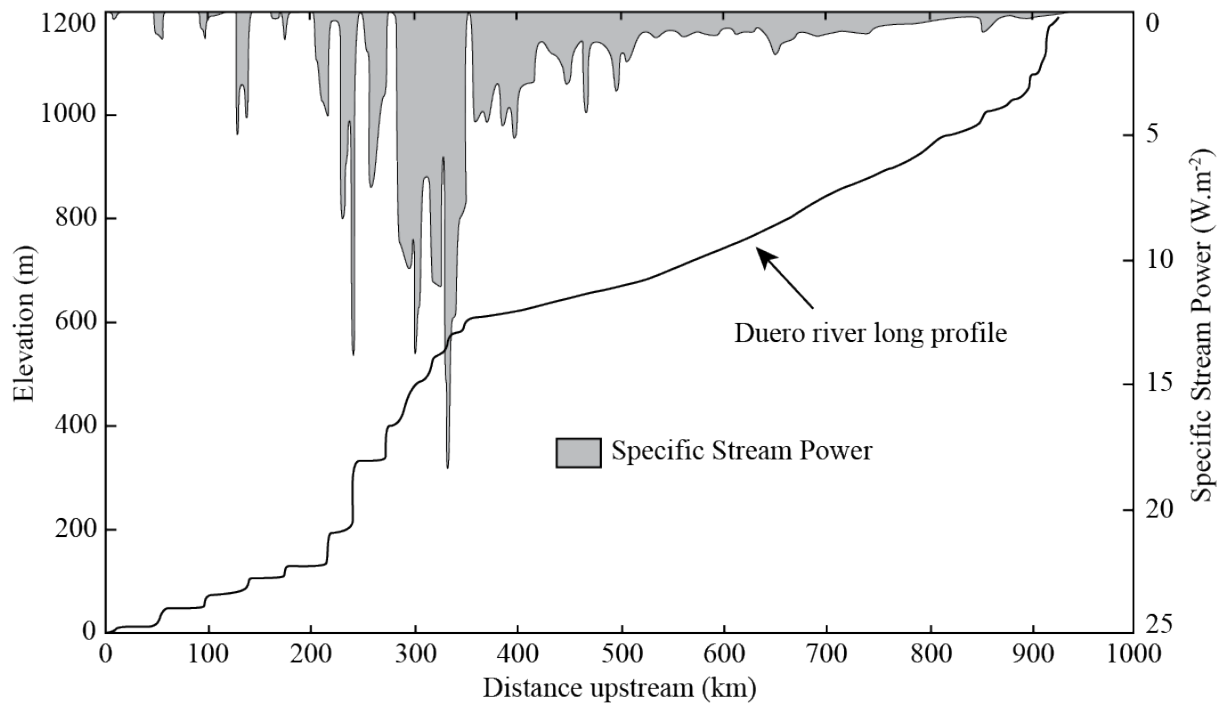


Figure 10

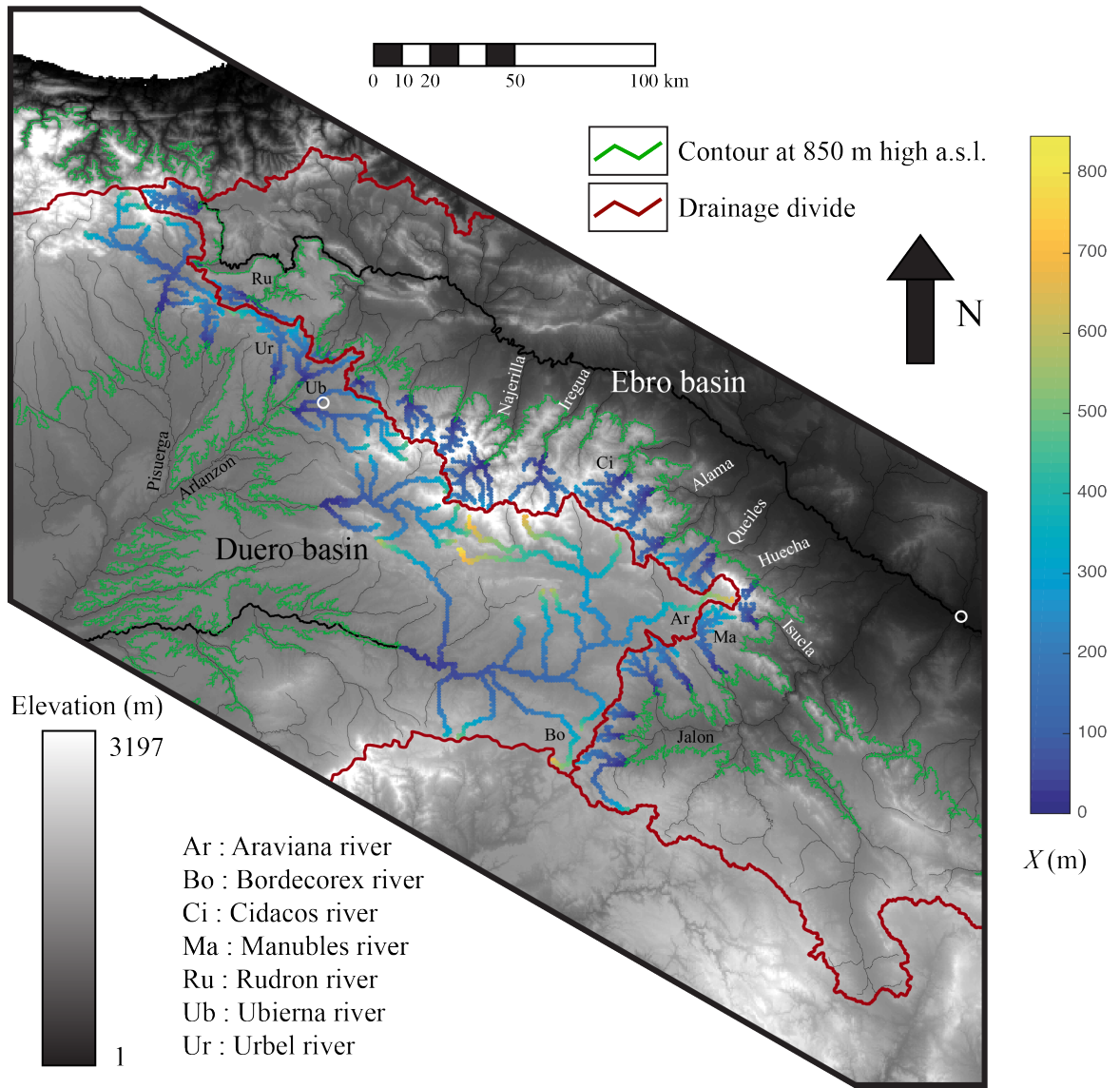


Figure 11